

Regulation of TFEB and TFE3 activity in skeletal muscle remodeling

Inaugural-Dissertation

to obtain the academic degree

Doctor rerum naturalium (Dr. rer. nat)

submitted to

the Department of Biology, Chemistry, Pharmacy

of Freie Universität Berlin

by

Cristina Pablo

From Valencia, Spain

June 2019

*"I was taught that the way of progress
is neither swift nor easy"*

- Marie Curie

This work was carried out from October 2013 to December 2018 under the supervision of Univ.-Prof. Dr. med. Jens Fielitz at the Experimental and Clinical Research Center (ECRC), a joint cooperation of the Max Delbrück Center for Molecular Medicine and the Charité Medical Faculty, Berlin.

1st Reviewer: Prof. Dr. med. Simone Spuler

Institute for Chemistry and Biochemistry Department of Biology, Chemistry,
Pharmacy Freie Universität, Berlin

and

Department of Muscle Sciences and University
Outpatient Clinic for Muscle Disorders
Experimental and Clinical Research Center, Berlin

2nd Reviewer: Univ.-Prof. Dr. med. Jens Fielitz

Experimental and Clinical Research Center, Berlin

and

Department of Internal Medicine B
Universitätsmedizin, Greifswald

Date of defense: 13.12.2019

I declare that I have completed the submitted dissertation independently and without the use of sources and aids other than those indicated. I further declare that the dissertation presented here has not been submitted in the same or similar form to any other institution for the purpose of obtaining an academic degree.

Acknowledgements

I would like to thank in first place Prof. Jens Fielitz for giving me the opportunity to join his lab and develop myself as a scientist. His dedication for research and his trust on me were always good reasons to move forward.

This work could not have been possible without all the members of AG Fielitz. Danke Sibylle for being the best German teacher among many other things. *Am Ende, wird alles Gut.* I would also like to thank Dr. Melanie Kny and Alexander Hahn for all these years of adventures in cell culture and their help with experiments. Special thanks to Dr. and friend Dörte Lodka, you have been always a great help in every professional and personal difficult moment. I hope this lasts for many other years.

To all my friends, the ones who are always present and those that passed by my life in the last years, I am grateful for your patience and support during my PhD. I do not want to forget about that person who came to the rescue in every critical situation, big thank you for your support.

Gracias también a mi hermano, a mi tita y a mi abuela por haber hecho de mi la persona que soy. Por último, quiero dedicar completamente este trabajo a mi padre. Por ser la persona que me lo ha dado todo y me ha enseñado a luchar para conseguir cualquier meta.

Table of content

List of abbreviations	I
List of figures	III
List of tables	V
Summary	VI
Zusammenfassung	VIII
1. Introduction	1
1.1 Skeletal muscle	1
I. Structure and physiology	1
II. Muscle differentiation	4
III. Hypertrophy and atrophy	5
1.2 Muscle remodeling	6
I. Ubiquitin proteasome system	6
II. Autophagy-lysosomal pathway	7
A. Autophagosome formation	8
B. Trigger autophagy	9
C. Monitoring autophagy	9
III. UPS-Autophagy crosstalk	11
1.3 MuRF1	12
I. Transcriptional regulation	13
1.4 MiTF/TFE family members of transcription factors	13
I. Transcription factor EB	14
II. Transcription factor 3	15
III. Microphthalmia-associated transcription factor	16
1.5 Histone deacetylases	16
1.6 Protein kinase D family	17
2. Aim of the study	19
3. Material and methods	20

3.1 Plasmids and Vectors	20
I. Plasmids	20
II. Transformation	21
3.2 Cell Culture	21
I. Gelatin Coating	21
II. COS7	21
A. Transfection	22
B. Measurements of luciferase and fluorescence signals	22
C. Co-Immunoprecipitation (Co-IP)	22
III. Plat-E cells for retrovirus production	23
A. Transfection of Plat-E cells	23
B. Retrovirus production	23
VI. C2C12 myoblast cell line	24
A. Cultivation and differentiation of C2C12 cells	24
B. Starvation and Chloroquine treatment	24
C. Transfection	25
D. Retroviral transduction	25
E. siRNA Transfection	25
3.3 TFEB knockout mice	26
I. Generation	26
II. Isolation of muscle and organs from adult mice	26
3.4 Immunofluorescence	26
I. Immunostaining protocol	26
II. Antibody list	27
III. Image acquisition and analysis	28
A. Routine cell culture image acquisition	28
B. Confocal imaging	28
C. Image processing and analysis	28

3.5 Protein Analysis	28
I. Preparation of protein lysates	28
II. SDS-PAGE and immunoblotting	28
III. Densitometric quantification	30
IV. Proteomics	30
A. Generation of samples	30
B. Proteomic analysis	30
3.6 mRNA Analysis	31
I. RNA Isolation and cDNA synthesis	31
A. Tissue homogenization and lysis	31
B. Cell lysis	32
C. RNA isolation	32
D. cDNA synthesis	32
II. Quantitative Real Time PCR	32
3.7 Statistics	33
4. Results	34
4.1 Role of MiTF/TFE family members in MuRF1 induction	34
I. Microphthalmia-associated transcription factor family (MiTF/TFE) members TFEB and TFE3 transcriptionally regulate <i>Trim63</i> -expression	34
II. Class IIa Histone deacetylases inhibit TFEB and TFE3 mediated increase in MuRF1 expression	35
III. Protein kinase D family members attenuate HDAC mediated inhibition of TFEB- and TFE3-induced MuRF1 expression	36
IV. TFEB and TFE3 share same HDAC5-interacting domain	40
V. TFEB and TFE3 compete for the activation of MuRF1 expression	42
4.2 TFEB in muscle protein homeostasis: UPS and Autophagy	43
I. TFEB knock down reduces autophagic flux <i>in vitro</i>	44
II. Deletion of <i>Tfeb</i> does not affect the expression of autophagy genes	44
III. TFEB overexpression is not sufficient to stimulate autophagy	46

4.3 Muscle specific <i>Tfeb</i> knockout mice do not show muscle phenotype	49
4.4 Overexpression of TFEB impairs myoblast fusion <i>in vitro</i>	51
5. Discussion	58
5.1 Role of MiTF/TFE family members in MuRF1 expression	58
5.2 Regulation of TFEB- and TFE3-induced MuRF1 expression	59
5.3 Nuclear localization of TFEB and TFE3	61
5.4 TFEB role as master regulator of autophagy in muscle cells	61
5.5 Deletion of <i>Tfeb</i> in muscle does not affect muscle growth <i>in vivo</i>	63
5.6 TFEB overexpression impairs myogenic differentiation	64
6. Bibliography	66

Abbreviations

ACN	acetonitrile
ALP	autophagy-lysosome pathway
ATP	adenosine triphosphate
bHLH	basic helix loop helix
BSA	bovine serum albumin
cDNA	complementary DNA
cKO	conditional knockout
DAPI	4',6-diamidino-2-phenylindole
DMEM	Dulbecco's Modified Eagle Medium
DMSO	dimethylsulfoxide
DNA	deoxyribonucleic acid
EDTA	ethylene diamine tetraacetic acid
ER	endoplasmic reticulum
FA	formaldehyde
FBS	fetal bovine serum
<i>g</i>	gravitational acceleration
GAPDH	glyceraldehyde 3-phosphate dehydrogenase
GFP	green fluorescent protein
GR	glucocorticoid receptor
h	hour
HDAC	histone deacetylases
HRP	horseradish peroxidase
IGF	insulin-like growth factor
LC-MS	liquid chromatography–mass spectrometry
<i>LacZ</i>	gene encoding beta-galactosidase
LC3	microtubule-associated protein 1 light chain 3 (MAP1LC3)
LZ	leucine zipper
MB	myoblast
MHC	myosin heavy chain

MiTF	microphthalmia-associated transcription factor
mM	millimolar
MOI	multiplicity of infection
MRF	myogenic regulatory factor
mRNA	messenger ribonucleic acid
MS	mass spectrometry
mTOR	mechanistic target of rapamycin
NaCl	sodium chloride
nM	nanomolar
PBS	phosphate buffered saline
PCR	polymerase chain reaction
PI3K	phosphoinositide 3-kinase
PKD	protein kinase D
ppm	parts per million
PVDF	polyvinylidene difluoride
qPCR	quantitative PCR
RLU	relative luciferase units
RNA	ribonucleic acid
RT	room temperature
SDS-PAGE	sodium dodecyl sulfate-polyacrylamide gel electrophoresis
SEM	standard error of the mean
siRNA	small interfering RNA
TBS-T	Tris-buffered saline with Tween 20
TFEB	transcription factor EB
TFE3	transcription factor E3
Tris	trisaminomethane
Triton X-100	polyethylene glycol p-(1,1,3,3-tetramethylbutyl)-phenyl ether
Tween-20	polyoxyethylene (20) sorbitan monolaurate
U	unit
UPLC	ultra-performance liquid chromatography
UPS	ubiquitin proteasome system
WT	wildtype

List of figures

Fig. 1. Muscle structure _____	1
Fig. 2. Organization of myofibril _____	3
Fig. 3. Schema of myogenesis _____	4
Fig. 4. Ubiquitin proteasome system _____	7
Fig. 5. The process of macroautophagy in mammalian cells _____	9
Fig. 6. Autophagy pathway and autophagic flux _____	11
Fig. 7. Schematic diagram of MuRF1 protein structure and their potential protein-protein interaction domains _____	12
Fig. 8. MiTF/TFE family members structure _____	14
Fig. 9. Model of TFEB function and regulation of lysosomal biogenesis and autophagy _____	15
Fig. 10. Class IIa histone deacetylase (HDAC) members _____	17
Fig. 11. Ang II/PKD1/HDAC5 signaling pathway regulates TFEB-mediated MuRF1 expression _____	18
Fig 12. <i>Tfeb</i> and <i>Tfe3</i> increase <i>Trim63</i> -expression _____	34
Fig 13. Class IIa HDAC family members inhibit TFEB-mediated MuRF1 expression _____	35
Fig 14. Class IIa HDAC family members inhibit TFE3-mediated MuRF1 expression _____	36
Fig 15. PKD1 promotes nuclear export of class IIa HDAC _____	37
Fig 16. Each PKD family member restores TFEB-mediated MuRF1 expression inhibited by HDAC4, HDAC5 and HDAC7 _____	38
Fig 17. PKD1 promotes nuclear export of class IIa HDAC releasing its interaction with TFE3 _____	39
Fig. 18. Each PKD family member restores TFE3-mediated MuRF1 expression inhibited by HDAC4, HDAC5 and HDAC7 _____	41
Fig. 19. HDAC5 binds TFEB and TFE3 by the same association domain _____	42
Fig. 20. TFEB and TFE3 redundantly regulate activity of MuRF1 promoter _____	43
Fig. 21. Depletion of TFEB in C2C12 mouse skeletal muscle myotubes may have an effect in autophagy flux _____	45
Fig. 22. RNA expression data reveals almost no changes in autophagy genes due to absence of TFEB or fasting _____	46
Fig. 23. TFEB overexpression does not induce transcription of most autophagy-related genes _____	47
Fig. 24. Most autophagy markers are not modulated by a stable TFEB overexpression _____	48

Fig. 25. Deletion of <i>Tfeb</i> does not result in muscle phenotype_____	50
Fig. 26. Autophagic genes are not transcriptionally downregulated in <i>Tfeb</i> ^{-/-} mice_____	50
Fig. 27. TFEB expression blocks C2C12 myotube differentiation_____	52
Fig. 28. TFEB inhibits myogenic differentiation of C2C12 cells_____	53
Fig. 29. Downregulated myogenic differentiation markers confirm undifferentiated myotubes phenotype_____	53
Fig. 30. Proteomic analysis of lysates from TFEB-GFP and control GFP transduced C2C12 myotubes at day 0, 1, 3 and 5 of differentiation_____	55
Fig. 31. Proteomic analysis of lysates from TFEB-GFP and control GFP transduced C2C12 myotubes at day 0, 1, 3 and 5 of differentiation_____	56
Fig. 32. Proteomic analysis of lysates from TFEB-GFP and control GFP transduced C2C12 myotubes at day 0, 1, 3 and 5 of differentiation_____	57

List of Tables

Table 1. cDNA expression plasmids_____	20
Table 2. Buffers used in Co-Immunoprecipitation_____	23
Table 3. List and working dilution of antibodies used in this study_____	27
Table 4. List and composition of buffers needed for Western Blot_____	29
Table 5. List of qRT PCR primers_____	33

Summary

Muscle is a highly dynamic and plastic tissue that adapts to varying loading conditions by changes in muscle mass and fiber type composition. Muscle mass is mainly regulated by changes in protein synthesis and protein degradation. A decrease in protein synthesis and or an increase in protein degradation will lead to a reduction in protein and eventually muscle mass, which is called muscle atrophy. Most proteins are degraded via two proteolytic systems: the ubiquitin proteasome system (UPS) and the autophagy-lysosome pathway (ALP). Muscle RING-finger-1 (MuRF1) is an E3 ligase considered a key mediator of UPS-mediated muscle atrophy. Recently, our group demonstrated that the transcription factor EB (TFEB) is involved in muscle remodeling by directly activating *Trim63*/MuRF1 expression and described the protein kinase D1 (PKD1)/histone deacetylase 5 (HDAC5)/TFEB axis as regulator of muscle atrophy. Because TFEB belongs to the microphthalmia family (MiTFE, TFEB, TFE3) of transcription factors, we hypothesized that TFEB shares its transcriptional activity towards *Trim63*/MuRF1 with the MiTF-family members. Similarly, class IIa HDACs and PKDs belong to respective families with close structural, regulatory, and functional properties. Therefore, I investigated the interaction and functional significance of these three families. I demonstrated that class IIa HDACs physically interact with and directly inhibit the activity of TFEB and TFE3 towards *Trim63*/MuRF1. I showed that the PKD-family redundantly relieves HDAC-mediated inhibition of TFEB and TFE3. Altogether I propose a mechanistic basis for the control of muscle atrophy via the PKD/HDAC/TFEB-TFE3 axis. Besides that, TFEB is known to be a master regulator of lysosomal biogenesis and autophagy. However, if this function has physiological implications for skeletal muscle is uncertain. To address this question, I performed muscle-specific gain- and loss-of-function experiments both *in vitro* and *in vivo*. We generated a muscle specific *Tfeb* knockout mice; importantly, we did not observe a difference in autophagy-mediated protein degradation in muscle. In the *in vitro* part, I successfully established a retrovirus-based strategy to stably overexpress *Tfeb* in C2C12 muscle cells. My results suggest that TFEB does not induce ALP mediated protein degradation in C2C12 cells. Although the vast majority of studies support TFEB as master regulator of ALP, I propose that the effects of TFEB on ALP-mediated protein degradation are different between muscle and non-muscle cells. Interestingly, I found in my study that overexpression of TFEB in C2C12 myoblasts attenuates myoblast differentiation and keeps these cells in at an undifferentiated blast stage. Using a proteomics-based approach we found that TFEB-overexpression resulted in a reduction of proteins in charge of cell-cell fusion and cytoplasmic architecture such as α -actin, actinin, muscle specific cadherin and most of tropomyosin isoforms. Additionally, we found an increased amount of the proliferation marker Ki67 indicative for the incompetence of C2C12 cells to exit the cell cycle, to differentiate and to generate

muscle fibers upon TFEB overexpression. Accordingly, late differentiation markers such as myosin heavy chain proteins were greatly reduced in TFEB treated C2C12 cells.

In summary, my thesis sheds new light on the transcriptional regulation of the MiTF-family of transcription factors in myocytes and implicates that TFEB is involved in myogenic differentiation. Although TFEB is known as a master regulator of ALP-mediated protein degradation in non-myocytes, my data argue for alternative functions of TFEB in myocytes.

Zusammenfassung

Muskel ist ein hochdynamisches und plastisches Gewebe, das sich durch Änderungen der Muskelmasse und der Fasertypzusammensetzung an unterschiedliche Belastungsbedingungen anpasst. Die Muskelmasse wird hauptsächlich durch Veränderungen der Proteinsynthese und des Proteinabbaus reguliert. Eine Verringerung der Proteinsynthese und / oder eine Zunahme des Proteinabbaus führt zu einer Verringerung der Proteinmenge und schließlich der Muskelmasse, was als Muskelatrophie bezeichnet wird. Im Muskel werden die meisten Proteine über zwei proteolytische Systeme abgebaut: das Ubiquitin-Proteasom-System (UPS) und den Autophagie-Lysosom-Weg (ALP). Muskel-RING-Finger-1 (MuRF1) ist eine E3-Ligase, die hauptsächlich im Muskel exprimiert wird und ein Hauptmediator der UPS-vermittelten Muskelatrophie ist. Kürzlich hat unsere Gruppe gezeigt, dass der Transkriptionsfaktor EB (TFEB) durch direkte Aktivierung der *Trim63*/MuRF1-Expression Muskelatrophie vermittelt. In diesem Zusammenhang haben wir zeigen können, dass die Proteinkinase D1 (PKD1) / Histondeacetylase 5 (HDAC5) / TFEB-Achse die Aktivität von TFEB und dadurch Muskelatrophie reguliert. Da TFEB zur Mikrophthalmie-Familie (MITF, TFEB, TFE3) von Transkriptionsfaktoren gehört, haben wir angenommen, dass nicht nur TFEB, sondern auch andere MITF-Familienmitglieder die Transkription von *Trim63* / MuRF1 regulieren. Desgleichen zeigen die Klasse IIa HDAC- und die PKD-Familie ein hohes Maß an Übereinstimmung in strukturellen, regulatorischen und funktionellen Eigenschaften. Daher untersuchte ich die Interaktion und funktionelle Bedeutung dieser drei Familien. Ich kann zeigen, dass Klasse IIa HDACs physikalisch mit TFEB und TFE3 interagieren und darüber deren transkriptionelle Aktivität gegenüber *Trim63*/MuRF1 direkt hemmen. Ich konnte auch zeigen, dass die gesamte PKD-Familie die HDAC-vermittelte Hemmung von TFEB und TFE3 aufhebt. Meine Daten implizieren einen neuen Mechanismus für die Kontrolle der Muskelatrophie über die PKD / HDAC / TFEB-TFE3-Achse. Darüber hinaus ist TFEB als Hauptregulator der lysosomalen Biogenese und Autophagie bekannt. Ob diese Funktion jedoch physiologische Auswirkungen auf die Skelettmuskulatur hat, ist weniger gut untersucht. Um diese Frage zu beantworten, führte ich muskelspezifische Funktionszu- und -abnahme-Experimente sowohl in vitro als auch in vivo durch. Wir haben dafür muskelspezifische *Tfeb* Knockout-Mäuse generiert und diese phänotypisiert. Wir konnten keinen Unterschied im ALP-vermittelten muskulären Proteinabbau zwischen den knockout- und Wildtyp-Tieren beobachten. Im in-vitro-Teil habe ich erfolgreich eine Retrovirus-basierte Strategie etabliert, um TFEB in C2C12-Muskelzellen stabil über zu exprimieren. Meine Ergebnisse implizieren, dass TFEB den ALP-vermittelten Proteinabbau in C2C12-Zellen nicht induziert. Obwohl die überwiegende Mehrheit der Studien zeigen, dass TFEB als Hauptregulator des ALP funktioniert, zeigen meine Daten, dass die sich Effekte von TFEB auf den ALP-vermittelten Proteinabbau zwischen Muskel- und Nicht-Muskelzellen unterscheiden. Zusätzlich konnte ich zeigen,

dass eine Überexpression von TFEB in C2C12-Myoblasten die Myoblastendifferenzierung verhindert, so dass diese Zellen in einem undifferenzierten Blastenstadium bleiben. Unter Verwendung eines Proteomics-basierten Ansatzes fanden wir, dass die TFEB-Überexpression zu einer Verringerung derjenigen Proteine führte, die für die Zell-Zell-Fusion und die cytoplasmatische Architektur verantwortlich sind, wie z. B. α -Actin, Actinin, muskelspezifisches Cadherin und die meisten Tropomyosin-Isoformen. Zusätzlich fanden wir eine erhöhte Menge des Proliferationsmarkers Ki67, was darauf hindeutet, dass die Überexpression von TFEB dazu führt, dass die C2C12-Zellen den Zellzyklus nicht verlassen können, um zu Myotuben zu differenzieren. Konsequenter Weise waren späte Differenzierungsmarker wie Myosin-Schwerkettenproteine in TFEB-behandelten C2C12-Zellen stark reduziert.

Zusammenfassend wirft meine Arbeit ein neues Licht auf die Regulation der MITF-Familie von Transkriptionsfaktoren in Myozyten und impliziert, dass TFEB an der myogenen Differenzierung beteiligt ist. Obwohl TFEB als Hauptregulator des ALP-vermittelten Proteinabbaus in Nicht-Myozyten bekannt ist, sprechen meine Daten für alternative Funktionen von TFEB in Myozyten.

1. Introduction

Muscle is one of the four primary tissues of the body. The muscle system is responsible for contraction and generation of active movement, resisting gravity to maintain posture, opening and movement of internal tracts and for generation of body heat. In the human body, there are three main types of muscle: smooth muscle, cardiac muscle, and skeletal muscle. Given that the main interest of this work is focused on skeletal muscle, this section is a detailed outline of the skeletal muscle.

1.1 Skeletal muscle

I. Structure and physiology

Skeletal muscle consists of a number of muscle fibers lying parallel to one another and are bundled together by connective tissue. In general, the number of individual muscle fibers determines muscle size. During development muscle fibers are formed by fusion of many smaller myocytes called myoblasts. Therefore, one striking feature is the presence of multiple nuclei in a single muscle fiber. The two most abundant proteins are actin and myosin comprising about 70-80 % of the total protein content of a single myofiber. Myosins assemble to form thick filaments, whereas thin filaments primarily consist of the protein actin. Three thick filaments surround each thin filament (Sherwood, L. Human physiology: From cells to systems, 2007).

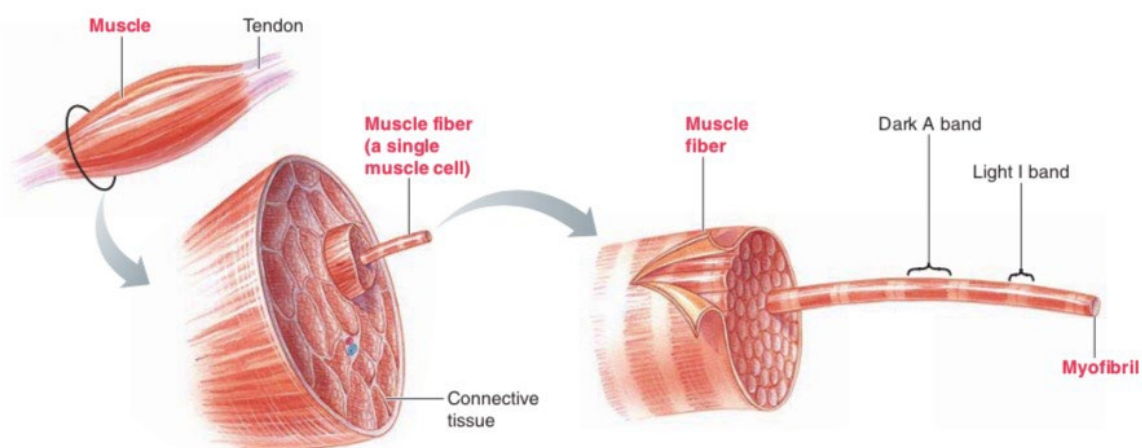


Fig. 1. Muscle structure. The smallest structural units of skeletal muscle are myofibrils. Myofibrils are specialized contractile elements consisting of thick and thin filaments. Several myofibrils are organized together to form muscle fibers. Eventually, a number of muscle fibers lying parallel to each other and bundled together by connective tissue form a skeletal muscle Modified from Sherwood, L. Human physiology: From cells to systems, 2007.

Myosin is the main molecular motor of muscle. A total of eleven sarcomeric myosin genes with their corresponding protein products have been described in mammals (Weiss *et al.*, 1999; Berg *et al.*, 2001; Desjardins *et al.*, 2002). A myosin molecule is a protein consisting of two identical subunits; the myosin tails are intertwined and two globular heads projecting out at one end. The myosin heads form the cross bridges between the thick and thin filaments. Two twisted strands of spherical actin, together with tropomyosin and troponin form thin filaments. Each actin molecule has a special binding site for attachment with the myosin cross bridge. This binding of myosin to actin molecules at the cross bridges results in energy-consuming contraction of the muscle fiber. However, in a state of a relaxed muscle fiber the position of tropomyosin and troponin prevents myosin to bind to actin. Tropomyosin molecules are threadlike proteins that lie end-to-end along the actin spiral. In this position, tropomyosin covers the actin sites that myosin binds to which prevents muscle contraction. Troponin is another thin filament; it is a protein complex made out of three subunits: troponin T binds to tropomyosin, troponin I to actin, and troponin C binds Ca^{2+} . The binding of troponin to Ca^{2+} results in a change of the ternary structure in a way that tropomyosin slips away from its blocking position allowing myosin binding to actin, hence muscle fiber contraction.

When viewed with an electron microscope, myofibers display alternating dark and light bands, these are A-bands and I-bands. The A-band is made up of a stacked set of thick filaments along with the portions of the thin filaments that overlap on both ends of the thick filament. I-band consist of the remaining portion of the thin filament that do not project into the A-band. In the middle of the I-band the dense Z-line is located. The area between two Z-lines is called a sarcomere, which is the functional unit of skeletal muscle. During growth, muscle increases in length by adding new sarcomeres, as opposed to an increase in the size of the sarcomeres. Not shown in the figure, single strands of a highly elastic and giant protein named titin, attaches to the sarcomere and to myosin helping to stabilize and align the thick filaments contributing to the mechanical and physiological properties of muscle (Sherwood, L. Human physiology: From cells to systems, 2007).

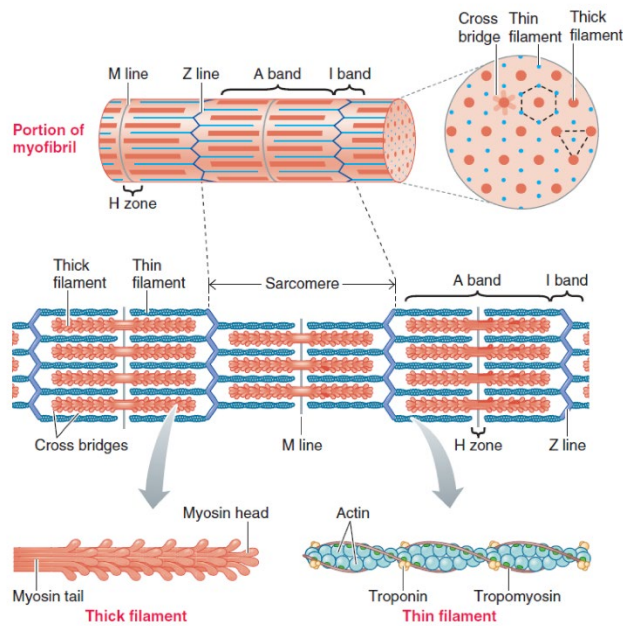


Fig. 2. Organization of myofibrils. Cross section of a myofibril. Myofibrils are assembled of repeated structures called sarcomeres, which is the basic and functional unit of muscle that allows contraction. The thin and thick filaments form partially overlapping layers giving the appearance of dark and light bands. A-bands, dark, are mainly thick filaments, whereas I-bands contain only thin filaments. Thick filaments are composed by the protein myosin. In the case of thin filaments, two twisted long chains of actin molecules are complemented with tropomyosin and troponin. Modified from Sherwood, L *Human physiology: From cells to systems*. 2007.

Another feature of muscle tissue is the abundance of mitochondria to accomplish the high-energy demands due to muscle contraction. Mitochondria form a three-dimensional network that generates the energy needed for muscle contraction and provides it to the sarcomeres. Some mitochondria are localized very close to the sarcolemma reducing the diffusion distance for oxygen transported from the capillaries. Another population of mitochondria is located in the inter-myofibrillar space. Number and size of mitochondria are plastic and depend on activity; an increase in the number of mitochondria was observed during endurance training. In the same way, aging impairs calcium release and muscle activation. This may contribute to muscle weakness in elderly people. Some congenital and acquired neuromuscular diseases and obesity are associated with abnormalities in the muscle mitochondrial network (Sherwood, L. *Human physiology: From cells to systems*, 2007).

Classified by their biochemical capacities, there are three major types of muscle fibers: slow-oxidative (type I), fast oxidative (type IIa) and fast-glycolytic (type IIb). The two main differences are their speed of contraction and the type of enzymatic machinery they primarily use for ATP formation (Sherwood, 2007). Fast fibers have higher myosin ATPase activity. Therefore, ATP can be converted fast resulting in a fast twitch of the myofiber. According to the ATP-synthesizing ability, fibers equipped with

oxidative phosphorylation yield more ATP than anaerobic glycolysis. Oxidative fibers are therefore more resistance to fatigue.

II. Muscle differentiation

During skeletal muscle development and muscle regeneration, myoblasts fuse to form multinucleated myofibers. The specialized skeletal muscles to be formed with different contractile and metabolic properties are determined by the activity of specific transcription factors, the myogenic regulatory factors (MRFs). In all the anatomical sites where skeletal muscle forms, determination and terminal differentiation of muscle are governed by four MRFs: myogenic factor 5 (MYF5), muscle-specific regulatory factor 4 (MRF4), myoblast determination protein (MYOD) and myogenin. All these factors seem to have specific functions within the process of myogenic differentiation. For example, MYOD and MYF5 are muscle-specific transcription factors and constitute a cross-regulatory transcriptional network responsible of muscle cell determination and myogenic differentiation (Braun and Gautel, 2011). In contrast, myogenin is essential for the terminal differentiation of committed myoblasts (Berkes and Tapscott, 2005).

Myoblast fusion requires cell recognition, migration, adhesion and membrane coalescence (Millay *et al.*, 2016). Cytoskeletal reorganization occurs before and after myoblast fusion, which has been demonstrated in several studies showing dynamic changes in murine myoblast fusion in vitro (Duan and Gallagher, 2009; Novak *et al.*, 2009). The best described signaling pathway involved in actin dynamics in mice is dependent on M-cadherin through a complex that mediates actin break down and recycling of the cell membrane as fusion proceeds (Charrasse *et al.*, 2007). In addition to actin, numerous other proteins with diverse cellular functions have been associated with myoblast fusion. However, besides myomaker, which is absolutely required for myoblast fusion in mice (Millay *et al.*, 2013; Millay *et al.*, 2016), none of these proteins is muscle-specific.

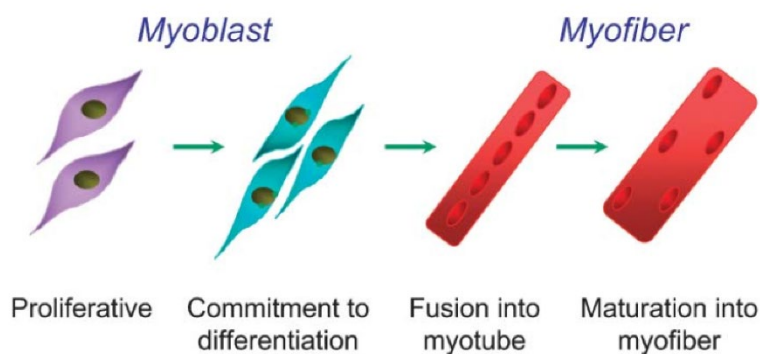


Fig. 3. Schema of myogenesis. Cell-derived myoblasts further proliferate, commit to differentiation and fuse to form myotubes, which then mature into myofibers. Modified from Zammit *et al.*, 2006

In different stages of differentiation, specific myosin heavy chain (MHC) isoforms are expressed. Therefore, these MHCs are utilized as late differentiation markers. Embryonic and slow MHC is the first myosin to be expressed (*MYH3*) (Schiaffino and Reggiani, 2011), fetal and neonatal fibers transiently express perinatal MHC (*MYH8*), while the adult myosin isoform is *MYH1*. Likewise, α -actin (*ACTA1*), is a part of the contractile apparatus, which can be used as a marker for the final stage of myogenesis.

III. Hypertrophy and atrophy

Muscle is a highly dynamic and plastic tissue that adapts to varying loading conditions by changes in muscle mass and fiber type composition. Muscle mass is mainly regulated by changes in protein synthesis and protein degradation. An increased protein synthesis or a decrease in protein degradation will lead to an increased protein content and hypertrophy. On the contrary, a decrease in protein synthesis and or an increase in protein degradation will lead to a reduction in protein and eventually muscle mass, which is called muscle atrophy. Both, atrophy and hypertrophy, occur in physiological conditions, as in a sedentary lifestyle, during and post pregnancy, after birth in the newborn and in response to exercise training. Or on the contrary, can be triggered by pathological conditions as in end-stage heart failure, end-stage renal disease, inflammation and neurological disorders (Goldberg, 1969; Du Bois *et al.*, 2015).

Muscle atrophy is an active process controlled by specific signaling pathways and transcriptional programs (Goldberg, 1969; Bodine *et al.*, 2001; Gomes *et al.*, 2001). Several studies revealed two novel muscle-specific ubiquitin ligases whose expression is relatively low in resting skeletal muscle but significantly increased within 24 h of inactivity. One E3 ligase identified was muscle RING-finger 1 (really interesting new gene 1, MuRF1/*Trim63*) (Bodine and Baehr, 2014). The other protein was an F-box domain protein, muscle atrophy F-box (MAFbx/*Fbxo32*/Atrogin-1). The two genes are selectively expressed in skeletal muscle and rapidly increased during muscle atrophy. Many functions of MuRF1 and Atrogin-1 in skeletal muscle continue to be investigated, but they are thought to involve the binding of selective substrates for ubiquitination and degradation by 26S proteasome (Bodine and Baehr, 2014). The importance of these atrophy genes in muscle wasting was confirmed by studies inducing muscle atrophy in transgenic mice. Specifically, atrogin-1/*Fbxo32* and MuRF1/*Trim63* knockout mice showed less denervation-induced muscle atrophy compared to wildtype mice (Baehr *et al.*, 2011) implicating that they are key factors for muscle atrophy.

1.2 Muscle remodeling

Most proteins are degraded via two proteolytic systems: the ubiquitin proteasome system (UPS) and the autophagy-lysosome pathway (ALP). In skeletal muscle and heart, these two systems are coordinately regulated to remove proteins and organelles in atrophying cells (Milan *et al.*, 2015).

I. Ubiquitin proteasome system

UPS-mediated proteolysis includes two essential steps: ubiquitination, which tags target proteins with a chain of ubiquitin molecules; and the degradation of ubiquitinated proteins by the proteasome.

Ubiquitin is the most studied modifier protein that can be covalently attached to the side chain of a lysine residue of a target protein via a process known as ubiquitination. The process of ubiquitin-mediated substrate delivery to 26S proteasomes starts with an activating enzyme, E1, that transfers ubiquitin to the E2 ubiquitin conjugating enzyme. The E2 transfers the ubiquitin to the substrate with the help of E3 enzymes. E3 enzymes are the rate limiting and specificity assuring enzymes in this cascade.

Once the to-be-removed protein is tagged with four or more ubiquitin moieties, it is recognized by the proteasome for degradation. The proteasome is a large multi-subunit protease found in the cytosol, both free and attached to the endoplasmic reticulum (ER) and in the nucleus of eukaryotic cells. Normally a functional proteasome consists of two subcomplexes: a 20S proteolytic core and two regulatory particles (19S) binding to 20S. Altogether forming the 26S proteasome. This structure recognizes ubiquitin-tagged proteins and transfers them to the catalytic core where they are degraded. The yield of this degradation process are small peptides that are re-used for synthesizing new proteins.

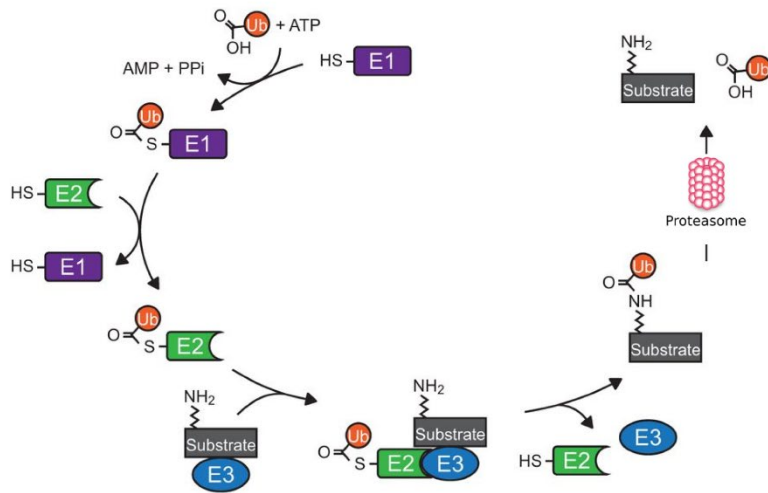
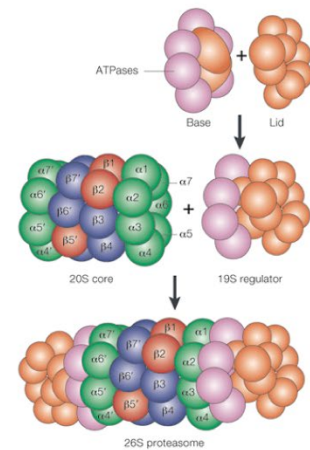
A**B**

Fig. 4. Ubiquitin proteasome system. A) Protein targeting for removal by ubiquitin requires the action of three hierarchically ordered enzymes: E1 activates ubiquitin, E2 acts as a carrier and E3, in last term, is in charge of transferring ubiquitin to the target protein. Modified from Li and Machner, 2017. **B)** Proteasome is a multiprotein complex containing one 20S subunit and two 19S regulatory cap subunits that associate with each end of the 20S core particle. Modified from Kloetzel, 2001.

II. Autophagy-lysosomal pathway

Autophagy is a fundamental and conserved protein and organelle degrading pathway that is characterized by the formation of double-layered vesicles, named autophagosomes, around intracellular cargo for delivery to lysosomes and proteolytic degradation. (Barth *et al.*, 2010). Quite distinct from endocytosis-mediated lysosomal degradation of extracellular and plasma membrane proteins, as autophagosomes engulf parts of the cytoplasm, autophagy is generally thought to be a non-selective degradation system. Remarkably, this is in contrast to the UPS, which specifically recognizes ubiquitinated proteins for proteasomal degradation (Mizushima, 2007). There are three types of autophagy: macroautophagy, microautophagy and chaperone-mediated autophagy. In general, the term autophagy refers to macroautophagy unless otherwise specified. Recently it has been demonstrated that autophagy plays a role many different physiological and pathological pathways, such as adaptation to starvation, intracellular and organelle clearance, anti-aging or cell death (Mizushima, 2005).

Autophagy consists of several sequential steps, such as sequestration, transport to lysosomes, degradation and utilization of degradation products, which are described here.

A. Autophagosome formation

Membrane dynamics during autophagy are highly conserved from yeast to plants and animals. In the first steps of autophagosome formation, cytoplasmic constituents are sequestered by a unique membrane called the phagophore, which is a flat organelle like a Golgi cisterna. Complete sequestration by the elongating phagophore results in formation of autophagosome, which is typically a double-membraned organelle (Mizushima, 2007).

Core proteins essential for autophagosome formation and lysosomal delivery of autophagic cargo are grouped by their functional and physical interactions into five complexes: (I) the Unc-51 like autophagy activating kinase (ULK) complex, (II) autophagy-related protein (ATG) 9, (III) class III PI3K complex, (IV) WD repeat domain phosphoinositide-interacting (WIPI) protein and their physical interaction partner ATG2 and (V) two ubiquitin-like proteins, ATG12 that conjugates with ATG5 and ATG8 family proteins (Dikic and Elazar, 2018). According to current understanding, phagophore formation involves activation of ULK1 complex and PI3K complex together with the recruitment of ATG9-containing vesicles, which may deliver additional lipids and proteins contributing to membrane expansion. The ATGs most prominently implicated in phagophore expansion are the Ub-like ATG8 family members, which is thought to occur on ER exit sites. The autophagosome undergoes maturation by a maturation process consisting of expansion and sealing of the phagophore, which involves gradual clearance of ATGs from the nascent autophagosome outer membrane and recruitment of the machinery responsible for lysosomal delivery and the machinery that mediates fusion with the lysosome (Dikic and Elazar, 2018). In the final degradation step, autophagosomes fuse with lysosomes where the inner membrane of autophagosome and the cytoplasm-derived materials contained in autophagosomes are then degraded by lysosomal hydrolases. Once macromolecules have been degraded, monomeric units as amino acids are exported to the cytosol for reuse (Mizushima, 2007). Although many ATG proteins are conserved between yeast and mammals, several mammalian-specific factors that modulate the functions of ATG proteins have been identified. Among them, the best studied is Beclin-1.

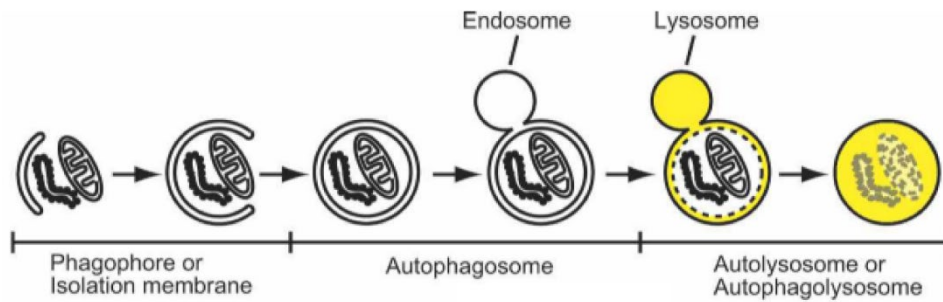


Fig. 5. The process of macroautophagy in mammalian cells. A portion of cytoplasm is enclosed by a phagophore to form an autophagosome. The outer membrane of the autophagosome subsequently fuses with the endosome and then the lysosome and the internal material is degraded. Modified from Mizushima, 2007.

B. Triggers of autophagy

Autophagy is an adaptive process that occurs in response to different forms of stress, including nutrient deprivation, growth factor depletion, infection and hypoxia. However, the most typical trigger of autophagy is nutrient deprivation. How cells sense amino acid concentration is not fully understood. Some reports point to the presence of other amino acid signaling pathways involving PI3-kinase and Beclin-1 (Mizushima, 2007). However, no matter the signal, an outcome of an inhibition of the master cell growth regulator serine/threonine kinase mechanistic target of rapamycin (mTOR) will always result in induction of autophagy.

ULK1-ATG13 complex is activated by autophosphorylation when it dissociates from mTOR under starvation conditions. Like ATG13-ULK complex, transcription factor EB (TFEB) was recently described as a master regulator that controls autophagy by directly activating mTOR (Di Malta *et al.*, 2017).

Other transcriptional regulators were also implicated in the regulation of autophagy in different systems. For example, the epigenetic reader bromodomain-containing protein 4 (BRD4) was reported to suppress the transcriptional program of genes needed for autophagosome biogenesis (Sakamaki *et al.*, 2017). Also FOXO proteins were shown to regulate autophagy in C2C12 muscle cells (Zhao *et al.*, 2007; Dikic and Elazar, 2018).

C. Monitoring autophagy

Autophagy is involved in several physiological and pathological processes. It is a dynamic and complicated process that requires dynamic rather than static measurements. Therefore, a scientific need to accurately identify, quantify and manipulate autophagy in cells aroused in

the last years. New techniques, including monitoring autophagy as a dynamic process and autophagy modulation, have been developed.

As described before, the process of autophagosome formation involves two major steps: nucleation and elongation of the isolation membrane. The ULK kinase complex is important for the nucleation step, whereas the ATG12-ATG8-conjugation systems are important for elongation step (Mizushima *et al.*, 2010). In mammalian cells, most of the ATG proteins are observed on isolated membranes (e.g., ULK1, ATG13, Beclin-1 or ATG12) but not on complete autophagosomes. However, only microtubule-associated protein light chain 3 (LC3), a mammalian homolog of yeast ATG8, is known to localize to autophagosomes, and therefore, this protein is widely used as marker for autophagosomes (Kabeya *et al.*, 2000; Mizushima *et al.*, 2004; Mizushima *et al.*, 2010).

Soon after synthesis, LC3 is processed at its C-terminus by ATG4 and becomes LC3-I. LC3-I is subsequently conjugated by phosphatidylethanolamine (PE) to become LC3-II. In contrast to the cytoplasmic localization of LC3-I, LC3-II associates with both the outer and inner membranes of the autophagosome. After fusion with the lysosome, LC3 on the outer membrane is cleaved off by ATG4, and LC3 on the inner membrane is degraded by lysosomal enzymes. Therefore, a useful method to quantitate the number of cellular autophagosomes is to track LC3-I to LC3-II conversion by immunoblotting. LC3-II usually correlates well with the number of autophagosomes (Kabeya *et al.*, 2000; Mizushima *et al.*, 2010).

However, a common misconception is the notion that increased numbers of autophagosomes in cells invariably correspond to increased cellular autophagy activity. Given that the autophagosome is an intermediate structure in a dynamic pathway, the number of autophagosomes observed at any specific time point is a function of the balance between the rate of their generation and the rate of their conversion into autolysosomes. Thus, autophagosome accumulation may represent either autophagy induction or suppression of steps in the autophagy pathway downstream of autophagosome formation. Different methods are often needed to distinguish between basal levels of autophagy, induction or suppression of either downstream or upstream steps of autophagy. The term “autophagy flux” is used to denote the dynamic process of autophagy synthesis and degradation of autophagic substrates (Mizushima *et al.*, 2010). Under these conditions, a biochemical assay coupled with an inhibitor of lysosomal activity by protease inhibitors such chloroquine or bafilomycin A will block autophagy in *in vitro* experiments by impairing autophagosome fusion with lysosomes rather than by affecting the acidity of this organelle as it was assumed for a long time (Mauthe *et al.*, 2018).

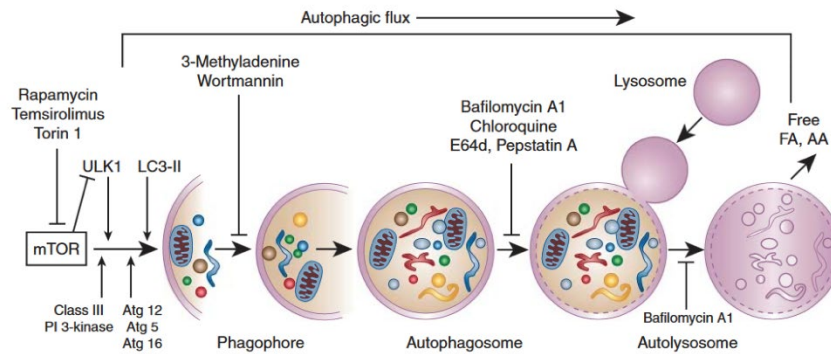


Fig. 6. Autophagy pathway and autophagic flux. Several lysosomal inhibitors as Bafilomycin A1, protease inhibitors and Chloroquine are used to block autophagy in different stages of autophagosome-lysosome fusion. On the other hand, Rapamycin and Torin-1 have been classically autophagy inducers. Modified from Kaushal, 2012.

Besides LC3, other autophagy substrates can be used to monitor autophagic flux. A change in the understanding of autophagy as a non-selective degradative pathway was recently made. Studies revealed that specific substrates are degraded preferentially by autophagy, of which the best studied example is p62/Sqstm1 (Mizushima *et al.*, 2010). P62 is selectively incorporated into autophagosomes through direct binding to LC3 and is efficiently degraded (Bjørkøy *et al.*, 2005). Thus, the amount of p62 in cells inversely correlates with autophagy activity. That is, p62 accumulates in autophagy-deficient cells (Mizushima and Yoshimori, 2007). Of note, it is not yet clear whether p62 is degraded through autophagy or partially through the UPS. Moreover, p62 can be transcriptionally regulated, which may complicate interpretation of p62 levels as an indicator for autophagy flux (Mizushima *et al.*, 2010).

III. UPS-Autophagy crosstalk

The fact that proteasome inhibition induces autophagy in many cell lines provides an indication for a connection between the two systems. Studies demonstrated a proteasome-to-autophagy shift to compensate for a reduced capacity in protein degradation. In 2009 Qiao and Zhang showed that inhibition of autophagy resulted in an increased proteasome activity in colon cancer cells, as indicated by an upregulation of proteolytic activity and expression of proteasome subunits. In another study performed in David Rubinsztein's group, no change in proteasomal activity was shown upon autophagic inhibition in HeLa cells. However, they monitored high levels of p62 that would sequester ubiquitinated proteins, hence delaying their shuttling towards the proteasome (Korolchuk *et al.*, 2009).

Besides the compensatory function of autophagy upon proteasome impairment, both systems interact through the mutual control of their key components in order to adjust the specific needs of the cell. For example, p62 mediates degradation of E3 ligases in oxidative stress response. In addition, p62 also sets a link between autophagy and proteasome-mediated protein degradation in DNA repair processes (Hewitt *et al.*, 2016). These findings suggest that p62 might function as a central stress sensor that mediates communication between UPS and autophagy. Moreover, LC3 can undergo proteasomal degradation as well. The most striking fact is that both degradation systems use ubiquitination as a labeling system for their substrates (Dikic, 2017). However, how the final destiny of the tagged substrate is decided, remains unclear.

1.3 MuRF1

Muscle RING finger proteins are striated muscle-specific proteins involved in regulation of muscle mass and cardiomyocyte development. MuRF1 contains a canonical N-terminal RING domain characteristic of RING-E3 ligases followed by a MuRF family conserved region, a zinc-finger domain (B-box), two leucine-rich coiled-coil domains, a COS-box and an acidic C-terminal tail (Foletta *et al.*, 2011). The RING finger domain has ubiquitin ligase capabilities, targeting sarcomeric proteins such as troponin I, titin and slow myosin heavy chain for degradation. This targeting occurs through the coordinated placement of polyubiquitin chains on these substrates, which, once four or more ubiquitin moieties have been attached to the substrate, are recognized by the proteasome and degraded (Willis *et al.*, 2009). MuRF1 specifically localizes to the M line in the sarcomere.



Fig. 7. Schematic diagram of MuRF1 protein structure and their potential protein-protein interaction domains. MuRF1 consists of 353 amino acids and contains a RING domain, a MuRF family conserved region (MFC), a B-box, two coiled-coiled regions (CC), a COS-box and an acidic tail (AT). Modified from Foletta *et al.*, 2011.

I. Transcriptional regulation

The expression of *MuRF1/Trim63* is regulated by transcription factors of the forkhead box (FoxO) protein family (Stitt *et al.*, 2004). The group of David Glass demonstrated that the insulin-like growth factor (IGF) / phosphoinositide 3-kinase (PI3K) / protein kinase B (Akt) pathway, which had previously been shown to induce hypertrophy (Bodine *et al.*, 2001), suppresses atrophy by down regulating *MuRF1*. Later, in 2008, Waddell and co-workers showed that FOXO transcription factors directly bind to the *MuRF1/Trim63* promoter. However, not all FOXO family members equally activate the FOXO binding motif in the *MuRF1/Trim63* promoter. In addition, they also described a palindromic glucocorticoid response element (GRE) in the proximal region of the *MuRF1/Trim63* promoter that directly binds the glucocorticoid receptor (GR) (Waddell *et al.*, 2008). They also showed that FOXO1 and an activated GR synergistically activate *MuRF1/Trim63* expression. These data explained how the synthetic glucocorticoid dexamethasone increases the expression of *MuRF1/Trim63*.

In parallel, myogenin was also shown to regulate muscle wasting. Myogenin, which is a basic helix-loop-helix (bHLH) transcription factor and an essential MRFs for skeletal development, regulates both muscle development and neurogenic atrophy. Moresi and colleagues found that adult mice lacking myogenin are resistant to denervation induced muscle atrophy. In this case, *myogenin*-knockout mice failed to up-regulate *MuRF1* indicating that *MuRF1* is transcriptionally regulated by myogenin (Moresi *et al.*, 2010).

1.4 MiTF/TFE family members of transcription factors

The MiTF/TFE family of basic helix-loop-helix leucine zipper transcription factors (bHLH-LZ) encodes four family members: MiTF, TFE3, TFEB, and TFEC. All of them share the same structure of protein domains that include three critically important regions. The basic motif binds to specific areas of DNA while the helix-loop-helix and leucine-zipper motifs are critical for their dimerization (Steingrímsson *et al.*, 2002; Martina *et al.*, 2014). Every family member is able to regulate gene expression by its binding to the DNA consensus sequence known as E-box (CANNTG, where N means any of the four nucleobases) located in the promoter region of their downstream target genes. Efficient DNA-binding and successful transcriptional activation of target genes requires dimerization, either homo- or heterodimerization. However, a dimerization with other bHLH-LZ-containing proteins such as, FOXO or MYC, has not been observed so far. The roles of TFEB-family members in the development and proliferation of specific tissues is well described. There is also evidence that the MiTF/TFE family is involved in nutrient sensing and maintenance of cellular homeostasis.

MiTF is predominantly expressed in melanocytes, osteoclasts, mast cells, macrophages, NK cells, B cells and heart, whereas TFE3 and TFEB are expressed ubiquitously and in multiple cell types

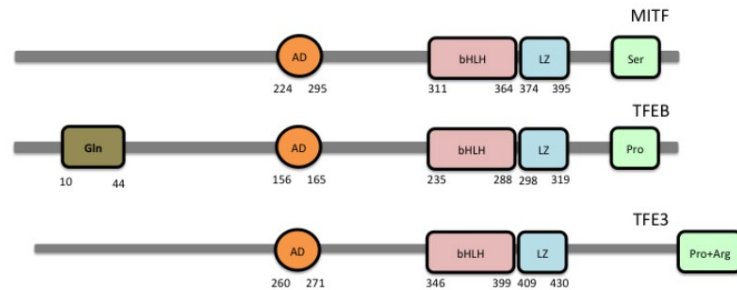


Fig. 8. MiTF/TFE family members structure. The entire family members share common structural characteristics. **AD**: transactivation domain, **bHLH**: basic-helix-loop-helix domain, **Gln**: glutamine rich region, **LZ**: leucine zipper region, **Pro**: proline rich region, **Pro + Arg**: proline + arginine rich region, **Ser**: serine rich region. Modified from Nabar and Kehrl, 2017.

I. Transcription factor EB

TFEB was shown to be essential in the signal transduction processes required for normal vascularization of the placenta. *Tfeb* knockout mice die at embryonic day E9.5-10.5 because defective placental vascularization (Steingrimsson *et al.*, 1998).

TFEB was shown to directly bind to CLEAR elements in the promoter region of TFEB target genes regulating their expression (Palmieri *et al.*, 2011; Sardiello *et al.*, 2009). The CLEAR network, Coordinated Lysosomal Expression and Regulation, is a specific network of genes that contain one or more copies of the regulatory motif GTCACGTGAC in their promoter. The CLEAR network is comprised of several classes of genes, including genes that belong to the lysosomal complex and genes that participate in lysosomal biogenesis and function (Sardiello and Ballabio, 2009). TFEB overexpression results in an increased number of lysosomes and higher levels of lysosomal enzymes, enhancing thus lysosomal activity. Hence, TFEB was characterized as a master regulator of lysosomal function (Sardiello *et al.*, 2009).

Many other genes not involved in lysosomal biogenesis are also controlled by TFEB. For example, genes involved in autophagy (Palmieri *et al.*, 2011). TFEB induces the biogenesis of autophagosomes (Settembre and Ballabio, 2011) and clearance of lipid droplets and damaged mitochondria (Nezich *et al.*, 2015; Mansueto *et al.*, 2017). Altogether, TFEB coordinates a transcriptional program able to control the main cellular degradative pathways and to promote intracellular clearance. In line with the role of TFEB in degradative pathways, our group demonstrated recently that TFEB is involved in muscle

remodeling by directly activating MuRF1/*Trim63* expression. Therefore, inducing proteasome-mediated protein degradation in muscle (Du Bois *et al.*, 2015).

Importantly, TFEB does not regulate the basal transcription of its targets but rather their expression levels in response to environmental cues. In resting cells, under nutrient-rich conditions, TFEB is mostly cytosolic and inactive (Sardiello *et al.*, 2009 and Settembre *et al.*, 2011). Upon starvation or condition of lysosomal dysfunction, TFEB rapidly translocates to the nucleus and activates the transcription of its target genes. In sufficiently fed cells, the kinase complex mTOR phosphorylates TFEB at several serine/threonine residues, including serine 211 and serine 142 (Settembre and Ballabio, 2011; Martina *et al.*, 2012). Phosphorylated S211 functions as a binding site for the cytosolic chaperone protein 14-3-3, which keeps TFEB sequestered in the cytosol probably through masking its nuclear transport signal (Roczniak-Ferguson *et al.*, 2012). When nutrient levels are low, mTOR is inactivated, 14-3-3 dissociates from TFEB, and TFEB is free to translocate into the nucleus. Therefore, TFEB is involved in the transcriptional regulation of starvation-induced autophagy and lysosomal biogenesis (Settembre *et al.*, 2011). Because the promoter region of TFEB contains a CLEAR element, it enhances its own expression as well. This auto-regulatory feedback loop is particularly relevant to achieve a sustained response under prolonged starvation conditions (Martina *et al.*, 2014).

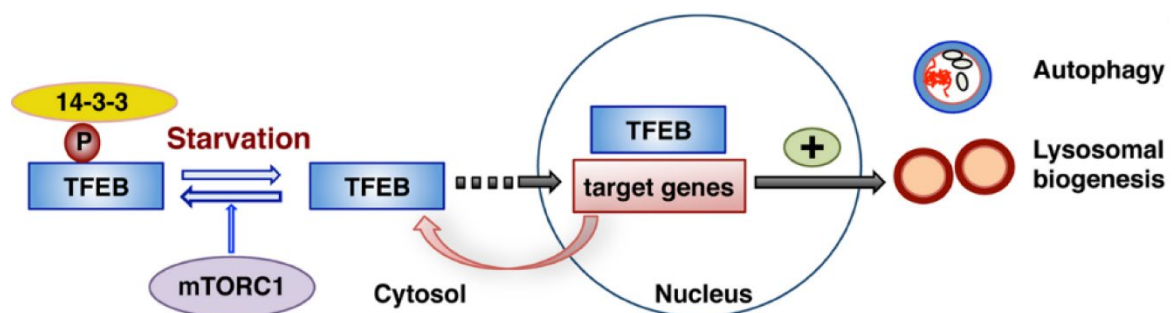


Fig. 9. Model of TFEB function and regulation of lysosomal biogenesis and autophagy. TFEB plays a critical role in the adaptation of cells to nutrient deprivation. TFEB translocates to the nucleus under starvation conditions to promote autophagy and lysosomal biogenesis. At the same time, TFEB auto-regulatory feedback loop (pink arrow) results in increased TFEB levels under prolonged starvation conditions. Modified from Martina *et al.*, 2014.

II. Transcription factor 3

TFE3 is, as TFEB, a ubiquitously expressed protein that regulates expression of target genes through binding to E-boxes in their promoter region. TFE3 was identified as a protein that binds to the mE3 motif within the immunoglobulin heavy-chain enhancer and was implicated in humoral immunity

(Beckmann *et al.*, 1990). TFE3 shares important roles in osteoclast development with MiTF, where both proteins are functionally redundant (Steingrímsson *et al.*, 1998). Its subcellular localization is also regulated by mTOR-mediated phosphorylation and involves serine residues that are conserved in TFEB and TFE3 (S321) (Martina *et al.*, 2012; Roczniak-Ferguson *et al.*, 2012).

Recent evidence suggests that TFEB may not be the only member of the MiTF/TFE family involved in nutrient sensing, since amino acid sequence alignment revealed that the domain binding between TFEB and 14-3-3 is also present in TFE3. Meaning, these transcription factors may share the same mechanism of activation (Peña-Lopis *et al.*, 2011; Martina and Puertollano, 2013). Investigators showed that TFE3 also binds CLEAR elements and induces lysosomal biogenesis and autophagy upon activation (Martina *et al.*, 2014). Although TFEB and TFE3 are partially redundant in terms of their ability to induce lysosomal biogenesis in response to starvation, both must be present for a maximal response (Martina *et al.*, 2014).

III. Microphthalmia-associated transcription factor

To date, nine MiTF isoforms have been described (Bharti *et al.*, 2008; Steingrímsson, 1998). The MiTF isoforms differ in their amino-terminal regions, and their alternative promoters mediating tissue-dependent expression. In contrast with the rest of family members, MiTF is predominantly expressed in melanocytes, osteoclasts, mast cells, macrophages, NK cells and B cells (Martina *et al.*, 2014). MiTF is critical for the development and differentiation of neural crest-derived melanocytes and retinal pigmented epithelium.

The participation of MiTF in lysosomal biogenesis is less clear partially due to the multiple different isoforms of MiTF. Microarray based analyses showed a strong correlation between the expression of one of the MiTF variants enriched in melanoma and some lysosomal genes containing CLEAR elements (Ploper *et al.*, 2015). However, it is thought that the ability of MiTF/TFE family members to heterodimerize with each other may influence the relative contributions of MiTF to lysosomal gene expression.

1.5 Histone deacetylases

Posttranslational modifications of histones, for example, plays a crucial role in disease development by modulating gene transcription. The histone deacetylases (HDAC) are a class of histone modification enzymes that remove acetyl groups from lysine residues on histones. In addition, HDACs deacetylate numerous non-histone substrates that govern a wide array of biological processes,

basically because their repressive influence in transcription (Li and Seto, 2016). 18 human HDACs, which are grouped in four classes, have been described so far. There are two classes of HDACs that can be distinguished by their structures and expression patterns. Class I HDACs (HDAC1, HDAC2 and HDAC3) are ubiquitously expressed and are mainly composed of a catalytic domain. In contrast, class II HDACs (HDAC4, HDAC5, HDAC7 and HDAC9) display more restricted expression patterns and contain an N-terminal extension (Vega *et al.*, 2004). HDAC5 and HDAC9 are highly enriched in muscle, HDAC4 in brain and some part of the skeleton and HDAC7 is enriched in endothelial cells and T-cell precursor (Haberland *et al.*, 2009).

Histone acetylation has been implicated in denervation-dependent changes in skeletal muscle gene expression. Mice lacking HDAC4 and HDAC5 in skeletal muscle fail to up-regulate myogenin and also preserve muscle mass following denervation. Both HDACs are upregulated in skeletal muscle upon denervation (Moresi *et al.*, 2010).

Subcellular localization and activity of class II HDACs is regulated by phosphorylation. Indeed, protein kinase D (PKD) phosphorylates class II HDACs on the serine residues that mediate nuclear export via binding of the 14-3-3 chaperone. Nuclear export of class II HDAC then relieves their repression activity towards transcription factors, such as MEF2 (Fielitz *et al.*, 2008; Kim *et al.*, 2008).

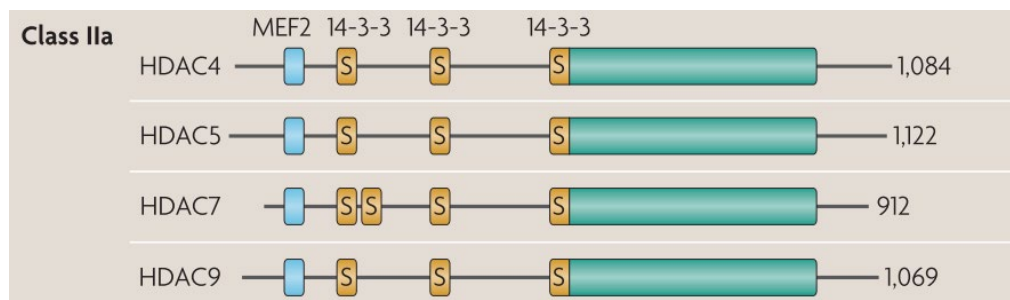


Fig. 10. Class IIa histone deacetylase (HDAC) members. Green rectangles indicate the conserved HDAC domain; numbers following HDAC domain indicate number of amino acids. Myocyte enhancer factor 2 (MEF-2)-binding sites, marked by a blue square. Sites for the 14-3-3 chaperone protein binding are also shown. Modified from Haberland *et al.*, 2009.

1.6 Protein kinase D family

Protein kinase D (PKD) is an evolutionary conserved stress dependent serine/threonine protein kinase family with structural, enzymological, and regulatory properties different from the protein kinase C (PKC) family members. PKD1, the most studied member of the family, is implicated in the

regulation of a complex array of fundamental biological processes, including signal transduction, cell proliferation and differentiation, membrane trafficking, secretion, immune regulation, cardiac hypertrophy, angiogenesis and cancer (Ha *et al.*, 2009; Rozengurt *et al.*, 2005; Rozengurt, 2011; Sundram *et al.*, 2011).

PKD1 directly binds to and phosphorylates HDAC5 promoting its nuclear export. This mechanism is involved in the pathophysiology of cardiomyocyte hypertrophy *in vitro* and cardiac hypertrophy and remodeling *in vivo* (Vega *et al.*, 2004; Fielitz *et al.*, 2008). Our laboratory described that PKD1 regulates muscle atrophy through the Angiotensin II/PKD1/HDAC5/TFEB axis; PKD1 phosphorylates HDAC5 and mediates binding of 14-3-3, which leads to nuclear export of HDAC5. Absence of HDAC5 relieves repression of TFEB causing an increase in *Trim63*/MuRF1 expression which in turn results in an increased protein degradation in skeletal muscle (Du Bois *et al.*, 2015).

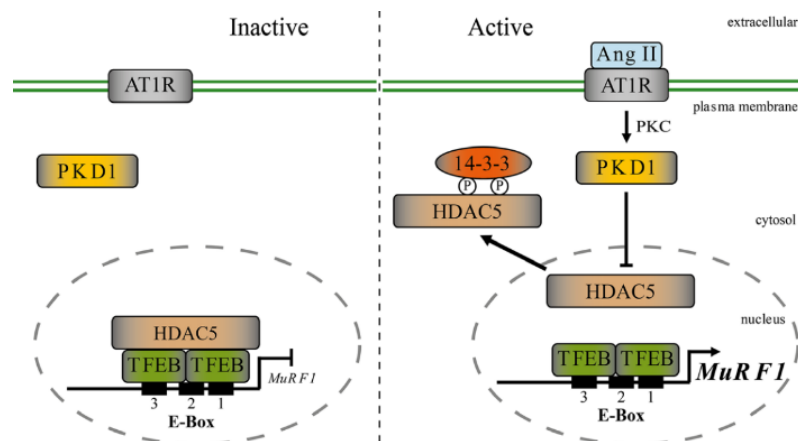


Fig. 11. Ang II/PKD1/HDAC5 signaling pathway regulates TFEB-mediated MuRF1 expression. The PKD1/HDAC5/TFEB/MuRF1 axis mediates angiotensin II-induced skeletal muscle atrophy. Nuclear TFEB specifically binds to E-boxes 1, 2 and 3 of the MuRF1 promoter. PKD1 together with HDAC5 controls TFEB activity over MuRF1. Modified from Du Bois *et al.*, 2015.

2. Aim of the study

In this study, we wanted to bring insight in the role of TFEB in muscle remodeling by investigating TFEB activity in the two protein degrading pathways, the UPS and ALP, in skeletal muscle. Given that TFEB belongs to the family of MiTF-transcription factors consisting of other members, in the first part of the project, we hypothesized that TFEB shares its transcriptional activity towards *Trim63* with other MiTF-family members. Similarly, class IIa HDACs and PKDs belong to respective families with close structural and regulatory properties. Therefore, we aimed to investigate their functional significance in muscle remodeling of the PKD/HDAC/TFEB-TFE3 axis.

Most proteins are degraded via two proteolytic systems: the UPS and the ALP, and TFEB is known as a master regulator of lysosomal biogenesis and autophagy. Thus, in the second part, we investigated the role of TFEB involvement in ALP-mediated protein degradation in skeletal muscle by performing gain- and loss-of-function experiments *in vivo* and *in vitro*.

3. Material and Methods

3.1 Plasmids and Vectors

I. Plasmids

The cDNA expression plasmids used in this work and their source are listed in Table 1.

Table 1. cDNA expression plasmids.

Vector name	Insert	Backbone	Tag	Rereference
Hs_ <i>Trim63</i> -luc	Human MuRF1 promoter	pGL3-Basic	None	Du Bois <i>et al.</i> , 2015
FLAG-HDAC4	Full length human <i>HDAC4</i>	pcDNA™3.1 (+)	N-FLAG	Vega <i>et al.</i> , 2004
FLAG-HDAC5	Full length human <i>HDAC5</i>	pcDNA™3.1 (+)	N-FLAG	Song <i>et al.</i> , 2006
FLAG-HDAC7	Full length human <i>HDAC7</i>	pcDNA™3.1 (+)	N-FLAG	Chang <i>et al.</i> , 2006
HDAC5-Myc deletion mutants	Diverse indicated deletion mutants of human <i>HDAC5</i>	pcDNA™3.1 (+)	C-Myc	Song <i>et al.</i> , 2006
FLAG-Tfeb	Full length mouse isoform 1 Transcription Factor EB	pcDNA™3.1 (+)	N-FLAG	Du Bois <i>et al.</i> , 2015
Tfeb-Myc/His	Full length mouse isoform 1 Transcription Factor EB	pcDNA™3.1 (+)	C-Myc	Du Bois <i>et al.</i> , 2015
Myc-PRKD1	Full length human <i>PKD1</i>	pcDNA™3.1 (+)	C-Myc	Kim <i>et al.</i> , 2008
FLAG-PRKD2	Full length human <i>PKD2</i>	pcDNA™3.1 (+)	N-FLAG	Prof. Jens Fielitz, unpublished
FLAG-PRKD3	Full length human <i>PKD3</i>	pcDNA™3.1 (+)	N-Flag	Prof. Jens Fielitz, unpublished
pMP71-IRES eGFP	IRES eGFP	pMP71	-	Dr. Franziska Schmidt, unpublished
pMP71-Tfeb IRES eGFP	IRES eGFP and full length isoform 1 Tfeb	pMP71	N-Flag	Dr. Franziska Schmidt, unpublished

Material and Methods

II. Transformation

All bacteria transformations for cDNA expression plasmids and retroviral plasmids were performed in XL-1Blue electrocompetent cells (Stratagene). DNA was purified using the NucleoBond® Xtra Maxi DNA purification kit (Macherey-Nagel GmbH & Co. KG) according to manufacturer's protocol.

3.2 Cell Culture

Cell culture work was performed under sterile and aseptic conditions. Every cell line was kept in an incubator (Thermo Fisher Scientific) with the standard conditions of 37°C temperature, 5% CO₂ and 95% humidity.

I. Gelatin Coating

In order to ensure proper cell attachment during immunostaining methods, chambered cover slips (μ -Slide 8 Well chambers; ibidi GmbH) and glass coverslips contained in 6-well plates (BD Falcon™) were to gelatin coated. For that, a final 0.2% gelatin working solution was prepared diluting the corresponding amount from the stock 2% gelatin (Sigma-Aldrich®) in sterile PBS (PAA). The 0.2% gelatin solution was poured into the well and incubated for 20 min at room temperature. Afterwards, the excess of gelatin solution was aspirated, and plates were used for seeding.

II. COS7

The monkey kidney fibroblast-like cell line COS7 (ATCC® CRL-1651™) was cultured in standard cell culture conditions using Dulbecco's Modified Eagle Medium (DMEM) 4.5 g/l glucose (Sigma-Aldrich®), L-Glutamine (Sigma-Aldrich®), 10% fetal bovine serum (Biochrom GmbH) and 1% Penicillin-Streptomycin (Sigma-Aldrich®).

Cells were splitted every 2-3 days before reaching confluency with 2 ml of Trypsin-EDTA (Sigma-Aldrich®). Subcultivation ratio of 1:5 to 1:10 was routinely used.

For cryopreservation, cells were counted after trypsinization and resuspended in freeze medium consisting of 90% FBS and 10% DMSO (Carl Roth GmbH + Co. KG). 1 ml aliquots of $1 \cdot 10^6$ cell/ml were set in Cryovial® tubes (Simport), placed in a Cryofreezing container (Nalgene™, Thermo Fisher Scientific) and transferred and stored -80°C for 48h and before they were placed into tanks with liquid nitrogen tanks for long-term storage.

Material and Methods

A. Transfection

COS7 cells were transfected with FuGENE[®]6 (Promega) transfection reagent according to the manufacturers protocol. Transfection was performed at ~70% confluency using a 1:3 DNA:FuGENE[®]6 ratio.

B. Measurements of luciferase and fluorescence signals

The Luciferase Assay System (Promega) was used to quantify gene expression with reporter gene constructs. In this assay, COS7 cells were seed (section II.A) in a 24-well plate in duplicates and transfected with the indicated expression plasmids. 24 h after transfection cells were rinsed with ice-cold PBS and lysed with 200 μ L Luciferase Cell Culture Lysis Reagent (Promega) at -80°C. To pellet cell debris, lysates were collected and centrifuged at 1000g for 3 min. For luciferase activity, 50 μ L of lysate supernatant was pipetted in triplicates into 96-well plates and placed into the luminometer (FluorStar Optima, BMG-Labtech). The injector automatically added 50 μ L Luciferase Assay Reagent per well and immediately read and recorded relative light units (RLU).

To correct for differences in protein loading, the expression of LacZ was quantitated. For that, 10 μ L lysate was analyzed with FluoReporter[®] *lacZ*/Galactosidase Quantification Kit (Invitrogen[™], Thermo Fisher Scientific) according to manufacturer's instructions. Fluorescence values of the *lacZ*/Galactosidase assay were used to normalize luciferase values of each individual sample.

C. Co-Immunoprecipitation (Co-IP)

COS7 cells were transfected with FuGENE[®]6 (Promega) transfection reagent according to the manufacturers protocol. 24 h after transfection (Section II.A), 200 μ L lysis buffer was added to the cells and incubated for 10 min. Cells were harvested with the help of a cell scraper, transferred to a 1.5 ml Eppendorf tube and incubated further for 30 min at 4°C in a rotating shaker. Afterwards, cell debris was pelleted by centrifugation and discarded, and the remaining supernatant was used for further analysis. 40 μ L of the lysate (20%) was collected from the lysate as input control. The remaining supernatant was filled up with lysate buffer to a total volume of 1 ml. For immunoprecipitation, 30 μ L of PBS-washed glycerol-free ANTI-FLAG M2 affinity gel (Sigma-Aldrich[®]) was added to each sample and the mixture was incubated for 4 h incubation at 4°C in a rotating shaker. Afterwards, the ANTI-FLAG M2 affinity gel was pelleted by centrifugation and the supernatant was discarded. Then the affinity gel was washed for 5 times using phosphate buffer. The elution of proteins bound to the affinity gel was performed using 60 μ L of 2x SDS-PAGE Sample

Material and Methods

Buffer and boiled for 5 min at 95°C. The sample buffer-protein mixture was stored at -20°C and used for further analysis.

Table 2. Buffers used in Co-Immunoprecipitation

Buffer	Composition
Phosphate buffer	150 mM Phosphate Buffer 150 mM NaCl + H ₂ O
Lysis Buffer	1x Protease Inhibitor 0.5% Triton X100 + Phosphate Buffer

III. Plat-E cells for retrovirus production

Platinum-E (Plat-E, Cell Biolabs, Inc.) is a potent retrovirus packaging cell line based on the 293T line, designed for transient production of high-titer ecotropic retrovirus. Plat-E cells were handled and treated in standard conditions (Section II). Culture medium consisted of DMEM 4.5 g/l glucose with 1% L-Glutamine (Sigma-Aldrich®) supplemented with 10% FBS, 1 µg/ml Puromycin (Sigma-Aldrich®), 10 µg/ml Blastidin (Thermo Fisher Scientific) and 1% Penicillin-Streptavidin.

A. Transfection of Plat-E cells

Transfection of Plat-E cells was performed with Lipofectamine®3000 (Invitrogen™, Thermo Fisher Scientific) with a working DNA:reagent ratio of 1:2, according to manufacturer's instructions.

B. Retrovirus production

48 h after transfection, virus-containing supernatant was collected and filtered using 0.45-µm Minisart® filter (Sartorius AG) to prevent Plat-E cells contamination. For large-scale virus production the supernatant was concentrated with Lenti-X Concentrator (Clontech) following manufacturer's instructions. The resulting virus-containing pellet was resuspended in 1 ml sterile PBS, aliquoted and store at -80°C. Retroviral titer was determined by flow cytometry GFP detection (BD

Material and Methods

FACSCanto™ II, BD Biosciences) using a dilution series of virus transduced cells. Adequate negative and positive controls were used in order to determine the correct FACS gating conditions.

VI. C2C12 myoblast cell line

The mouse myoblast cell line C2C12 (ATCC® CRL-1772™) was used for myocyte specific analyses. This cell line differentiates into mature myotubes, forming contractile proteins and producing characteristic muscle proteins (Yaffe and Saxel, 1977). C2C12 cells were cultivated and kept under ~80% confluency in order to maintain their ability to differentiate. C2C12 cells were handled and treated according to the standard cell culture conditions (Section II).

A. Cultivation and differentiation of C2C12 cells

The base medium for C2C12 cells, growing medium, consisted of DMEM 1 g/l glucose, 1% L-Glutamine (Sigma-Aldrich®), 10% FBS and 1% Penicillin-Streptomycin.

For differentiation, C2C12 myoblasts were trypsinized and plated in the desired plate format ($1.5 \cdot 10^6$ cells/well in 6-well plates or $7 \cdot 10^3$ cells/well in the case of μ -Slide 8 Well chamber). Differentiation was routinely induced after 48 h of plating, once the cells had reached 100% confluency, by the change from growing to differentiation medium. Differentiation medium consisted of DMEM 1 g/l glucose, 1% L-Glutamine, 1% FBS and 1% Penicillin-Streptomycin. To obtain completely differentiated myotubes, culture medium was replaced daily for 5 to 7 consecutive days.

B. Starvation and Chloroquine treatment

C2C12 myoblasts and differentiated myotubes were treated equally for starvation experiments. Depending on the experimental requirements, growth medium was replaced with PBS or serum-free growth medium and cultures were incubated for different time points (1-14 h) before cell harvest.

Chloroquine (Sigma-Aldrich®) was used as an autophagosome-lysosome fusion inhibitor to quantify autophagic flux. For every individual experiment, a chloroquine working solution was freshly prepared by dissolving the solid reagent in sterile H₂O and used at a final concentration of 50 μ M for 2 h in cell culture.

Material and Methods

C. Transfection

Prior to transfection, C2C12 cells were cultivated in growing medium without antibiotics for at least 24 h. Transfection of C2C12 cells was performed at 60% confluence by using Lipofectamine[®]3000 in a 1:2 DNA:reagent ratio, according to manufacturer's instructions. Samples were analyzed 24 h or 48 h after transfection as indicated.

D. Retroviral transduction

Myoblast were plated 24 h prior to viral infection at a confluency of ~20% in full growth medium. The infection mix was prepared with the needed retroviral particles to reach a multiplicity of infection (MOI) of 0.7. Additionally, infection mix contained Polybrene (Santa Cruz Biotechnology, Inc.) at a final concentration of 6 µg/µl and growing medium until complete infection volume. Cells were treated with the retroviral infection mix (e.g. 2 ml/well for 6-well plate format), the plates were sealed with Parafilm[®] (Bemis Company, Inc.) and centrifuged at 800 g for 90 min at a temperature of 32°C (Beckman Coulter[®]). After centrifugation, medium was replaced with fresh growing medium and cells incubated for indicated time points (usually 24 to 72 h).

E. siRNA Transfection

Synthetic small interfering RNA (siRNA) targeting *Tfeb* was used in order to block TFEB expression in muscle cells (ON-TargetPlus SMARTpool, Dharmacon). After careful optimization, a concentration of 100 nM siRNA was chosen as an optimal working concentration. The day before siRNA transfection, C2C12 myoblast were plated at a confluency of ~20% in antibiotic free growing medium. The corresponding ON-TARGETplus Non-targeting siRNA Pool was used as a negative control. All transfections were performed in triplicates following DharmaFECT manufacturer's instructions (Dharmacon).

3.3 TFEB knockout mice

I. Generation

The *Tfeb*^{loxp/loxp} (C57BL/6) mouse strain used in this research project was created from mice previously reported using a targeted allele and ES cell line from EUCOMM (Settembre *et al.*, 2011). We used *Tfeb*^{fl/fl} mice to generate mice with a muscle-specific deletion of *Tfeb* using Pax7-Cre mice (C57BL/6), which express the Cre recombinase under the control of the *Pax7* promoter (Griger *et al.*, 2017). Since Pax7, and therefore the CRE recombinase, is only expressed in the muscle cell lineage *Tfeb* was deleted in all muscle cells. *Tfeb*^{loxp/+;Pax7-Cre} and *Tfeb*^{loxp/+} were intercrossed to obtain muscle specific *Tfeb* knockout mice (*Tfeb*^{loxp/loxp;Pax7-Cre}) and littermate controls (*Tfeb*^{loxp/loxp}).

II. Isolation of muscle and organs from adult mice

All animal procedures were performed in accordance with the guidelines of the Max-Delbrück Center for Molecular Medicine and the Charité-Universitätsmedizin Berlin, and were approved by the Landesamt für Gesundheit und Soziales (LAGeSo, Berlin, Germany) for the use of laboratory animals and the Max-Delbrück Center for Molecular Medicine (X 9005/17), and followed the current version of German Law on the Protection of Animals. Adult mice were sacrificed by cervical dislocation. Organs and tissues were dissected and prepared. Isolated organs were washed in ice cold sterile PBS, immediately flash frozen in liquid nitrogen and stored at -80°C until usage.

3.4 Immunofluorescence

I. Immunostaining protocol

Cells were plated in 6-well plates on sterile coverslips or 8-well chamber μ -Slides. In both cases, wells were gelatin-coated prior to plating of the cells (Section I). At the experimental end point, cells were PBS-washed, fixed in 3.7% formaldehyde (FA) (Sigma- Aldrich®) for 10 min followed by 3x PBS washing steps, 1 ml for 5 min.

For immunostaining, coverslips were transferred to a dark incubation wet chamber. μ -Slide 8 Well samples were treated directly in the chamber. For every staining procedure, permeabilization and blocking was carried out in a single step with the following buffer: 0.3% Triton X-100, 0.5% goat serum (abcam) in PBS for at least 1 h at RT. Afterwards, cells were incubated with primary antibody at its working concentration (Table 3) diluted in blocking buffer at 4°C overnight. The next day, cells were washed 3 times with PBS before addition of the appropriate secondary antibody. Secondary antibodies

Material and Methods

conjugated with Alexa Fluor® were diluted in PBS and incubated for 2 h at RT. At last, samples were washed 3 times with PBS, followed by a final DNA staining step using PBS solution with 1:10.000 DAPI. Finally, coverslips were mounted on glass slides using Pro Long Gold Antifade mountant (Thermo Fisher Scientific), dried and stored in the dark at 4°C until imaging. The μ -Slide 8 Well chambers were kept in the dark in PBS at 4°C until imaging.

II. Antibody list

Table 3. List and working dilution of antibodies used in this study

Antibody	Host species	Provider	Cat. No.	Dilution	
				WB	IF
Primary				WB	IF
anti- α Actin	Mouse	Sigma-Aldrich	A3853	1:1000	
anti-DYKDDDDK (Flag Tag)	Rabbit	Cell Signaling Technology	2368	1:1000	1:1000
anti-Myc	Rabbit	Millipore	06-549	1:500	1:500
anti-MyH3	Mouse	Santa Cruz Biotechnology	sc-53091	1:500	1:100
anti-My32	Mouse	Sigma-Aldrich	M4276	1:500	1:200
anti-LC3	Rabbit	Cell Signaling Technology	2775s	1:500	1:500
anti-p62 (C-term specific)	Guinea Pig	Progen Biotechnik	GP62-C	1:1000	1:500
Secondary				WB	IF
anti-Mouse IgG-HRP	Horse	Cell Signaling Technology	7076	1:2000	
anti-Rabbit IgG-HRP	Horse	Cell Signaling Technology	7074	1:2000	
anti-Rabbit IgG-Alexa Fluor® 555	Goat	Invitrogen™, Thermo Fisher Scientific	A-21428		1:1000
anti-Rabbit IgG-Alexa Fluor® 488	Goat	Invitrogen™, Thermo Fisher Scientific	A-11034		1:1000
anti-Mouse IgG-Alexa Fluor® 555	Goat	Invitrogen™, Thermo Fisher Scientific	A-21422		1:1000
anti-Mouse IgG-Alexa Fluor® 488	Goat	Invitrogen™, Thermo Fisher Scientific	A-11001		1:1000

Material and Methods

III. Image acquisition and analysis

A. Routine cell culture image acquisition

Routine bright field and fluorescence cell imaging was performed using an inverted light microscope EVOS®FL Imaging System (Thermo Fisher Scientific) with 10x and 20x magnification objectives (my gratitude to the laboratory of Prof. S. Spuler, ECRC).

B. Confocal imaging

Multi-channel fluorescence images and Z-Stack scanning of immunostained fixed samples were acquired with the Zeiss LSM 700 confocal microscope (Carl Zeiss), mostly with 40x and 63x immersion oil objectives (my gratitude to the laboratory of Prof. S. Spuler, ECRC).

C. Image processing and analysis

All figures were prepared in Adobe Illustrator CC (Version 21.0.2). Digital images from immunofluorescence staining were processed with ZEN 2009 (Zeiss) and Fiji software (Schindelin *et al.*, 2012). Image brightness and contrast were modified to a better visualization of printed version. All images corresponding to the same figure were together and equally treated.

3.5 Protein Analysis

I. Preparation of protein lysates

Cultured cells were rinsed with 2 ml PBS and afterwards treated with 200 µL radioimmunoprecipitation assay buffer (RIPA lysis buffer) (Table 4), scraped from the bottom of the well with the help of a cell scraper, transferred to a 1.5 ml microcentrifuge tube and incubated on ice for 20 min. Tubes were then spun at 150.000 rpm at 4°C for 15 min to pellet cell debris. The protein-containing supernatant was either directly used for further analysis or stored at -80°C until usage.

II. SDS-PAGE and immunoblotting

Protein lysates were supplemented with the corresponding amount of 4x Laemmli buffer (Table 4) to the final concentration of 1x and boiled at 98°C for 5 min. 10 to 20 µl of the lysate were loaded onto 8% or 10% poly-acrylamide gels, resolved under denaturing conditions (Running Buffer, table 4) by SDS-PAGE and blotted (Transfer Buffer, table 4) onto Amersham Hybond P 0.45 µm PVDF membranes (GE Healthcare Life Sciences).

Material and Methods

After blotting, membranes were incubated with the corresponding blocking solution (5% bovine serum albumin (BSA)/ 1x Tris-buffered saline- 0.1% Tween 20 complemented (TBS-T) or 5% Milk/TBS-T), according to the needs of the specific antibody, for at least 1 h at RT. Subsequently membranes were incubated overnight at 4°C with its corresponding antibody and working dilution in blocking solution. The next day, membranes were washed 5 times in TBS-T for 10 min and incubated with the corresponding HRP-conjugated secondary antibody for 2 h at RT. The immunoblot signal was detected with SuperSignal™ West Pico PLUS Chemiluminescent Substrate (Thermo Fisher Scientific) and membranes processed using Curix 60CP (Agfa-Gevaert N.V.) in different exposure times.

Table 4. List and composition of buffers needed for Western Blot

RIPA Buffer	50 mM Tris HCl, pH 7.4 150 mM NaCl 1% NP-40 0.5% Sodium deoxycholate 0.1% SDS 1 mM EDTA in H ₂ O + 1x cOmplete™ EDTA-free Protease inhibitor*
4x Laemmli sample Buffer	12% SDS 25% Glycerol 150 mM Tris HCl pH 1 0.03% Bromophenol Blue 20% β-mercaptoethanol*
10x Tris-Glycine	30 g Tris Base 144 g Glycine + 1000 ml H ₂ O
Running Buffer	1x Tris-Glycine 10% SDS in H ₂ O
Transfer Buffer	1x Tris-Glycine 10% MeOH in H ₂ O
TBS-T	20 mM Tris Base 150 mM NaCl 0.1% Tween ® 20 in H ₂ O

*Freshly added before use

Material and Methods

III. Densitometric quantification

Developed films were scanned (HP Scanjet G4050) and the specific signals were determined from the image format TIFF by Fiji (Schindelin *et al.*, 2012). The optical density of each specific protein band (signal), as well as background of each individual film, were detected. Background values were subtracted from the corresponding protein band yielding a specific protein signal for each sample. To correct for differences in loading, this individual protein quantity was normalized to a reference protein, such as GAPDH or Actin.

IV. Proteomics

A. Generation of samples

Proteins were obtained by lysis of cells (~300.000 cells) in 0.5 % sodium dodecyl sulphate in 50mM Hepes, pH8.5, with 1X cOmplete protease inhibitor cocktail-EDTA (Merck). Cell solutions not exceeding 5.000 cells per μ l PBS were mixed with an equal volume of lysis buffer and heated at 95°C for 5 min according to Hughes *et al.*, 2014. To degrade chromatin, mixtures were incubated with 15.6 U benzonase (Novagen) for 30 min at 37°C. Protein concentrations were estimated with a bicinchoninic acid (BCA) assay (Pierce, Thermo Fisher Scientific).

B. Proteomic analysis

4 μ g of total protein from each sample were incubated with 2.5 mM Dithiothreitol (DTT) ultrapure, (Invitrogen, Thermo Fisher Scientific) for 30 min at 37 °C to reduce disulfide bonds. Subsequently protein was alkylated by addition of 10 mM iodoacetamide (Merck) for 15 min at 37°C. Afterwards, peptide extracts were prepared by an optimized SP3 protocol (Sielaff *et al.*, 2017). Briefly, protein was mixed with the magnetic SP3 beads in a ratio 1: 2 (w/v), and acetonitrile (ACN) was added to a final concentration of 70 %. The bead bound protein was washed two times with 70 % ethanol (200 μ l) before 180 μ l ACN was added. All supernatants were discarded. To prepare the protein for proteolysis at alkaline pH, 10 μ l ammonium bicarbonate (20 mM) was added. Proteolysis was obtained by digestion with trypsin (Promega) at a protease to protein ratio 1: 25 overnight at 37°C. The tryptic digestion was stopped by adding ACN to a final concentration of 95 %. After removal of the supernatant, bead bound peptides were washed again with ACN before elution in 2 % DMSO. Subsequent LC-MS/MS analyses were performed according to Kindt *et al.*, 2017. In detail, chromatographic separation of tryptic peptides was achieved on a reverse phase nano-Acquity UPLC column (1.7 μ m, 100 μ m i.d. \times 100 mm, Waters GmbH) using a 90 min non-linear gradient ranging from 2 to 60% ACN in 0.1% acetic acid at a flow rate of 400 nl/min. The nano-LC column was interfaced using electro spray ionization to an LTQ-Orbitrap Velos mass spectrometer (Thermo

Material and Methods

Fisher Scientific). Precursor ions of m/z range 325–1525 ($r=30.000$) were subjected to data dependent MS/MS fragmentation of top-20 peaks in the ion trap at a collision induced energy (CID) of 35%. Repetitive MS/MS acquisition was avoided by setting a dynamic exclusion of 60 s for already selected precursors.

Data analysis was carried out by MaxQuant (vs 1.5.3.8) software package developed by Jürgen Cox and Matthias Mann (Max Planck Institute of Biochemistry, Planegg, Germany) using the in-built Andromeda search engine. Spectra were matched against the Uniprot Sprot mouse database version 2018_05 using the following settings: precursor mass tolerance: 20 ppm, fragment mass tolerance: 0.5 Da, trypsin as cleavage enzyme, 1 missed cleavage, variable modification: oxidation on methionine and acetylation at the protein N-terminus, static modification: carbamidomethylation on cysteine residuals. Amino acid sequences identified at a false discovery rate (FDR) < 1% were annotated and only razor (Occam's razor principle) and unique peptides were used to calculate protein intensities.

For relative quantitation of protein abundance across samples the MaxQuant normalized Label Free Quantification (LFQ) intensities were used. All statistical tests were carried out in Genedata Analyst v 11.0.1 (GeneData) with log₁₀ transformed protein intensities. A two-groups Welch's t-test with multiple test correction (Benjamini Hochberg (BH)) was used to identify differences dependent on (i) TFEB expression level and (ii) the differentiation state of the cells. A nominal p-value, a BH corrected q-value and protein ratios (ratio of protein abundance in TFEB- and control-virus transduced cells) were calculated. For our analyses we used a p-value of < 0.05, and a protein ratio of < 0.5 and > 2.0 for calculation. N-way ANOVA was used for multiple group comparisons.

(Section IV gently provided by Dr. Elke Hammer, University Greifswald)

3.6 mRNA Analysis

I. RNA Isolation and cDNA synthesis

A. Tissue homogenization and lysis

To homogenize tissue samples from mice, 50 to 100 mg of tissue was transferred to a homogenization tube containing ceramic beads (Precellys® ceramic beads kit, Thermo Fisher Scientific) with 1 ml TRIzol™ Reagent (Invitrogen, Thermo Fisher Scientific). Samples were homogenized in a FastPrep-24 homogenizer for 3 cycles of 30 sec at a speed setting of 6.0 (MP Biomedicals, LLC.). Samples were placed on ice for 5 min between cycles and the lysate was transferred to a 1.5 ml Eppendorf® safe-lock microcentrifuge tube (Eppendorf AG).

Material and Methods

B. Cell lysis

Treated cells were typically plated in 6-well plates when prepared for RNA isolation. Culturing medium was removed, and the cell monolayer was washed with ice cold PBS. 1 ml TRIzol™ Reagent (Invitrogen, Thermo Fisher Scientific) was added directly to the cells and the cells were incubated on ice for 5 min before transferring trizol-lysate into a 1.5 Eppendorf® safe-lock microcentrifuge tube.

C. RNA isolation

200 µl chloroform (Carl Roth GmbH + Co. KG) was added to the Trizol-lysate mixture followed by 3 min incubation at room temperature and centrifugation for 15 min at 12.000g at 4°C. The aqueous phase containing RNA was obtained and transferred to a fresh Eppendorf tube. 500 µl isopropanol (Carl Roth GmbH + Co. KG) was added and spun at 12.000 g at 4°C for 20 min to precipitate RNA. In a final step, RNA pellets were washed with 1 ml ice-cold 80% ethanol and air-dried before resuspension in 20 µl of RNase-free water. The RNA yield and quality were measured using NanoDrop™ 2000 (Thermo Fisher Scientific).

D. cDNA synthesis

1 µg of high purity RNA was used as a template for cDNA synthesis using SuperScript® II Reverse Transcriptase-First Strand synthesis system with random hexamer primers (Invitrogen, Thermo Fisher Scientific), as indicated in the manufacturer's protocol. After cDNA synthesis, the removal of RNA template was achieved by incubation with RNase H (Sigma-Aldrich®) for 20 min at 37°C. cDNA was directly used for qRT-PCR, kept at 4°C or long-term stored at -20°C.

II. Quantitative Real Time PCR

1-2 ng of cDNA sample was routinely used as template for SYBR-based (FastStart Universal SYBR Green Master, Roche) quantitative real-time PCR. Three technical replicates per sample and primers pair used were performed. PCR was run in a StepOnePlus™ System (Applied Biosystem, Thermo Fisher Scientific) using 96-well plates and a standard running protocol. Expression levels were calculated using a standard curve and correlated to *Gapdh* expression to correct variances between samples. Data analysis was performed with StepOne Software v2.3 (Life Technologies, Thermo Fisher Scientific) and

Material and Methods

Excel (Microsoft Corporation). Displayed graphs were designed with GraphPad Prism 7 (GraphPad Software, Inc.).

Table 5. List of qRT PCR primers

Target	Forward (5'— 3')	Reverse (3'— 5')
<i>Atp9b</i>	AGGGCACAGCTCTAAGTTC	AGGTTGGCAAGGAAGGCT
<i>Atp6v0d1</i>	GCCATTCTGGTGGACACAC	TTTCGGATTATCTCGATGTTCA
<i>Atp6v1b2</i>	CGCTGATGTGTCTAACCAGTTG	CAGGTAAGGAGATCATCTGAGG
<i>Gapdh</i>	ATGGTGAAGGTCGGTGTGA	AATCTCCACTTTGCCACTGC
<i>Hexa</i>	ACTGGCACTTGGTGGACG	CCGAAGCCTTGCGTATTCA
<i>Malp1lc3b</i>	CGTCCTGGACAAGACCAAGT	ATTGCTGTCCCGAATGTCTC
<i>Mcoln1</i>	GCCATCTTCTATGCTGTGG	CACCACGGACATAGGCAT
<i>Myod</i>	AGCACTACAGTGGCGACTCA	GGCCGCTGTAATCCATCA
<i>Myog</i>	GCGATCTCCGCTACAGAGG	GCTGTGGGAGTTGCATTCA
<i>Myomaxin</i>	CCGTCGGATGTCAAGACAAC	GAGAGTAGAGGTCTCCAAGG
<i>Lamp1</i>	ACGATGCCTTCGAGGAGTT	CTGTCCTGAAGGGCCTGA
<i>Sqstm1</i>	AGACCCCTCACAGGAAGGAC	CATCTGGGAGAGGGACTCAA
<i>Tfeb</i>	GAGCTGGGAATGCTGATCC	CTTGAGGATGGTGCCTTTGT
<i>Tfe3</i>	AGCCTCCCAATATCACTG	CGCCTCTCTGTTCTCTG
<i>Trim63</i>	TGACATCTACAAGCAGGAGTGC	TCGTCTCGTGTTCTTGC
<i>Myomaker</i>	ATCGCTACCAAGAGGCGTT	CACAGCACAGACAAACCAGG
<i>Uvrug</i>	TCTGCTTACAGCTCAAGTCC	ATGATGGAGAGGGCGGAT
<i>Wipi1</i>	CGGCTACATGGGAAAGATG	CAGAGAAGTTCAGGCGTCCT

3.7 Statistics

All the experiments were performed at least three times. Values were expressed as mean \pm SEM. Statistical analysis was performed with unpaired Student's *t*-test using GraphPad Prism7 (GraphPad Software, Inc.) and Excel 2016 (Microsoft). *P* values less than 0.05 were considered statistically significant (**P* < 0.05; ***P* < 0.01; ****P* < 0.001).

4. Results

4.1 Role of MiTF/TFE family members in MuRF1 induction

I. Microphthalmia-associated transcription factor family (MiTF/TFE) members TFEB and TFE3 transcriptionally regulate *Trim63*-expression

In order to confirm that TFEB increases the expression of *Trim63* (MuRF1), I performed luciferase assays using *Trim63*-reporter gene constructs. As previously shown by our group, TFEB induced the *Trim63*/MuRF1 promoter in a dose-dependent manner (Fig. 12, A). Because TFEB belongs to the MiTF family (MiTF/TFE), I hypothesized that TFEB shares its transcriptional activity towards *Trim63* with the other family members. TFEB was initially described to be the only MiTF/TFE-family member binding to CLEAR elements in the promoter region of genes leading to an activation of gene expression (Palmieri *et al.*, 2011; Sardiello *et al.*, 2009). Recently also TFE3, like TFEB, was found to regulate gene expression through its ability to bind to E-box elements in CLEAR consensus sequences (Martina *et al.*, 2014).

To test if TFE3 induces *Trim63*/MuRF1 promoter, I performed luciferase reporter assays. I transfected COS7 cells with a reporter construct harboring the MuRF1 promoter and increasing amounts of a control vector or a TFE3 or MiTF containing cDNA expression plasmid. I observed that TFE3 increased *Trim63* expression within the range of ~30-50-fold activation compared to control-vector transfected samples (Fig. 12, B). On the contrary, even high doses of MiTF did not increase the *Trim63* expression (Fig. 12, C).

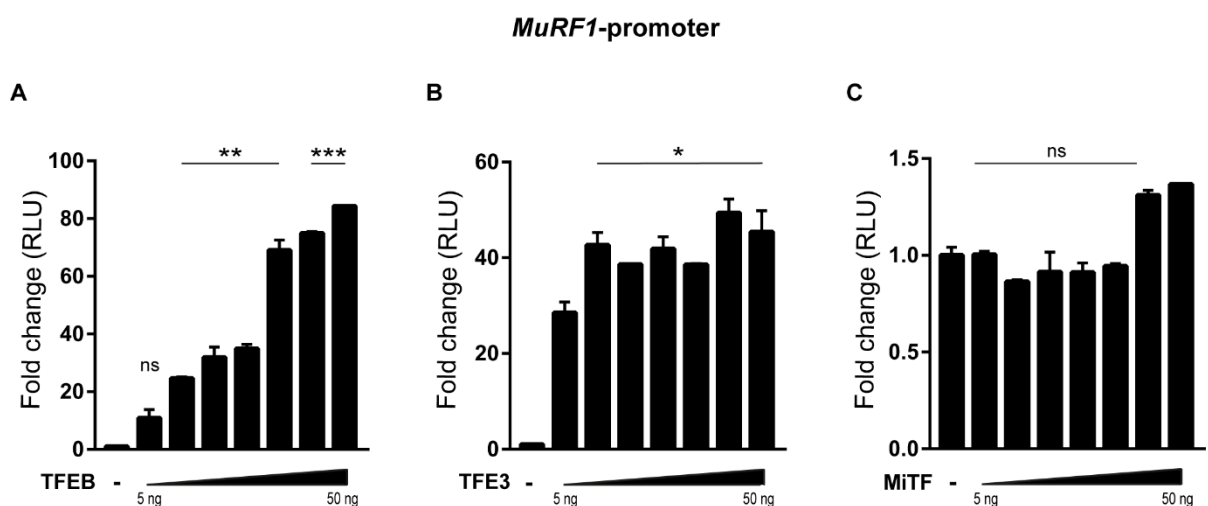


Fig 12. *Tfeb* and *Tfe3* increase *Trim63*-expression. MuRF1 promoter activity was measured by luciferase reporter assay. COS7 cells were cotransfected with human *MuRF1* promoter-luciferase reporter construct, pCMV-LacZ and increasing amounts of cDNA expression plasmids containing wild type *Tfeb* (A), *Tfe3* (B) or *Mitf* (C). Luciferase values normalized to pMV-LacZ. Bars show luciferase activity in relative luciferase units (RLU) expressed as fold-change versus cells transfected with control plasmid. Values are mean \pm SEM. * $p \leq 0.05$, ** $p \leq 0.01$, *** $p \leq 0.001$, ns= not significant (Student's T-test).

Results

II. Class IIa Histone deacetylases inhibit TFEB and TFE3 mediated increase in MuRF1 expression

It was previously reported that the class IIa histone deacetylases (HDACs), HDAC4 and HDAC5, inhibit the activity of the bHLH transcription factor myogenin that regulates MuRF1 expression (Moresi *et al.*, 2010). Consequently, we also demonstrated that TFEB physically interacts with HDAC5, that Tfeb and HDAC5 colocalized in myocytes *in vitro* and that HDAC5 inhibited TFEB-mediated MuRF1 expression (Du Bois *et al.*, 2015).

Based on these data, I hypothesized that not only HDAC5, but also HDAC4 and HDAC7 interact with TFEB and inhibit its transcriptional activity.

To test this hypothesis, I transfected COS7 cells with the MuRF1-reporter construct, a TFEB-FLAG containing cDNA expression plasmid and increasing amounts of HDAC4, HDAC5 and HDAC7. I transfected a *lacZ* containing plasmid in parallel and used the fluorescence values of the *lacZ*/Galactosidase assay to normalize the luciferase data. As shown in figure 13, TFEB increased *Trim63* expression. Increasing amounts of HDAC4 (Fig. 13, A), HDAC5 (Fig. 13, B) or HDAC7 (Fig. 13, C) inhibited TFEB-induced *Trim63* expression.

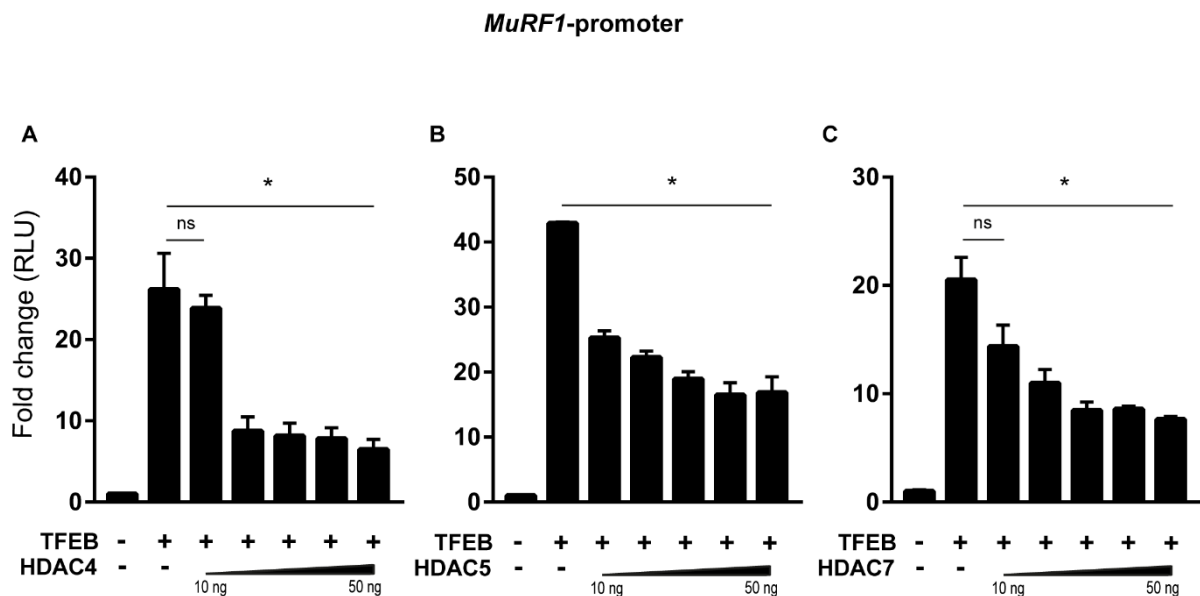


Fig 13. Class IIa HDAC family members inhibit TFEB-mediated MuRF1 expression. Luciferase activity was measured in COS7 cells coexpressing human *MuRF1* promoter-luciferase reporter construct with wild type *Tfeb*-FLAG and increasing amounts of *HDAC4* (A), *HDAC5* (B) or *HDAC7* (C). Luciferase values were normalized to pMV-LacZ. Bars show luciferase activity in relative luciferase units (RLU) expressed as fold change versus cells transfected with *Tfeb*-FLAG. Values are mean \pm SEM. * $p \leq 0.05$, ** $p \leq 0.01$, *** $p \leq 0.001$, ns= not significant (Student's T-test).

Because TFE3 belongs to the same family of bHLH transcription factors as TFEB, I hypothesized that the class IIa HDACs inhibit the activity of TFE3. Similarly, I transfected COS7 cells with the MuRF1-reporter construct, a TFE3-FLAG containing plasmid and increasing amounts of HDAC4, HDAC5 and

Results

HDAC7. Consistent with the results observed in TFE3, TFE3 increased the MuRF1 expression and addition of HDAC5, HDAC4 and HDAC7 inhibited this effect indicating that HDAC4, HDAC5 and HDAC7 negatively regulate TFE3-induced MuRF1 expression (Fig. 14).

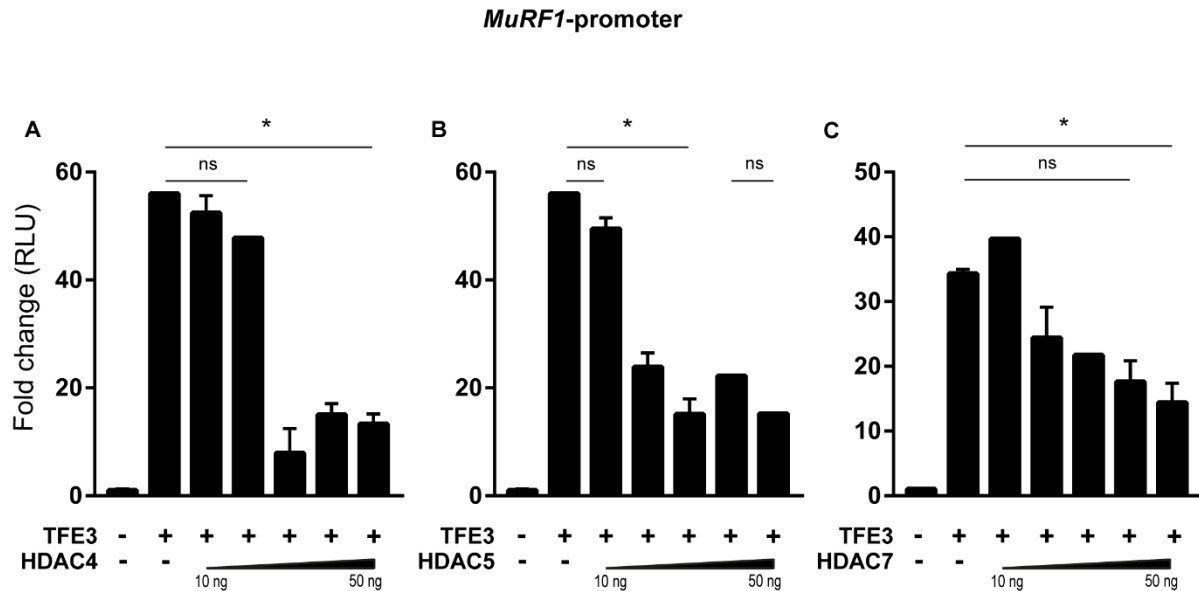


Fig 14. Class IIa HDAC family members inhibit TFE3-mediated MuRF1 expression. Luciferase activity measured in COS7 cells coexpressing human *MuRF1* promoter-luciferase reporter construct with *Tfe3*-FLAG and an increasing amount of *HDAC4* (A), *HDAC5* (B) or *HDAC7* (C). Luciferase values were normalized to pMV-LacZ. Bars show luciferase activity in relative luciferase units (RLU) expressed as fold change versus cells transfected with *Tfe3*-FLAG. Values are mean \pm SEM. * $p \leq 0.05$, ** $p \leq 0.01$, *** $p \leq 0.001$, ns= not significant (Student's T-test).

III. Protein kinase D family members attenuate HDAC mediated inhibition of TFEB- and TFE3-induced MuRF1 expression

We previously reported that the stress responsive serine/threonine kinase protein kinase D1 (PKD1) facilitates HDAC5 nuclear export, removing inhibition of TFEB and thereby increasing MuRF1 expression (Du Bois *et al.*, 2015). Therefore, I hypothesized that PKD1 also causes nuclear export of HDAC4 and HDAC7 which would relieve HDAC4 and HDAC7-mediated inhibition of TFEB.

To test this hypothesis and to investigate changes in subcellular localization of HDAC4, HDAC5 and HDAC7 I performed immunocytochemistry on transfected COS7 cells. As shown in Fig. 15, overexpressed TFEB colocalized with HDAC4, HDAC5 and HDAC7 in the nucleus (Fig 15, upper panel). However, when cotransfected with PKD1, HDAC4, HDAC5 and HDAC7 translocated to the cytoplasm whereas TFEB remained in the nucleus. PKD1 phosphorylates HDACs at several residues promoting sequestration of HDAC in the cytosol in a CRM1-dependent manner (Du Bois *et al.*, 2015; Vega *et al.*, 2004; Zhang *et al.*, 2002).

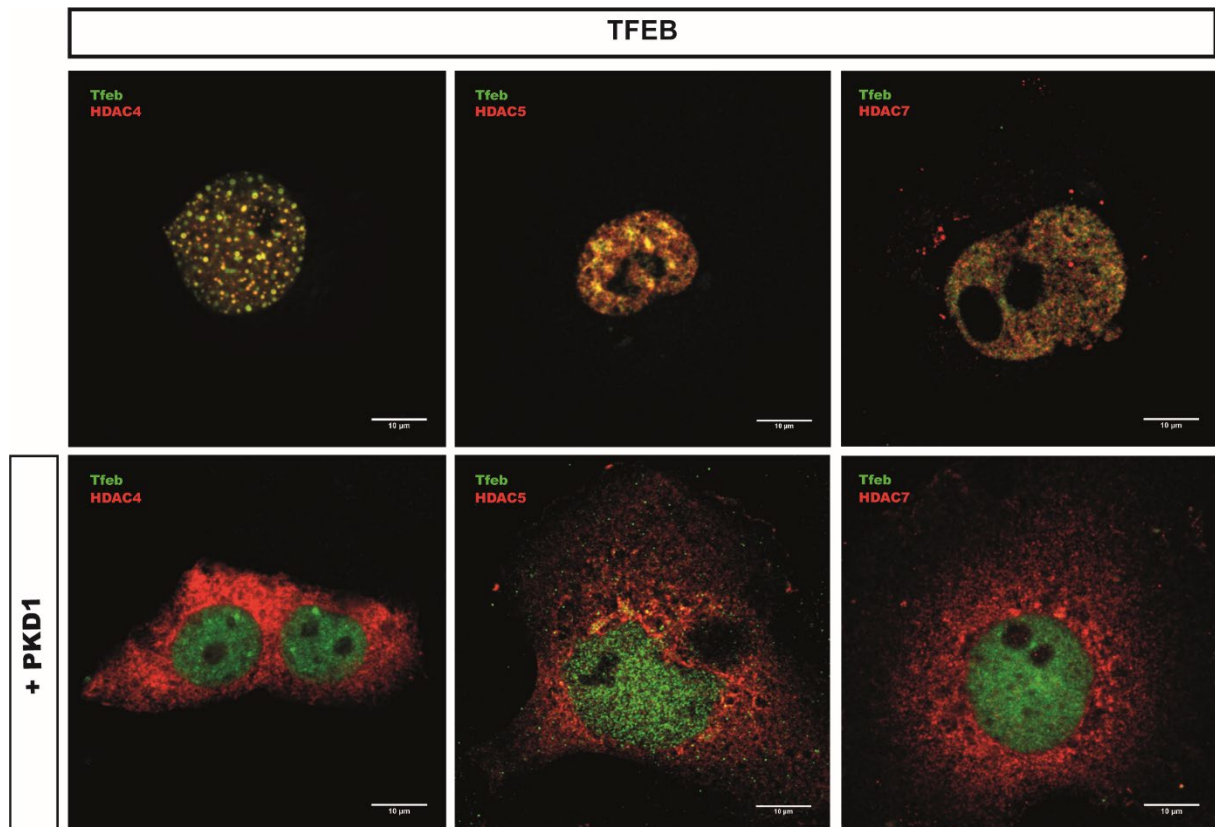


Fig 15. PKD1 promotes nuclear export of class IIa HDAC. COS7 cells were cotransfected with FLAG-TFEB, HDAC-Myc with or without PKD1-HA and double-stained against FLAG and Myc. Subcellular localization was analyzed by immunofluorescence confocal microscopy. Scale bars, 10 μ m. Images are representative of three independent experiments.

To determine if the dissociation between TFEB and HDAC4, HDAC5 and HDAC7 relieves the inhibitory effects of HDACs towards TFEB, I performed a luciferase-based reported gene assay. Moreover, because it is well known that PKD belongs to a family of kinases that share structural characteristics (Hayashi *et al.*, 1999), I reasoned that PKD2 and PKD3 have similar effects towards class IIa HDACs as PKD1. To investigate the effects of PKD1, PKD2 and PKD3 on HDAC mediated inhibition of the transcriptional activity of TFEB, I performed further luciferase assays (Fig. 16). I transfected COS7 cells with the MuRF1-luciferase reporter in combination with TFEB, HDAC4 (Fig. 16, A), HDAC5 (Fig. 16, B) or HDAC7 (Fig. 16, C) and in combination with PKD1, PKD2 or PKD3.

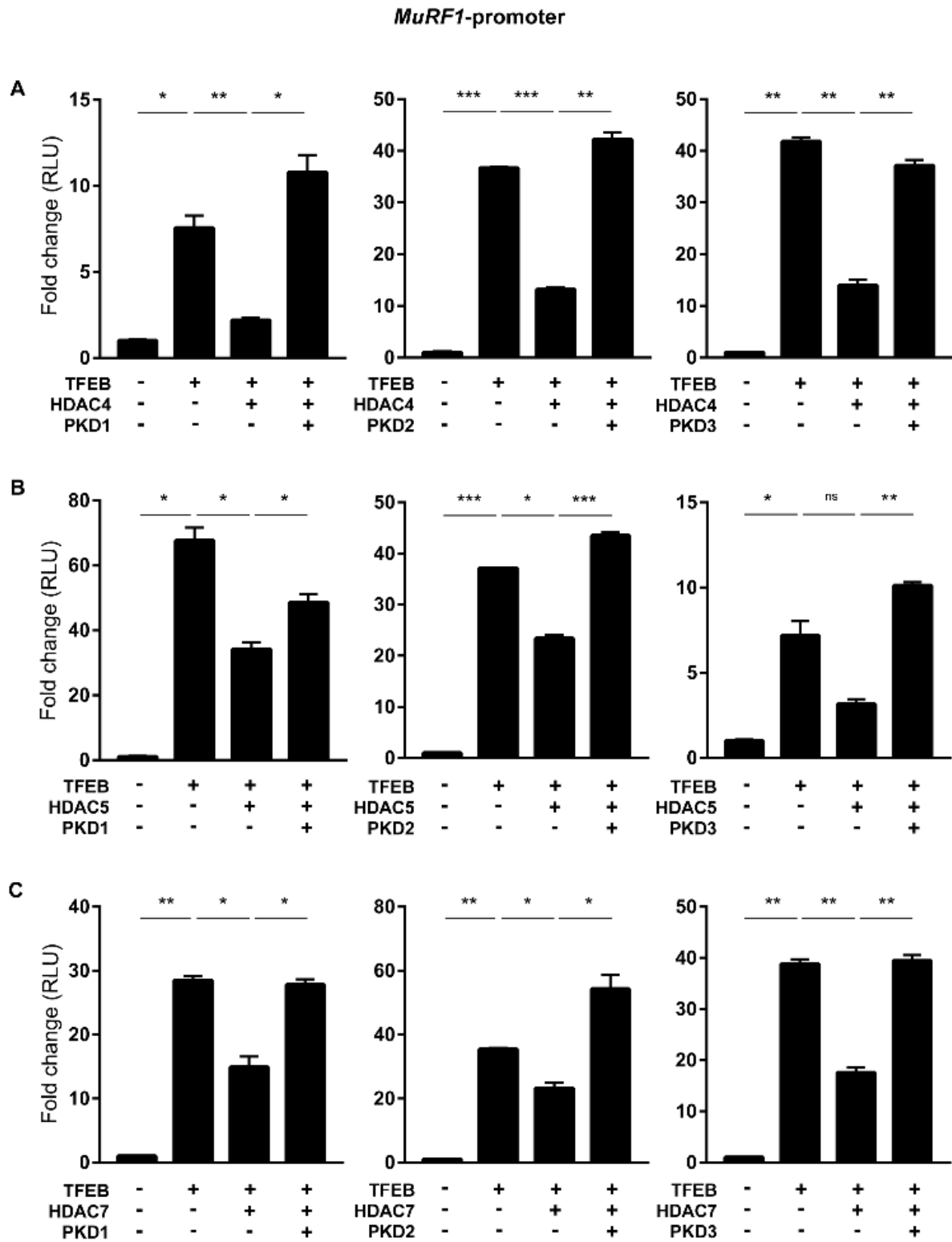


Fig 16. Each PKD family member restores TFEB-mediated *MuRF1* expression inhibited by HDAC4, HDAC5 and HDAC7. COS7 cells were transfected with expression plasmids encoding TFEB, HDAC and PKD together with human *MuRF1* promoter-luciferase reporter construct. Luciferase activity was assessed after 24h and values were normalized to pMV-LacZ. Bars show luciferase activity in relative luciferase units (RLU) expressed as fold change versus cells transfected with control plasmid. Values are mean \pm SEM. * $p \leq 0.05$, ** $p \leq 0.01$, *** $p \leq 0.001$, ns= not significant (Student's T-test).

Results

These data show that HDAC4, HDAC5 and HDAC7 decreased TFE3-induced MuRF1 expression. According to the initial hypothesis, PKD1, PKD2 and PKD3 attenuated the inhibitory effect of class IIa HDACs onto TFE3-induced MuRF1 expression.

In order to investigate if TFE3 shows a similar subcellular localization as TFE3, I transfected COS7 cells with TFE3 and performed immunocytochemistry. This experiment showed that TFE3 was localized to the nucleus (Fig. 17). Cotransfection of TFE3 and HDAC4, HDAC5 and HDAC7, respectively, revealed that TFE3 and those class IIa HDACs colocalized in the nucleus (Fig. 17, upper panel).

When PKD1 was cotransfected a nuclear export of HDAC4, HDAC5 and HDAC7 was detected. These data indicated that these class IIa HDACs regulate the activity of TFE3 and that PKD1 could reverse this effect (Fig. 17, lower panel).

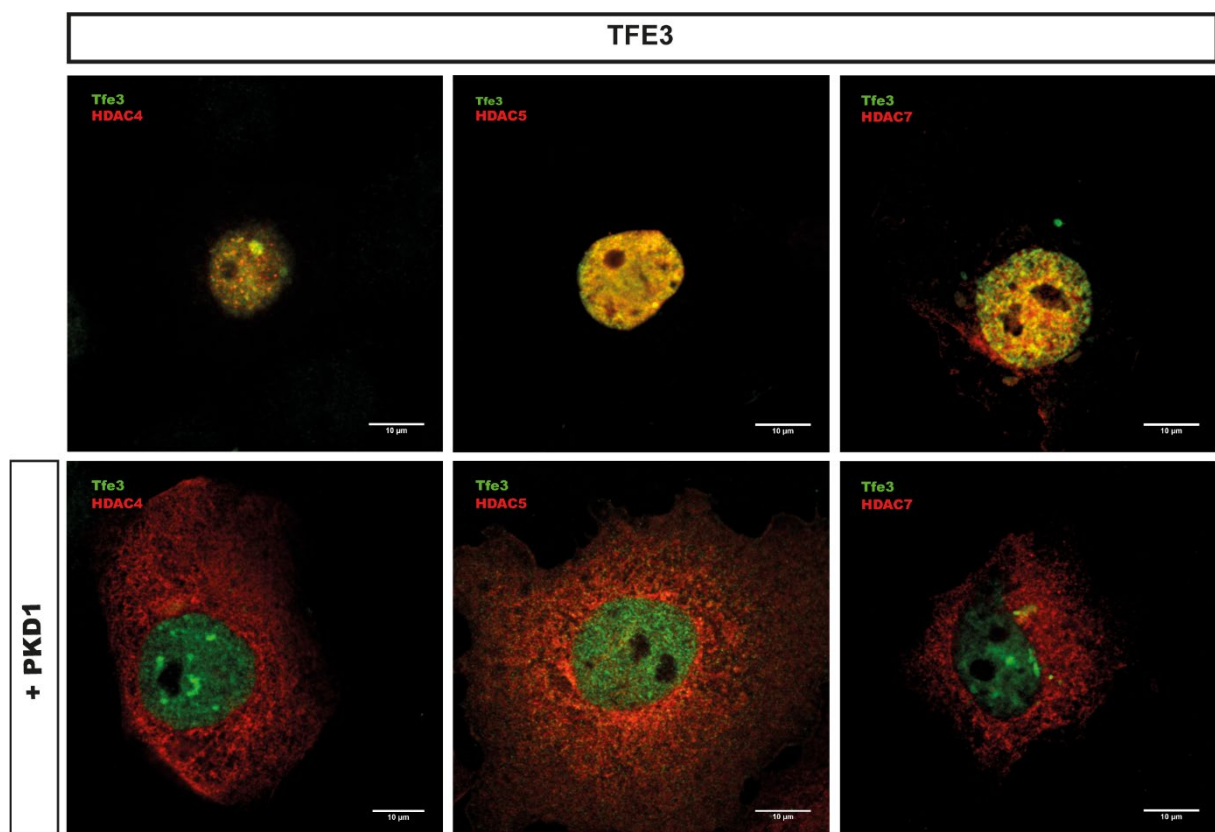


Fig 17. PKD1 promotes nuclear export of class IIa HDAC releasing its interaction with TFE3. COS7 cells were cotransfected with FLAG-TFE3, HDAC-Myc with or without PKD1-HA and double-stained against FLAG and Myc. Subcellular localization was analyzed by immunofluorescence confocal microscopy. Scale bars, 10 µm. Images are representative of three independent experiments.

Results

In order to test this hypothesis and to further investigate the functional significance of the TFE3/HDAC/PKD axis, I performed reporter gene assays.

Same as with TFEB, I found that TFE3 induced the MuRF1 expression and that class IIa HDACs inhibited this effect. In agreement with our hypothesis, either PKD1, PKD2 and PKD3 restored TFE3-mediated MuRF1 expression (Fig. 18).

All together, these data show a close relationship between class IIa HDACs (HDAC4, HDAC5 and HDAC7), the PKD family (PKD1, PKD2 and PKD3) and the TFE/MiTF family of transcription factors.

IV. TFEB and TFE3 share same HDAC5-interacting domain

To define the regions within HDAC5 responsible for the physiological interaction with TFEB, I used a series of HDAC5 deletion mutants were generated in our lab (Du Bois *et al.*, 2015); the HDAC5-deletion mutants are depicted in figure 19, C. Likewise, I used this approach to describe the domain within HDAC5 domain is responsible of its binding to TFE3 in order to repress its activity.

To elucidate the domain within HDAC5 that is responsible for its interaction with TFE3, I coexpressed wildtype FLAG-TFE3 and wildtype HDAC5-Myc or FLAG-TFE3 and HDAC5-Myc deletion mutants in COS7 cells and performed Co-Immunoprecipitation experiments (Co-IP). I found that TFE3 and HDAC5 coprecipitated with each other indicating a physical interaction between both proteins (Fig. 18. A, lane 3).

Further Co-IP experiments were performed to elucidate which region within HDAC5 is responsible for its binding to Tfe3. For these experiments I transfected wildtype Tfe3 with wildtype HDAC5 and the described HDAC5 deletion mutants into COS7 cells and performed co-immunoprecipitation experiments followed by Western blot analysis. I found that wildtype HDAC5, and the HDAC5 deletion mutants 1-664 and 51-C coprecipitated with Tfe3 (Fig. 18, B). These data indicate that HDAC5 binds to TFE3 by a small area in its N-terminal region of around 50 amino acids (Fig. 18, C).

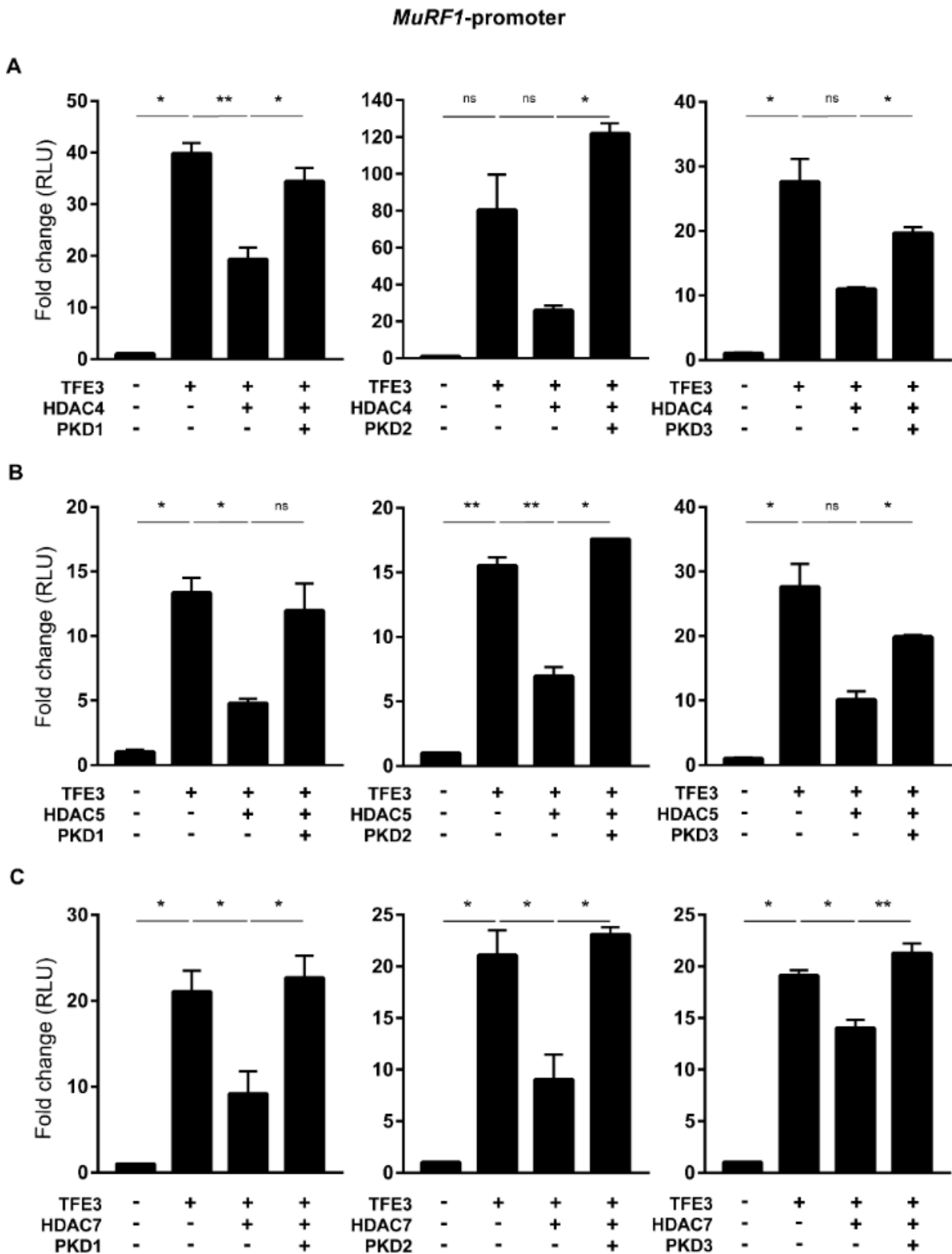


Fig. 18. Each PKD family member restores TFE3-mediated *MuRF1* expression inhibited by HDAC4, HDAC5 and HDAC7. COS7 cells were transfected with expression plasmids encoding TFE3, HDAC and PKD together with human *MuRF1* promoter-luciferase reporter construct. Luciferase activity was assessed after 24h and values were normalized to pMV-LacZ. Bars show luciferase activity in relative luciferase units (RLU) expressed as fold change versus cells transfected with control plasmid. Values are mean \pm SEM. * $p \leq 0.05$, ** $p \leq 0.01$, *** $p \leq 0.001$, ns= not significant (Student's T-test).

Results

V. TFEB and TFE3 compete for the activation of MuRF1 expression

Both transcription factors, TFEB and TFE3, bind to CLEAR elements in the promoter region of their target genes (Palmieri *et al.*, 2011; Settembre *et al.*, 2011; Martina *et al.*, 2014). Recent work by Jose A. Martina and coworkers showed a partial redundancy of TFEB and TFE3 in the ability to induce lysosomal biogenesis in response to starvation (Martina *et al.*, 2014). Moreover, first studies of the transcription factor family described the ability of TFEB and TFE3 to form and bind DNA as homo- or heterodimers (Fisher *et al.*, 1991) implicating that TFEB and TFE3 function redundantly. To investigate this possible redundant function of TFEB and TFE3, I performed reporter gene assays using the MuRF1 promoter. I cotransfected a MuRF1 luciferase construct with 20 ng of TFEB, TFE3 or both in COS 7 cells and analyzed the MuRF1 promoter activity by luciferase. As seen in Fig. 20, A, TFEB and TFE3 increased the activity of the MuRF1 promoter. However, there was no synergistic effect in the induction of the MuRF1 promoter when TFEB and TFE3 were cotransfected. These data indicate that TFEB and TFE3 function redundantly at the MuRF1 promoter.

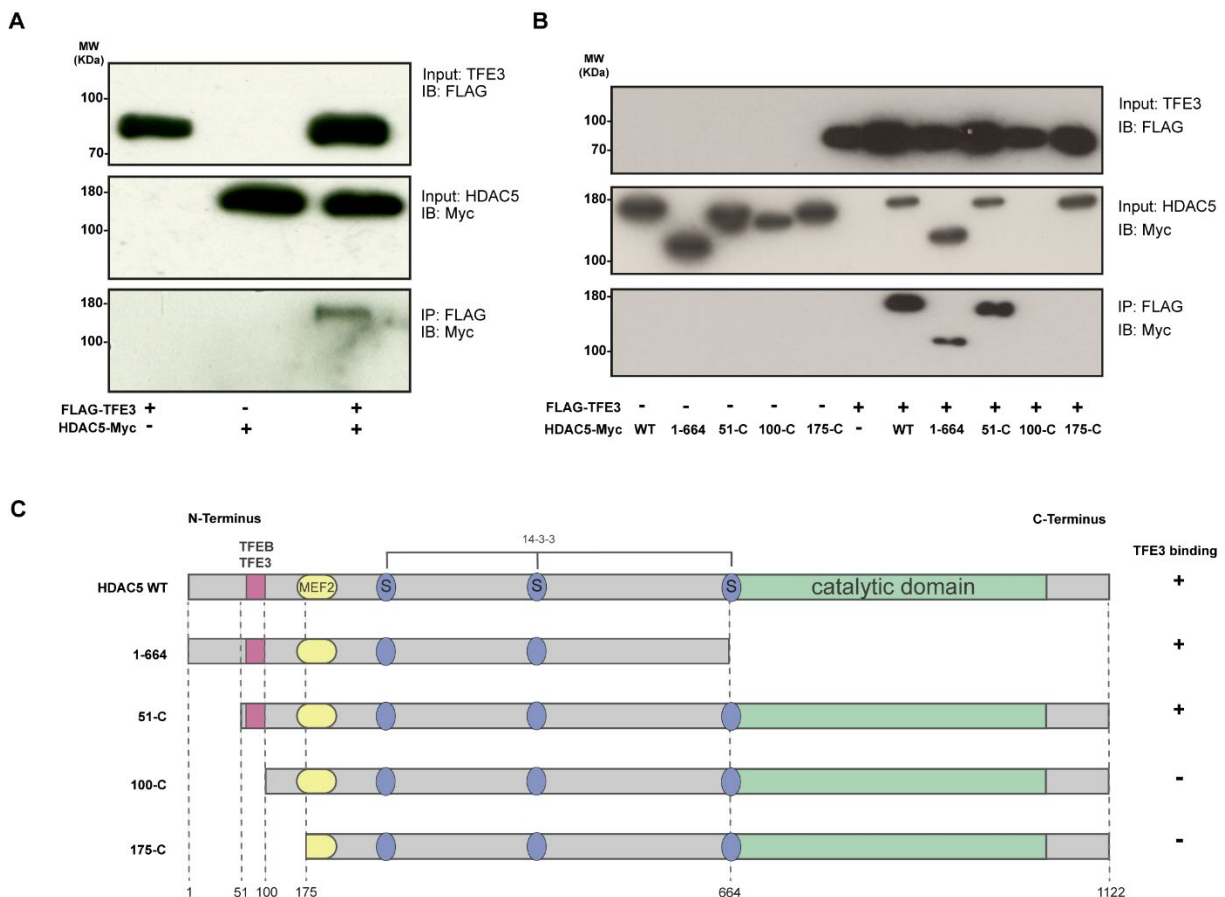


Fig. 19. HDAC5 binds TFEB and TFE3 by the same association domain. Western Blot analysis of Co-IP to show TFE3-HDAC5 relation was performed in COS7 cells by cotransfecting FLAG-TFE3 and HDAC5-Myc WT (**A**). Further binding site identification was established by a combination of Co-IP experiments using different HDAC5 mutants lacking determined areas (**C**) along with FLAG-TFE3, as indicated in (**B**). In every experiment, COS7 cells were used to obtain protein complexes that were immunoprecipitated against FLAG and detected with anti-FLAG or anti-Myc antibodies. Input proteins were detected by immunoblot (IB).

Results

Given that TFEB-TFE3 heterodimer was found to be the most effective form to induce gene expression, I reasoned that heterodimerization would be most likely the physiological conformation in the cell. Consequently, I investigated the strength of the interaction between TFE3 and TFEB. To test that, I cotransfected TFEB and TFE3, performed a Co-IP and exposed the heterodimer bound to sepharose to increasing salt concentrations. By western blot analysis I observed a quite strong signal of TFE3 and TFEB co-precipitating up to a NaCl concentration of 700 nM; the TFEB-TFE3 interaction was abolished by 900 nM NaCl (Fig. 20, B). My data indicate that TFEB and TFE3 form a stable, strong and efficient heterodimer.

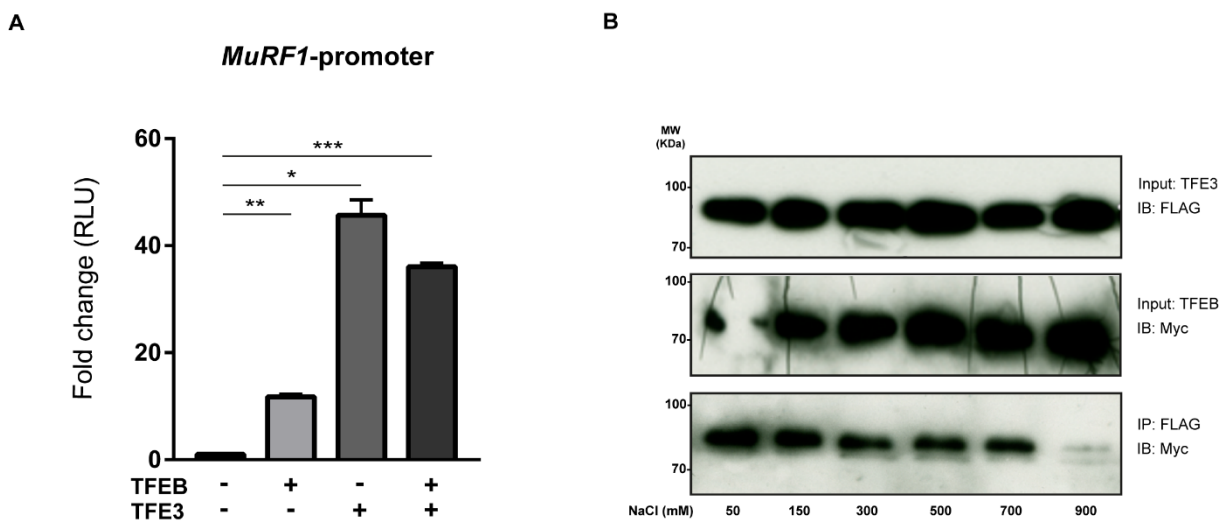


Fig. 20. TFEB and TFE3 redundantly regulate activity of MuRF1 promoter. (A) Luciferase assay in COS7 cells cotransfected with 20 ng of FLAG-TFEB expression plasmid alone or together with 20 ng FLAG-TFE3 and the human MuRF1 luciferase reporter construct for 24 h. Values were normalized to pMV-LacZ. Bars show luciferase activity in relative luciferase units (RLU) expressed as fold change versus cells transfected with control plasmid. Values are mean \pm SEM. * $p \leq 0.05$, ** $p \leq 0.01$, *** $p \leq 0.001$, ns= not significant (Student's T-test). **(B)** Prove of the stable TFEB-TFE3 association was tested by the transfection of 2 μ g FLAG-TFE3 together with 2 μ g TFEB-Myc in COS7 cells. Different samples were treated with an increasing amount of NaCl (from 50mM to 900mM). Protein complexes were immunoprecipitated against FLAG and detected with anti-FLAG or anti-Myc antibodies. Input proteins were detected by immunoblot (IB).

4.2 TFEB in muscle protein homeostasis: UPS and Autophagy

Our group described that TFEB is involved in UPS-dependent muscular protein degradation. Besides that, TFEB is known as a master regulator of lysosomal biogenesis and autophagy (Sardiello *et al.*, 2009; Palmieri *et al.*, 2011; Settembre *et al.*, 2011). However, the physiological role of TFEB in skeletal muscle is less well understood. To address this question, I performed muscle-specific gain- and loss-of-function experiments both *in vitro* and *in vivo*.

Results

I. TFEB knockdown reduces autophagic flux *in vitro*

To reduce TFEB in differentiated C2C12 myotubes, I transfected these cells with a pool of small interfering RNA (siRNA) targeting mouse *Tfeb*. A non-targeting pool of siRNA was used as a control. Five days differentiated myotubes were transfected with siRNA in a final concentration of 100 nM. After 24 h, RNA purified and quantitated residual *Tfeb* expression and the expression of TFEB target genes by qRT-PCR. In addition, I investigated the effects of TFEB onto autophagy. For that, I used chloroquine as a tool to measure autophagic flux since it inhibits lysosome-autophagosome fusion. As a consequence, LC3II-rich autophagosomes accumulate in the cell giving an estimate on “how fast” autophagy is working. A final concentration of 50 μ M chloroquine was administered to C2C12 cells 12 h prior to cell lysis. Western blotting (Fig. 21, A) and LC3II intensity quantification (Fig. 21, B) showed a higher content in LC3-II enriched vesicles in control-chloroquine treated samples compared to TFEB deficient myotubes. These results indicate that depletion of TFEB results in a decreased autophagic flux, which is in agreement with previously published work (Settembre *et al.*, 2011). However, when I quantified *Sqstm1/p62* which is another autophagy marker and was described as a TFEB target I obtained opposite results. p62 is supposed to be transcriptionally regulated by TFEB but as shown in Fig. 21, C and D no major changes in the p62 protein content were observed following knockdown *Tfeb* and compared to control-transfected samples.

II. Deletion of *Tfeb* does not affect the expression of autophagy genes

To follow up on the controversial outcome in protein analysis where TFEB had no clear effect on proteins involved in autophagy, I decided to test the expression of typical autophagy genes by RT-PCR. I focused on the expression of genes that have already been described as TFEB targets and to be involved in autophagy (Sardiello *et al.*, 2009; Settembre *et al.*, 2011; Palmieri *et al.*, 2011).

Day-5 differentiated myotubes were siTfeb- or control siRNA transfected in a final concentration of 100 nM, RNA purified after 24 h and used in qRT-PCR in order to quantify residual TFEB knock down efficiency and the expression of TFEB target genes.

Reduction of TFEB by siRNA did not lead to a significant down regulation of *Maplc3b* (LC3), *Lamp1*, *Sqstm1* (p62) and the genes encoding the v-ATPase subunits *Atp6v0d1* and *Atp6v1b2*, compared to control-transfected C2C12 myoblasts (Fig. 22, A). These data implicate that TFEB has different functions in muscle and non-muscle cells.

Results

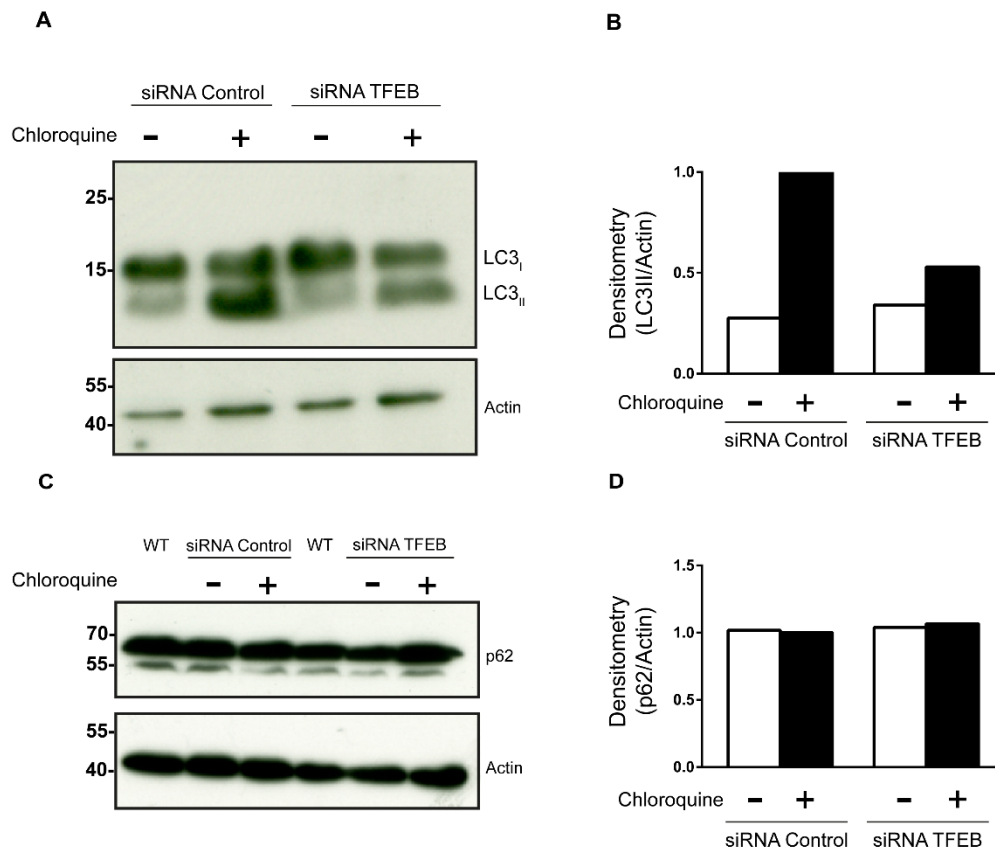


Fig. 21. Depletion of TFEB in C2C12 mouse skeletal muscle myotubes may have an effect in autophagy flux. siRNA-mediated knockdown of *Tfeb* in day-5 differentiated myotubes revealed a decreased LC3 lipidation and autophagy flux. Immunoblot of LC3 (**A**) and autophagic flux quantification by densitometry (**B**). (**C**) Immunoblot of autophagy marker p62. TFEB is not required for p62 induction in C2C12 myotubes (**D**). Data normalized to actin and expressed as fold change of chloroquine-treated control sample.

TFEB is a key element in the transcriptional response to starvation and controls autophagy by regulating autophagosome formation and autophagosome-lysosome fusion (Settembre *et al.*, 2011). Therefore, I investigated the effects of TFEB under physiological conditions. For that, I transfected five days differentiated C2C12 myotubes with siTFEB or siRNA control and starved the cells by incubation with serum-free medium for 12 h. From these cells I isolated RNA and performed qRT-PCR to quantify the autophagy genes *Maplc3b*, *Sqstm1*, *Uvrag*, *Atg9*, *Mcoln1*, *Wipi1* and *Hexa*. Reduction of TFEB did not result in a decreased induction of these typical autophagy genes, neither in normal physiological condition nor under starvation (Fig. 22, B). These results are in disagreement with previously published work in non-muscle cells.

To investigate the activation of TFEB in response to starvation, I performed a starvation experiment analyzing different time points covering the range of time points most commonly used in the literature. Day-5 differentiated myotubes were siTFEB- or siRNA control-transfected and exposed to starvation for up to 12 h. *Tfeb*, *Lamp1* and *Sqstm1* expression was quantitated in 1-hour intervals. The highest

Results

induction was achieved for every gene after 12 h with a maximum increase of 1.5-fold change (Fig. 22, C). A better knowledge in the process of starvation inducing autophagy would be needed to, ideally, be able to describe TFEB response to starvation and its role in autophagy.

Altogether, these data suggest that the effects of TFEB on ALP-mediated protein degradation are different between muscle and non-muscle cells.

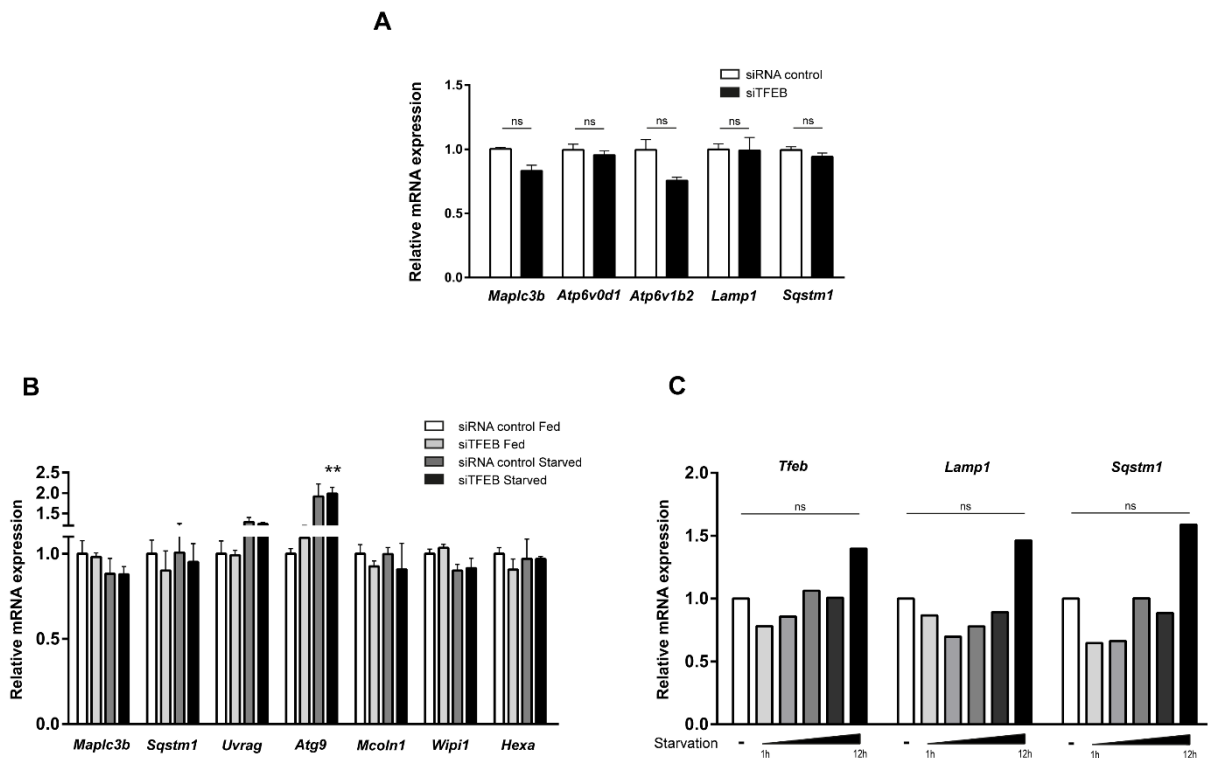


Fig. 22. RNA expression data reveals almost no changes in autophagy genes due to absence of TFEB or fasting. (A) Quantitative RT-PCR analysis of TFEB-depleted C2C12 myoblasts by siRNA. Data normalized to GAPDH and expressed as fold change of control-scramble transfected cells. **(B)** Day-5 differentiated myotubes were transfected with control scramble or siTFEB in a final 100 nM concentration and exposed to 12 h serum-free medium starvation or normally fed, as indicated in graph legend. Data normalized to GAPDH and expressed as fold change of fed siRNA control. Data representative of two different experiments. **(C)** Expression analysis of day-5 differentiated myotubes exposed to a serum deprivation time-course. Data normalized to GAPDH and expressed as fold change of fed myotubes. Values are mean \pm SEM. ** $p \leq 0.01$, ns= not significant (Student's T-test).

III. TFEB overexpression is not sufficient to stimulate autophagy

To gain a better insight into the role of Tfeb in muscle, I explored the effects of Tfeb overexpression on the transcriptional regulation of autophagy in C2C12 cells. For these experiments, I used a transient lipid-base transfection method.

Results

I transfected C2C12 cells with 1 µg of pcDNA3.1-FLAG TFEB or a control pcDNA3.1 expression plasmid, harvested RNA and protein after 24 h and performed qRT-PCR and western blot analysis to quantify the expression and protein content of typical genes and proteins involved in autophagy-mediated protein degradation; *Maplc3b*, *Atp6v0d1*, *Atp6v1b2* and *Lamp1*. TFEB overexpression had no effect on the expression of LC3, *Lamp1* and one of the v-ATPase subunit genes at mRNA levels (Fig. 23, A). Accordingly, no major change in autophagic flux was found as seen in the total LC3 form after chloroquine treatment (Fig. 23, B).

C2C12 cells are difficult to transfect and transfection efficiency is often less than 20 %. Due to these poor rates of TFEB overexpression, I wondered whether non-transfected cells would mask the real TFEB effect. Therefore, I turned to a stable transfection approach using a retroviral vector already developed in our lab (I am very thankful to Dr. Franziska Schmidt) and created a stable TFEB-GFP overexpressing cell line. Consequently, I routinely transduce C2C12 myoblast with pMP71-TFEB GFP or the equivalent control pMP71-GFP virus (referred to as TFEB-treated and control-treated cells) and performed the experiments after 48 h. Then, C2C12 were starved with serum-free medium for 12 h. In agreement with the results obtained with transient overexpression, stable TFEB overexpression did not increase most of the autophagy genes either. Nevertheless, I observed a significant induction of p62 (Fig. 24, B). Accordingly to the RNA data, protein analysis also showed a trend towards a higher p62 protein content in TFEB-transfected, which however did not reach statistical significance (Fig. 24, C).

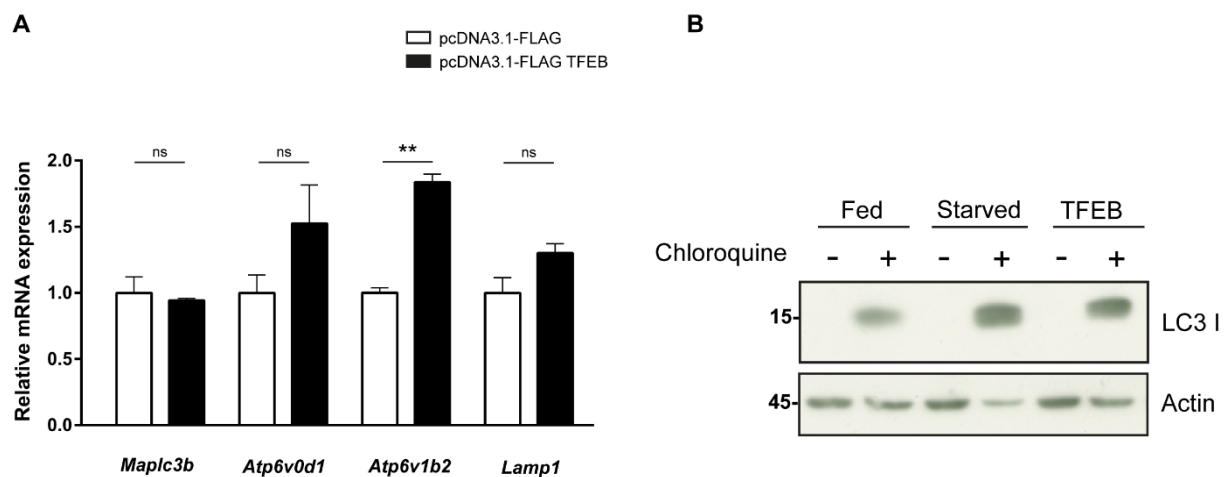
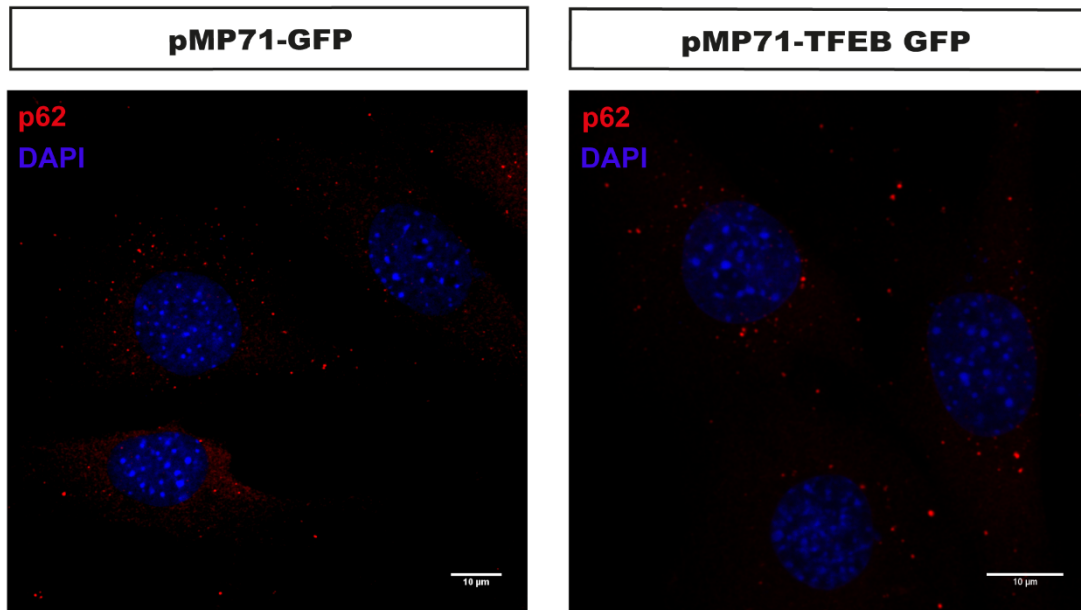
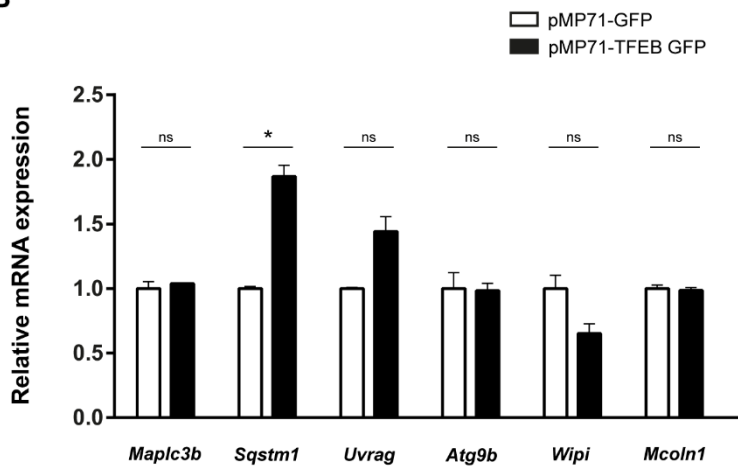


Fig. 23. TFEB overexpression does not induce transcription of most autophagy-related genes. (A) C2C12 myoblast were transiently transfected for 24 h and total RNA was extracted and analyzed by quantitative RT-PCR. Most of the representative genes did not exhibit significant changes compared to empty vector pcDNA3.1-FLAG. Data normalized to GAPDH and expressed as fold change of control plasmid-transfected. Values are mean \pm SEM. ** $p \leq 0.01$, ns= not significant (Student's T-test). **(B)** Cells were treated as in **(A)** and incubated with chloroquine for 12 h. Proteins were detected with antibodies against LC3 and actin.

A



B



C

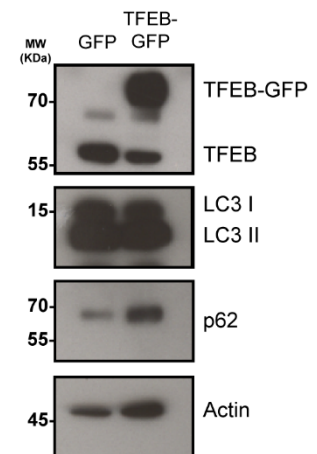


Fig. 24. Most autophagy markers are not modulated by a stable TFEB overexpression. p62 vesicle clearance evaluation in pMP71-TFEB treated muscle cells by immunofluorescence against SQSTM1/p62. Scale bars, 10 μ m. Representative images of two independent experiments (A). (B) Quantitative RT-PCR of autophagy genes from 48 h TFEB-transduced myoblasts. Data normalized to GAPDH and expressed as fold change of empty vector-transfected. Values are mean \pm SEM. ** $p \leq 0.01$, ns= not significant (Student's T-test). (C) Immunoblot analysis of p62, LC3 and TFEB that shows no increase in these autophagy markers in TFEB-overexpressing lysates.

p62 has the ability to form aggregates and for this reason is widely used as a predictor of autophagic flux. In the case of dysfunctional autophagy, p62 accumulates. On the contrary, it tends to degrade through autophagy pathway in a faster turnover when we observe an increased autophagy flux. As a last attempt to track p62 and better understand the significance of the results, I tested p62 in an immunofluorescence in C2C12 transduced cells and evaluated p62 vesicle clearance. Comparison of

Results

TFEB and control transduced staining did not reveal any sign of an enhanced autophagy flux as no clearance of p62 vesicles was observed in TFEB treated cells (Fig. 24, A).

Together, these data suggest that stable TFEB overexpression does not increase autophagic flux in muscle cells

4.3 Muscle specific *Tfeb* knockout mice do not show a muscle phenotype

Tfeb-null mice show defective placental vascularization and embryonic lethality at E9.5-10.5 (Steingrimsdottir *et al.*, 1998). Therefore, a conditional allele was generated to delete *Tfeb* in specific cell types. This mouse model allows deletion of *Tfeb* in specific cell type using a cell type specific CRE recombinase which allows mechanistical analysis of TFEB. In order to delete TFEB in the muscle cell lineage we crossed *Tfeb*^{loxP/loxP} with transgenic mice expressing the CRE recombinase under the control of the muscle-specific Pax7 promoter (referred to as *Tfeb*^{-/-}, cKO) (Murmah *et al.*, 2000). I used *Tfeb*^{loxP/loxP} (wildtype) littermates as controls. qRT-PCR and western blot analysis was used to confirm deletion of *Tfeb* in myocytes.

I measured the total body weight and heart weight of mice (control n=4, *Tfeb*^{-/-} n=3) and normalized it to the tibia length. Separately, I measured the weights of *Gastrocnemius and plantaris*, *Tibialis anterior*, *Soleus* and *Extensor digitorum longus* muscles and normalized to those tibia lengths. The appearance of *Tfeb*^{-/-} mice was indistinguishable in appearance from littermate. As seen in Fig. 25 no changes were observed in muscle mass of any of the tested muscles in *Tfeb*^{-/-} mice compare to controls. Histological analysis also showed normal muscle architecture and absence of pathologic features (data not shown). From these data, I conclude that the deletion of TFEB in the muscle cell lineage has no effect on the general morphology of the skeletal muscle.

To further characterize the role of TFEB in skeletal muscle, I analyzed if deletion of *Tfeb* affects protein degradation pathways *in vivo*. I isolated RNA from control and *Tfeb*^{-/-} mice (control n=4, *Tfeb*^{-/-} n=3) and quantified by qRT-PCR gene expression of MuRF1 (*Trim63*) and p62 as marker of autophagy (*Sqstm1*). No significant downregulation of both of the direct TFEB targets was found in any of the muscles analyzed compared to wildtype controls (Fig. 26, A). Accordingly, in terms of protein levels, no major changes were observed in LC3II/I conversion or p62 (Fig. 26, B). The maintenance of p62 and LC3 in *Tfeb*^{-/-} knockout mice was consistent with the siRNA results described *in vitro*. These data suggest that TFEB plays a minor role in ALP-mediated protein degradation in skeletal muscle.

Results

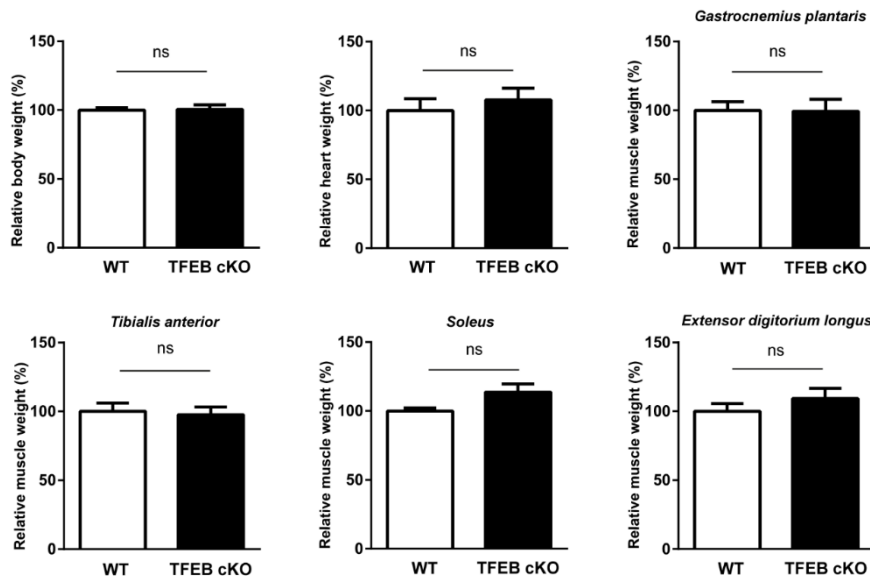


Fig. 25. Deletion of *Tfeb* does not result in muscle phenotype. Weight control of heart, *Gastrocnemius plantaris*, *Tibialis anterior*, *Soleus* and *Extensor digitorum longus* muscle of *Tfeb*^{-/-} and control WT mice. Data normalized to tibia length. Bars show values relative to WT animals. Control n=4; *Tfeb*^{-/-} n=3. Values are mean ± SEM. ns= not significant (Student's T-test).

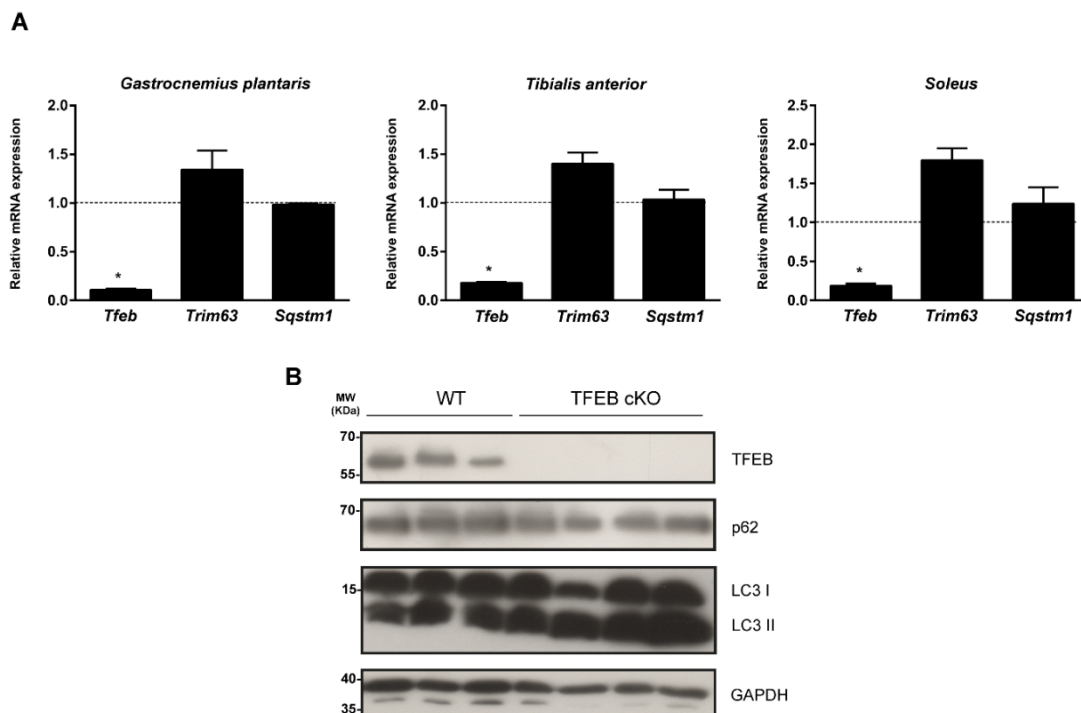


Fig. 26. Autophagic genes are not transcriptionally downregulated in *Tfeb*^{-/-} mice. (A) Quantitative RT-PCR analysis of *Tfeb*, *Trim63* (MuRF1) and *Sqstm1* (p62) mRNA expression in *Gastrocnemius plantaris*, *Tibialis anterior* and *Soleus* muscle of *Tfeb*^{-/-} and control mice. Data normalized to GAPDH. Bars show results relative to WT animals (dotted line). Control n=4; *Tfeb*^{-/-} n=3. Values are mean ± SEM. *p ≤ 0.05, ns= not significant (Student's T-test). (B) Immunoblot showing complete deletion of TFEB in lysates of *Tfeb*^{-/-} in *Gastrocnemius plantaris* (upper panel). Bottom part shows p62 and LC3 analysis, where no changes in LC3 lipidation and p62 protein content was observed.

4.4 Overexpression of TFEB impairs myoblast fusion *in vitro*

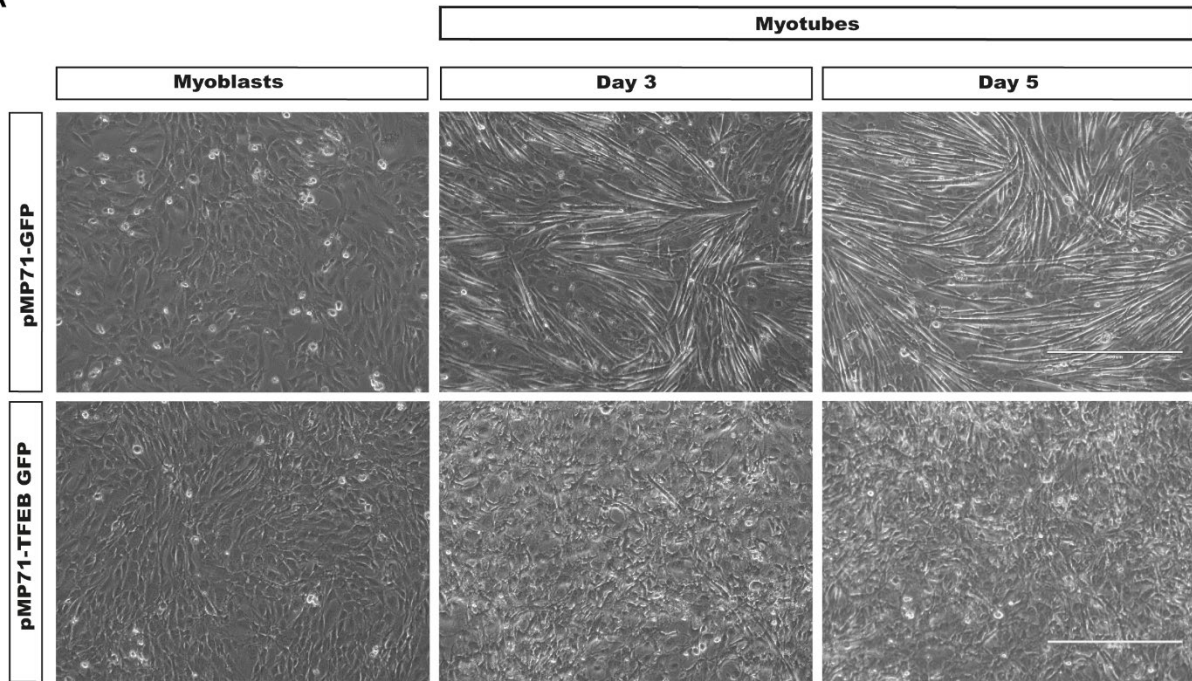
To test the effect of TFEB overexpression on myogenic differentiation, I used the retroviral system described under section X. I cultivated C2C12 myoblasts until ~50-60 % confluency and transduced these cells with a MOI of 0.7. With this approach I reached a transduction efficiency of ~90%. 24 h after transduction I induced myogenic differentiation.

Morphological analysis showed a marked impairment in the ability of C2C12 myoblast to differentiate when TFEB was stably overexpressed (Fig. 27, A lower panel). In a normal growing state, C2C12 cells pause in the G1 phase, exit permanently the cell cycle and eventually differentiate and fuse to form multi-nucleated myotubes (Perry and Rudnicki, 2000). This differentiation phenotype was consistently observed for control lentivirus transfected C2C12 cells. However, TFEB transfected cells stayed in an undifferentiated myoblast state along the whole 7 day-differentiation experiment. These cells would proliferate until reaching 100 % confluency and then enter in a “stand-by state” where cells would neither proliferate any longer nor start to die, as I did not observed detachment from culture surface. As mentioned, myoblasts transfected with the control GFP retroviral particles underwent normal myogenic differentiation (Fig. 27, A upper panel). These data suggested that stable overexpression of TFEB causes a deficient myogenic differentiation.

To investigate the effect of TFEB on a molecular level, I quantified the expression of *bona fide* markers of myogenic differentiation. In particular, I focused on the two classical myogenic regulatory factors (MRFs), MyoD and myogenin and two recently described muscle-specific proteins myomaker and myomaxin. Myomaker is a plasma membrane protein that mediates myoblast fusion, an essential step for the formation of multi-nucleated muscle fibers. Whereas myomaxin is involved in regulation of muscle cytoarchitecture, that is working as an anchor between Z-disc and cytoskeleton proteins. For this purpose, I transduced C2C12 in ~50-60 % confluency at MOI=0.7 and induced myogenic differentiation 24 h after transduction. I isolated RNA of undifferentiated myoblasts and days 1, 3 and 5 of differentiation to perform qRT-PCR.

I observed a typical expression pattern for MyoD and myogenin with a time dependent increase during myogenic differentiation and fusion, and their decrease upon completed differentiation in GFP-transduced differentiating C2C12 myotubes (Fig. 28). In contrast and in line with our observations, TFEB-GFP transduced myoblast showed a significant downregulation of all MRFs during differentiation. In addition, I found a decreased expression of myomaxin and myomaker in TFEB-GFP transduced differentiating C2C12 myotubes as well. My data indicate that, overexpression of TFEB inhibits differentiation of C2C12 myoblast as well as myotube fusion.

A



B

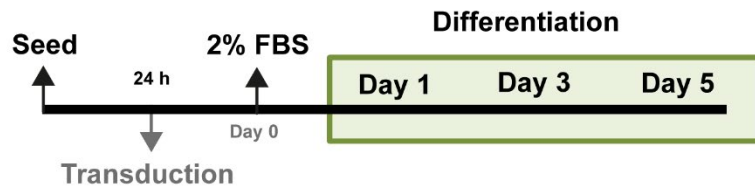


Fig. 27. TFEB expression blocks C2C12 myotube differentiation. (A) Representative differential interference contrast (DIC) images of control GFP (upper part) and TFEB-GFP (bottom part) transduced myoblast along the 5-days differentiation process. **(B)** Workflow timeline of C2C12 transduction and further differentiation for better understanding of the experimental procedure.

I found a consistent decrease in the MyoD protein content in TFEB-transduced myotubes from the myoblast stage (MB, day 0) to the final day of differentiation (day 5) compared to GFP-transduced myotubes. I observed similar effect for myogenin as well (Fig. 28).

In order to analyze late differentiation markers, I quantitated the effects of TFEB overexpression on the myosin heavy chain protein content. As expected, the amount of myosin heavy chain was greatly reduced in TFEB-transduced myocytes when compared to GFP-treated cells (Fig. 29, lanes 6 and 7).

Results

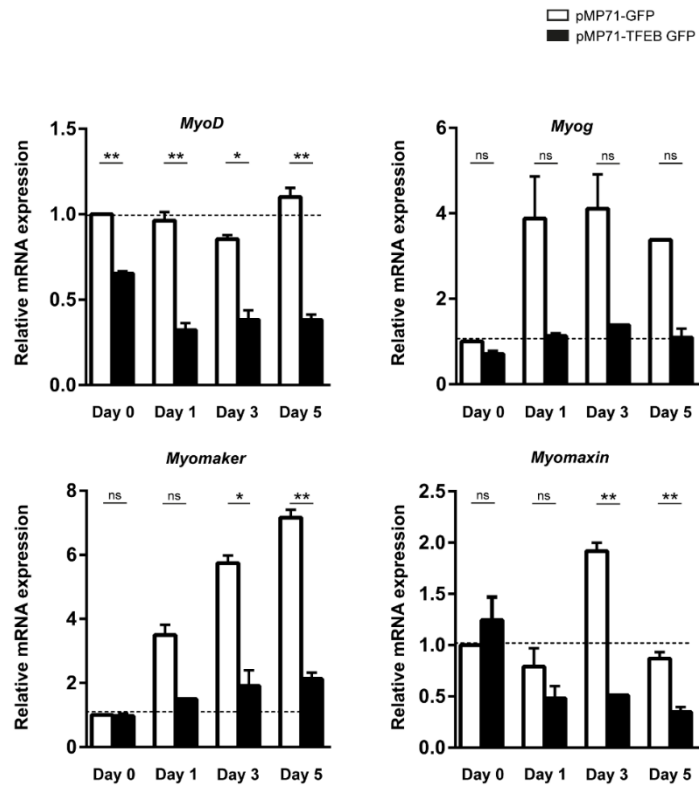


Fig. 28. TFEB inhibits myogenic differentiation of C2C12 cells. Quantitative RT-PCR analysis of the myogenic regulatory factors MyoD (*Myod1*), myogenin (*Myog*), myomaker (*Mymk*) and *myomaxin* in TFEB-GFP transduced versus control-GFP differentiating myotubes. Data normalized to GAPDH and expressed as fold change of control-GFP transduced differentiation day 0 myotubes. Values are mean \pm SEM. * $p \leq 0.05$, ** $p \leq 0.01$, ns= not significant (Student's T-test).

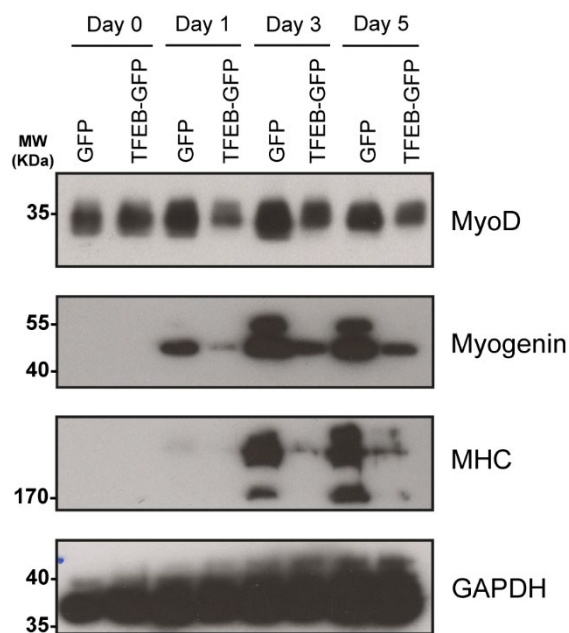


Fig. 29. Downregulated myogenic differentiation markers confirm undifferentiated myotubes phenotype. Total protein extracts of TFEB GFP or GFP-transduced C2C12 myoblasts in day 1, day 3 and day 5 of differentiation were analyzed by western blot. A downregulation of myogenic regulatory factors and myosin heavy chain was observed in TFEB-transduced cells.

Results

To elucidate molecular consequences of TFEB overexpression in myoblasts and to understand the mechanisms by which myoblast fusion and myotube differentiation was inhibited in TFEB-overexpressing myoblasts, a proteomics-based analysis using mass spectrometry was performed. For this experiment a similar experimental approach as mentioned above was used; including analysis of GFP signal by fluorescence microscopy and TFEB overexpression by western blot analysis.

We performed mass spectrometry analysis of 3 biological replicates of TFEB- and control GFP-transduced C2C12 myoblasts on different time point: day 0, day 1, day 3 and day 5. For further analysis we only used the data when proteins were detected in all three biological replicates. Using this method, we identified a total of 3.121 of proteins with 3 significant values in at least one of the 4 experimental groups (day 0, day 1, day 3 and day 5).

Because the formation of muscle requires the migration, differentiation and fusion of myoblast, I first investigated if the differentiation phenotype was reflected by changes of proteins involved in cell migration and adhesion. Overexpression of TFEB was associated with a decrease of most of the integrins (Fig. 30, A), indicative for deficient cell migration.

Numerous proteins involved in cell-cell adhesion and actin dynamics are implicated in myoblast fusion. Cadherins have been shown to be essential for the control of morphogenetic processes and may provide a trigger for terminal muscle differentiation. Transcripts from a particular cadherin, *Cdh15*, are expressed in myoblasts and upregulated in myotube-forming cells. In line with this, I observed a reduction of CDH15 in TFEB-treated myotubes during the 5 days of differentiation. The same reduction was observed for catenins and tight junction proteins as well (Fig. 30, B).

Abnormal expression of proteins responsible of cell-cell junctions and myoblast fusion, demonstrate a failure of these processes preventing a proper muscle fiber development.

Results

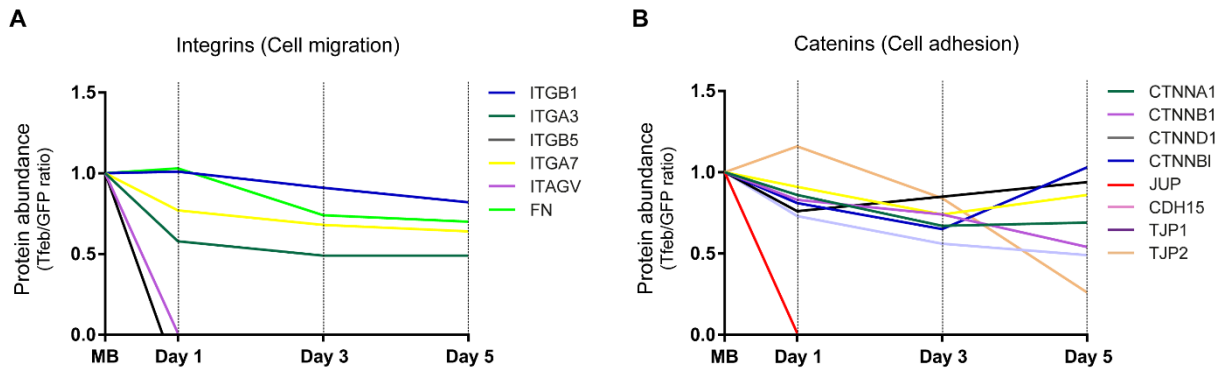


Fig. 30. Proteomic analysis of lysates from TFEB-GFP and control GFP transduced C2C12 myotubes at day 0, 1, 3 and 5 of differentiation. Relative quantification of protein abundance in TFEB-transduced myotubes along differentiation process. **(A)** Integrins, implicated in cell migration. **(B)** Catenins, Cadherin and Tight junction proteins regulate cell-cell adhesion. Data normalized to protein expression in GFP-control transduced myotubes.

Additionally, myoblast fusion requires cell–cell interaction followed by membrane coalescence and actin dynamics that drive the fusing cells to merge. Dysfunction of one or more of these steps will delay or attenuate muscle formation. Therefore, I analyzed and clustered myosins, proteins of the contractile apparatus and muscle proteins to have a better view on TFEB mediated alteration of myoblast differentiation.

As seen in Fig. 31, A, the content of all myosins is low in TFEB-transduced myotubes throughout the entire time course. This is accompanied by a dramatic drop of the terminal differentiation marker creatine kinase M-type (CKM).

In addition to the myosins, several other proteins contained in the contractile apparatus were decreased in response to TFEB overexpression as well (Fig. 31, B). Several types of actin, including muscle specific α -actin (ACTA1), muscle actinin (ACTN3), and cytoplasmatic actins (ACTB and ACTG1) were reduced in response to TFEB overexpression. Most of tropomyosin isoforms, which take part of contractile system as well as part of cytoskeleton (TPM1, TPM2 and TPM3), were accordingly diminished.

In agreement with what we observed so far, other typical muscular proteins desmin, filamin and laminin slightly decreased by TFEB overexpression; confirming myoblast migration was altered. Interestingly, I observed the most dramatic change in Titin. The total protein abundance of titin was reduced by approximately 50% just within the first day of differentiation and it is almost vanished at day 5 (Fig. 31, C). Pointing towards the incompetence of C2C12 to differentiate and generate muscle fibers upon TFEB overexpression.

Results

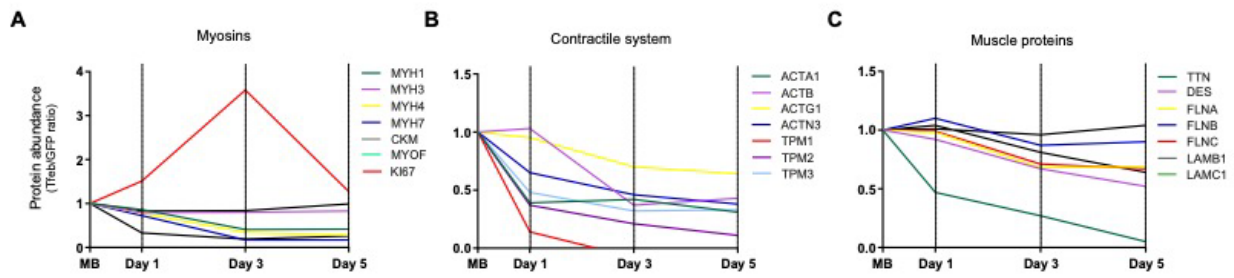


Fig. 31. Proteomic analysis of lysates from TFEB-GFP and control GFP transduced C2C12 myotubes at day 0, 1, 3 and 5 of differentiation. Relative quantification of protein abundance in TFEB-transduced myotubes along differentiation process. **(A)** Myosins and proliferation marker Ki67. **(B)** Actin and tropomyosin take part in contractile apparatus but also as an important part of cell cytoskeleton. **(C)** Muscle specific proteins. Data normalized to protein expression in GFP-control transduced myotubes.

Remarkably TFEB overexpression was accompanied by an increase in the proliferation marker Ki67. Once myogenic precursor cells start to differentiate into myotubes they irreversibly withdraw from the cell cycle. This cell cycle exit occurs at the beginning of differentiation and is required for normal expression of the contractile apparatus (Walsh and Perlman, 1997). Therefore, Ki67 is only weakly expressed or absent in differentiating myotubes. However, our proteomics data showed that TFEB-transduced C2C12 myotubes had a more than 3-fold higher Ki67 protein content compared to control transduced myotubes (Fig. 31, A). These data are in line with the morphological analysis of TFEB-transduced muscle cells, which do not differentiate and stay in cell cycle and proliferative stage during the 5 days of differentiation.

TFEB was newly described as a regulator of mitochondrial biogenesis in skeletal muscle increasing respiratory chain complex activity and ATP production (Mansueto *et al.*, 2017). To examine the effects of TFEB on the mitochondrial network in differentiating C2C12 cells, I quantitated and clustered the number of proteins involved in mitochondrial bioenergetics described by Mansueto and colleagues. I found that TFEB overexpression resulted in an increase of proteins involved in mitochondrial function (Fig. 32, B). These data independently confirmed that TFEB plays a role in mitochondrial biogenesis and show that overexpressed TFEB was biologically active in C2C12 cells. Together with my other experimental data these results show that TFEB has negligible effects on ALP-mediated protein degradation in myocytes. The fact that I found an effect of TFEB on the protein content of all the proteins involved in the mitochondrial respiratory chain that were recently reported to be regulated by TFEB proved my results to be true.

Finally, we analyzed if overexpression of TFEB caused an increase in lysosomal biogenesis and autophagy. However, mass-spectrometry data revealed no significant effect of TFEB on any of the proteins involved in these pathways; with the only exception of p62. As shown in the protein

Results

abundance graph (Fig.32, A), most of lysosomal-related proteins remained unchanged during differentiation irrespective of TFEB overexpression. These data indicate that TFEB has only minor effects on lysosomal protein degradation in myocytes.

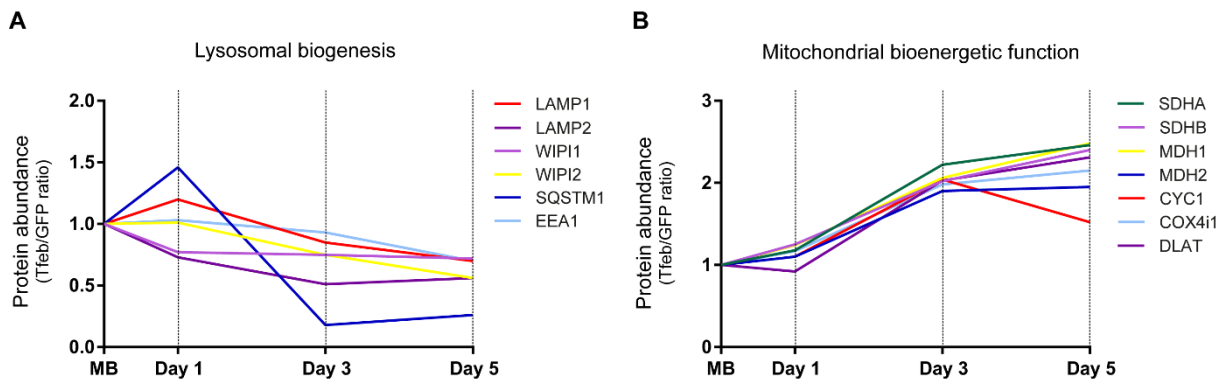


Fig. 32. Proteomic analysis of lysates from TFEB-GFP and control GFP transduced C2C12 myotubes at day 0, 1, 3 and 5 of differentiation. Relative quantification of protein abundance in TFEB-transduced myotubes along differentiation process. **(A)** Lysosomal biogenesis related proteins. **(B)** Mitochondrial bioenergetic function proteins. Data normalized to protein expression in GFP-control transduced myotubes.

5. Discussion

Muscle atrophy is characterized by a reduction in myofiber size due to a net loss of proteins. As occurring in many pathological conditions, a net loss of proteins results from unbalanced protein degradation due to malfunction of the main cellular protein degradation pathways, the UPS and ALP. However, muscle atrophy is a complex process that occurs as a consequence of a variety of stressors, and its pathophysiology is not well understood. Indeed, the molecules, mediators and cellular pathways that contribute to muscle atrophy are still being discovered (Bodine *et al.*, 2014). Owing to its involvement in intracellular clearance pathways, TFEB represents a very attractive therapeutic target for many human diseases, most importantly for diseases associated with or caused by lysosomal dysfunction. Most recently, another member of the MiTF/TFE family, TFE3, has been shown to bind CLEAR elements in the promotor region of ALP associated genes. TFE3 was therefore described as active participant in ALP regulation (Martina *et al.*, 2014). To follow up with our initial insights into TFEB as modulator of muscle atrophy, the aim of this study was, first, to describe the TFEB/HDAC/PKD axis and to test the importance of the other MiTF/TFE family members for regulation of MuRF1 expression through the HDAC/PKD pathway. Secondly, as TFEB was identified as a global modulator of intracellular clearance in non-muscle cells, I investigated if TFEB regulated ALP mediated protein degradation in myocytes as well and if this plays a role in muscle remodeling.

5.1 Role of MiTF/TFE family members in MuRF1 expression

Using a human cDNA library screening, our group searched for novel regulators of MuRF1 expression. TFEB was identified as one of the strongest transcriptional activators of MuRF1. We showed that TFEB regulates Angiotensin II (Ang II) - induced skeletal muscle atrophy by transcriptional control of MuRF1 (Du Bois *et al.*, 2015). I validated the ability of TFEB to activate MuRF1 expression and investigated if the other MiTF/TFE family members have comparable functions. Here, I identified TFE3 as another regulator of MuRF1 expression which indicates that it might play a role in skeletal muscle atrophy. TFE3 induced MuRF1 expression in a dose-dependent manner and to the same extent as TFEB.

However, even with very high amounts MiTF did not increase the MuRF1 expression. Such functional differences within the MiTF/TFE family were also observed by Martina and coworkers. They conclude that, despite sharing similar mechanisms of regulation with TFEB and TFE3, MiTF lacks the ability to induce lysosomal formation as they failed to increase expression of most of the lysosomal genes tested with TFEB and TFE3 in ARPE-19 cells (Martina *et al.*, 2014). This could be explained by the fact that

Discussion

MiTF preferably binds to M-box elements instead of E-boxes. A detailed study of MiTF structure and function revealed that an isoleucine in position 212 mediates and even favors the binding of MiTF to M-box motifs via a specific interaction with a thymidine base in position -4 in the M-box motif (Pogenberg *et al.*, 2012). Of note, M-boxes have a slightly different hexamer core sequence (CATGTG) as compared to a classical E-box (CACGTG) (Hamesath *et al.*, 1994; Martina *et al.*, 2014). However, in recent studies, the TFEB network of targets (CLEAR network) was characterized as E-box-like (Palmieri *et al.*, 2011). Therefore, differences in the recognition of and the binding to specific binding sites in the promoter region of genes could explain the observed behavior of MiTF compared to TFEB and TFE3.

Overall, my data suggest that TFE3 is possibly involved in skeletal muscle atrophy and that there are distinct differences in the function of TFEB, TFE3 and MiTF, which are possibly related to the ternary structure and DNA-binding activities of these transcription factors. Further studies are needed to decipher those differences in detail.

5.2 Regulation of TFEB- and TFE3-induced MuRF1 expression

In line with our previous studies and based on extensive reporter gene assays, colocalization studies by immunofluorescence and coimmunoprecipitation analyses, the results of my thesis demonstrate that all class IIa HDACs investigated directly inhibit TFEB-mediated MuRF1 expression. I found that beside HDAC5 also HDAC4 and HDAC7 directly bind to TFEB and inhibit TFEB-mediated MuRF1 expression. For the first time I showed, that all class IIa HDACs physically interact with and inhibit TFE3-induced MuRF1 expression.

According to Moresi *et al.* who showed that the activity of the bHLH transcription factor myogenin was strongest inhibited by HDAC4 and HDAC5 (Moresi *et al.*, 2010), I found that these HDACs were also the predominant HDACs inhibiting the activity of TFEB and TFE3. In addition to these findings, I demonstrate that also HDAC7, although with a slightly milder power, negatively regulates TFEB and TFE3. My results support our assumption that all three HDACs work together with TFEB and TFE3 to regulate MuRF1 expression.

Furthermore, I identified the binding domains responsible for the interaction of both HDAC5 and TFE3. Using different HDAC5 deletion mutants, I showed that TFE3 binds to small region (~ 50 amino acids) of the N-terminus of HDAC5. This result is in accordance with our previous data that identified the same region within HDAC5 responsible for its interaction with TFEB (Du Bois *et al.*, 2015). This result is also in accordance with the already known structural and functional homology of TFEB and TFE3 (Kauffman *et al.*, 2014; Martina *et al.*, 2014; Martina *et al.*, 2016; Salma *et al.*, 2017)

Discussion

As already shown, the activity and subcellular localization of class IIa HDACs is tightly regulated by PKD, which physically interacts with HDAC4, HDAC5 and HDAC7 and phosphorylates specific serine residues in these HDACs. Once these serine residues are phosphorylated the chaperone protein 14-3-3 binds to the HDACs and mediates their nuclear export. These observations suggested to me that PKD family members redundantly control the activity of class IIa HDACs (Vega *et al.*, 2004; Fielitz *et al.*, 2008). Based on immunocytochemistry and reporter gene assays I confirmed this hypothesis. I found that PKD directly phosphorylates HDAC4, HDAC5 and HDAC7, and promotes their nuclear export. My data provide a mechanistic basis for the control of muscle atrophy via the PKD/HDAC/TFEB-TFE3 axis.

However, due to the nature of the experiments, I am not able to demonstrate a direct physical binding between the participating members of the PKD/HDAC/TFEB-TFE3 axis. The results of coimmunoprecipitation experiments do not exclude the possibility of the involvement of additional proteins involved in these interactions. Taking part of a protein complex for example, which means a possible risk of additional up- or downregulation points interfering in the proposed route. What I can conclude, however, is that these proteins are related to the function of the final target. This assumption is subjected to further verification; a good answer would be given by a two-hybrid screening where protein-protein physical interactions are tested.

Further, it is unclear how different signals specifically activate particular MiT/TFE members and whether their homo- or heterodimerization leads to different responses in diverse tissues (Napolitano and Ballabio, 2016). Here I showed that, both, either homo- or heterodimerization could activate the MuRF1 promoter. However, my data show that the TFEB-TFE3 heterodimer is even more effective in inducing the MuRF1 expression as compared to TFEB alone.

Further studies are needed to investigate the redundancy of TFEB and TFE3 as well as their potential to form homo- and heterodimers in further detail especially in light of protein homeostasis in skeletal muscle.

5.3 Nuclear localization of TFEB and TFE3

For non-muscle cells, several authors showed that TFEB and TFE3 are localized to the cytosol and that they rapidly translocate to the nucleus upon starvation (Settembre *et al.*, 2011; Settembre *et al.*, 2012; Martina *et al.*, 2014). Once in the nucleus, both, TFEB and TFE3 bind to specific elements on the promoter region of their target genes and increase their expression. These target genes are important for the cell to adapt to nutrient deprivation (Settembre *et al.*, 2012; Martina *et al.*, 2014). As already mentioned, most studies that addressed the function of TFEB have been performed in a wide variety of non-muscle cell lines, such as the human cervical cancer line HeLa (Settembre *et al.*, 2011), the embryonic kidney cells HEK-293 (Settembre *et al.*, 2012), and human retinal ARPE-19 cells (Martina *et al.*, 2014). However, using myocytes I consistently found TFEB and TFE3 to be equally localized in cytosol and the nucleus. This distribution was independent of starvation conditions. This points towards different functions and or different regulators of TFEB and TFE3 in muscle and non-muscle cells. It could also be explained as a response to the stress that cells have been subjected to after the transfection process; i.e. it was shown by Martina and coworkers that TFE3 and TFEB are part of the integrated response to ER stress (Martina *et al.*, 2016).

5.4 TFEB role as master regulator of autophagy in muscle cells

Directly related with the function of TFEB as a mediator of muscle atrophy, my second aim was to investigate if TFEB is involved in the regulation of ALP-genes in muscle cells.

As expected, upon depletion of TFEB I found a reduction in the autophagic flux of differentiated C2C12 myotubes. In accordance with the literature (Settembre *et al.*, 2011), following siRNA-mediated knockdown of TFEB I found a reduced LC3I/LC3II conversion in myocytes. However, other autophagy markers, such as p62, were not differentially expressed.

One experimental difficulty that needed to be solved was to investigate if only the depletion or overexpression of TFEB is sufficient to investigate the function of TFEB as it has been shown that the activity of TFEB is regulated by changes in posttranslational modification and subcellular localization. Specifically, TFEB is phosphorylated and inactivated by an mTOR-dependent signal. However, during starvation TFEB is dephosphorylated and translocates to the nucleus where it activates the expression of its target genes. Therefore, it might be difficult to detect changes in direct TFEB-targets under non-stressed conditions

A further experimental challenge is that the UPS compensates for the loss of autophagy and degrades polyubiquitinated proteins, including p62. Therefore, a more generalist view and experimental design

Discussion

that addresses the cooperative work of the two protein degrading pathways would be helpful to quantify the interaction of these systems.

These controversial results led me to redesign the experimental set-up to more physiological conditions. When I induced starvation in five days differentiated C2C12 myotubes and knocked down TFEB, I did not observe any change in the expression of ALP-genes. In contrast, a significant and progressive increase of TFEB mRNA expression and protein levels starting as soon as 4 h after elimination of nutrients were reported for starved HeLa cells, mouse embryonic fibroblasts and hepatocytes (Settembre *et al.*, 2013). Notably, I could not show the same in C2C12 cells where 12 h nutrient depletion did not activate TFEB or increased the expression of TFEB target genes. It still remains open whether starvation is able to induce TFEB activation in muscle cells.

Because C2C12 cells are difficult to transfect, I successfully implemented a retroviral-based method to overexpress TFEB in this cell line. In contrast to lipotransfection of cDNA expression plasmids, which yields around 20% of transfection efficacy, I reached 95% of transduction efficacy for the retroviral system. This method allowed me to study the effects of TFEB overexpression in myocytes. My overexpression results are in line with the loss-of-function experiments, TFEB did not induce autophagy, as I could not show an upregulation of autophagy markers on either mRNA expression or protein content. In addition, I found that TFEB overexpression did not affect the clearance of p62-rich vesicles in C2C12 cells, indicating that overexpression of TFEB did not induce ALP. P62 is widely used as predictor of autophagic flux; however, many factors should be considered when used as a marker. P62 does not always inversely correlate with ALP-activity (Liu *et al.*, 2016).

Although the vast majority of studies support the theory that TFEB is a master regulator of autophagy and lysosomal biogenesis in non-muscle cells, my data suggest that TFEB is not sufficient to induce ALP mediated protein degradation in C2C12 cells.

My findings are supported by other groups. Gatto and coworkers demonstrated a delay in the progression of Pompe disease in TFEB-treated mice; however, they could not show an effect of TFEB on autophagy markers in muscle (Gatto *et al.*, 2017). In addition, the group of Andrea Ballabio investigated the role of TFEB in cell metabolism and mitochondrial biogenesis. In this study, the transcriptome of the skeletal muscle from mice overexpressing TFEB and *Tfeb*-knockout mice was analyzed and revealed that TFEB is involved in the regulation of genes involved in mitochondrial biogenesis and glucose homeostasis in muscle. However, they did not find any evidence that TFEB is involved in ALP mediated protein degradation in muscle in either the presence or absence of nutrients (Mansueto *et al.*, 2017).

Discussion

Another valuable contribution for the discussion would be to pointing out the relative abundance of distinct members of the MiT/TFE family in different tissues. It has been widely reported that TFE3 and TFEB heterodimerize and function redundantly. I hypothesize if there is a higher sensitivity in autophagy induction by TFE3 in skeletal muscle. Maybe due to a physiological greater abundance of TFE3.

5.5 Deletion of *Tfeb* in muscle does not affect muscle growth *in vivo*

Our group successfully generated a transgenic mouse in which we deleted *Tfeb* in the entire muscle-cell lineage. These animals resulted from an intercross of mice that harbored a conditional TFEB allele with transgenic mice, which expressed the CRE-recombinase under the control of the muscle-specific Pax7 promoter (a kind gift of the group of Carmen Birchmeier, MDC). The phenotyping results revealed that the absence of *Tfeb* in the muscle cell lineage had no effect on muscle growth or MuRF1 expression.

TFEB is extensively known to sustain autophagy, it is worth to underline that deletion of TFEB does not affect basal autophagy. Indeed, *Tfeb* knockout mice do not show any phenotype that may resemble features of the already described muscle-specific autophagy knockout mice (*Atg7^{-/-}*) shown by Masiero and coworkers (Masiero *et al.*, 2009). On the contrary, *Tfeb* knockout mice present the same muscle mass and histological organization as well as comparable expression levels of ALP genes. These results are in line with the aforementioned study performed by the group of Andrea Ballabio. His group showed that muscle-specific deletion of TFEB has no effect on the expression of ALP genes but instead results in accumulation of abnormal and dysfunctional mitochondria (Mansueto *et al.*, 2017).

My findings reveal unchanged levels of basal autophagy under conditions when TFEB is depleted in myocytes. A possible explanation for my results may lay in the redundancy of the MiT/TFE family members. The role and importance of functionality and heterodimerization of MiT/TFE family remains to be explored in skeletal muscle. Therefore, a potential strategy to overcome this problem would be the generation of a combined deletion of the MiT/TFE family.

Since TFEB is reported to regulate gene expression in response to starvation, I would suggest a second alternative stress factor, such as denervation-induced muscle atrophy, to investigate the role of TFEB in different pathologies.

5.6 TFEB overexpression impairs myogenic differentiation

In my study, I have shown that overexpression of TFEB in C2C12 myoblasts results in abnormal cell migration and myoblast fusion resulting in attenuated myogenic differentiation. A decreased expression of *myogenin* and *MyoD* as well as a reduction in myosin heavy chain protein content were observed in TFEB overexpressing myoblasts indicating that overexpression of TFEB inhibits myogenic differentiation. In addition, TFEB-transduced C2C12 cells consistently showed a decreased expression of myomaker and myomaxin. *mXina*-null mice, *myomaxin* knockout, present a disruption of intercalated disks and myofilament disarray in heart (Gustafson-Wagner *et al.*, 2007). Based on the similarities between heart and skeletal muscle, it is tempting to speculate that myomaxin is a direct target of TFEB and involved in the differentiation phenotype. Further studies are needed to investigate this hypothesis.

Together with our collaborators at the University Medicine Greifswald (FunGene, Prof. U. Völker), I performed a large-scale proteomics study, in order to better understand the function of TFEB in muscle cells. The outcome of this test was widely analyzed and initially inquired for typical TFEB targets, mostly related to the ALP. Consistent with my *in vivo* and *in vitro* data, we did not observe a major effect of TFEB on ALP mediated protein degradation. These results are still surprising since the most renowned effects of TFEB are related to autophagy control and lysosomal biogenesis.

However, we consistently found that TFEB positively affects the mitochondrial network of myoblasts and differentiating myotubes as well as throughout differentiation. I found proteins that improve the function of mitochondrial bioenergetics (Mansueto *et al.*, 2017). Including one of the major mitochondrial biogenesis master regulators in muscle, TFAM, which data is not included due to a mistake in data compilation of one of the biological replicates, but a trend of upregulation was noticeable. Together these results support my hypothesis that TFEB regulates gene expression and therefore protein synthesis in a tissue specific manner.

In mass-spectrometry, we did not identify myomaxin, myomaker and MuRF1. I explain this phenomenon as a common disadvantage of MS-proteomics. A protein that is not detected could mean that either the protein is not present, or the protein is present but not detected. For our analysis a protein first needed to be detected in every of the replicates and second it needs to be detectable above a certain threshold.

In addition, transcription factors and low abundant proteins are also often not detected by mass spectrometry. Identification of proteins also depends on the number and size of peptides resulting from the trypsin digest. Therefore, technical issues could have prevented the identification of myomaxin, myomaker and MuRF1 as well. In cases were mass spectrometry-based protein

Discussion

identification is difficult or even impossible this limitation can be overcome by targeted proteomics or simply by performing western blot analysis if the identity of the protein that needs to be detected and quantified is known.

Myomaxin is characterized as a Xin-related protein that plays a role in the regulation of muscle cytoarchitecture by directly interacting with α -actin (Huang *et al.*, 2006). Moreover, Xin proteins have been demonstrated to exist in a complex with N- and β -catenin, two proteins found in the adherens junctions (Sinn *et al.*, 2002; Gustafson-Wagner *et al.*, 2007). Since I observed that TFEB-transduced myoblasts are defective in cell fusion ability and motility I investigated this pathway. Indeed, I found that overexpression of TFEB caused a decrease in catenins and *Cdh15*, a cadherin specifically expressed in differentiated myotubes. These data are suggestive for the presence of disrupted adherens junctions and desmosomes that compromise their functionality. Accordingly, several forms of actin, muscle specific actinin and troponin were found to be downregulated as well. Likewise, I found that overexpression of TFEB caused a reduction in β -integrin and other integrin isoforms. Because integrins are a family of cell surface glycoproteins that have been shown to regulate myoblast fusion and assembly of muscle fiber cytoskeleton (Schwander *et al.*, 2003) it is tempting to speculate that their downregulation prevents differentiation and therefore contributes to the phenotype.

Reduced expression of many members of the myosin superfamily further supports the notion of an impaired myogenic differentiation due to TFEB overexpression as these proteins are used as late differentiation markers. Another surprising result of the proteomics analysis was the finding of highly expressed proliferation marker Ki67. Supporting my hypothesis that TFEB-transduced myoblasts subjected to differentiation medium do not exit the cell cycle and maintain their proliferative state.

Hence, I propose that TFEB participates in myogenic differentiation. Based on the observed defective cell-cell fusion and the apparent changes in the cytoskeleton, I hypothesize that TFEB controls myogenic differentiation by regulation of myomarker and myomaxin. Further studies are needed to investigate how TFEB regulates myomaxin and myomarker in myocytes. For instance, RNA sequencing and chromatin immunoprecipitation of TFEB transduced C2C12 myoblasts would give new insights into how TFEB represents an important part of this process. Cell fusion in muscle cells during the development and regeneration of skeletal muscle is a complex process that is so far not completely understood. Therefore, the study of the mechanistic role of TFEB in skeletal muscle development will also be an area of great interest.

6. Bibliography

Baehr, L. M., J. D. Furlow and S. C. Bodine (2011). "Muscle sparing in muscle RING finger 1 null mice: response to synthetic glucocorticoids." *The Journal of physiology* 589(Pt 19): 4759-4776.

Barth, S., D. Glick and K. F. Macleod (2010). "Autophagy: assays and artifacts." *J Pathol* 221(2): 117-124.

Beckmann, H., L. K. Su and T. Kadesch (1990). "TFE3: a helix-loop-helix protein that activates transcription through the immunoglobulin enhancer muE3 motif." *Genes Dev* 4(2): 167-179.

Berg, J. S., B. C. Powell and R. E. Cheney (2001). "A millennial myosin census." *Molecular biology of the cell* 12(4): 780-794.

Berkes, C. A. and S. J. Tapscott (2005). "MyoD and the transcriptional control of myogenesis." *Semin Cell Dev Biol* 16(4-5): 585-595.

Bharti, K., W. Liu, T. Csermely, S. Bertuzzi and H. Arnheiter (2008). "Alternative promoter use in eye development: the complex role and regulation of the transcription factor MITF." *Development (Cambridge, England)* 135(6): 1169-1178.

Bjorkoy, G., T. Lamark, A. Brech, H. Outzen, M. Perander, A. Overvatn, H. Stenmark and T. Johansen (2005). "p62/SQSTM1 forms protein aggregates degraded by autophagy and has a protective effect on huntingtin-induced cell death." *J Cell Biol* 171(4): 603-614.

Bodine, S. C. and L. M. Baehr (2014). "Skeletal muscle atrophy and the E3 ubiquitin ligases MuRF1 and MAFbx/atrogen-1." *American journal of physiology. Endocrinology and metabolism* 307(6): E469-E484.

Bodine, S. C., E. Latres, S. Baumhueter, V. K. Lai, L. Nunez, B. A. Clarke, W. T. Poueymirou, F. J. Panaro, E. Na, K. Dharmarajan, Z. Q. Pan, D. M. Valenzuela, T. M. DeChiara, T. N. Stitt, G. D. Yancopoulos and D. J. Glass (2001). "Identification of ubiquitin ligases required for skeletal muscle atrophy." *Science* 294(5547): 1704-1708.

Braun, T. and M. Gautel (2011). "Transcriptional mechanisms regulating skeletal muscle differentiation, growth and homeostasis." *Nat Rev Mol Cell Biol* 12(6): 349-361.

Charrasse, S., F. Comunale, M. Fortier, E. Portales-Casamar, A. Debant and C. Gauthier-Rouvière (2007). "M-cadherin activates Rac1 GTPase through the Rho-GEF trio during myoblast fusion." *Molecular biology of the cell* 18(5): 1734-1743.

Desjardins, P. R., J. M. Burkman, J. B. Shrager, L. A. Allmond and H. H. Stedman (2002). "Evolutionary Implications of Three Novel Members of the Human Sarcomeric Myosin Heavy Chain Gene Family." *Molecular Biology and Evolution* 19(4): 375-393.

Di Malta, C., D. Siciliano, A. Calcagni, J. Monfregola, S. Punzi, N. Pastore, A. N. Eastes, O. Davis, R. De Cegli, A. Zampelli, L. G. Di Giovannantonio, E. Nusco, N. Platt, A. Guida, M. H. Ogmundsdottir, L. Lanfrancone, R. M. Perera, R. Zoncu, P. G. Pelicci, C. Settembre and A. Ballabio (2017). "Transcriptional activation of RagD GTPase controls mTORC1 and promotes cancer growth." *356(6343): 1188-1192.*

Dikic, I. (2017). "Proteasomal and Autophagic Degradation Systems." *Annu Rev Biochem* 86: 193-224.

Dikic, I. and Z. Elazar (2018). "Mechanism and medical implications of mammalian autophagy." *Nature Reviews Molecular Cell Biology* 19(6): 349-364.

Du Bois, P., C. Pablo Tortola, D. Lodka, M. Kny, F. Schmidt, K. Song, S. Schmidt, R. Bassel-Duby, E. N. Olson and J. Fielitz (2015). "Angiotensin II Induces Skeletal Muscle Atrophy by Activating TFEB-Mediated MuRF1 Expression." *Circ Res* 117(5): 424-436.

Duan, R. and P. J. Gallagher (2009). "Dependence of myoblast fusion on a cortical actin wall and nonmuscle myosin IIA." *Dev Biol* 325(2): 374-385.

Fielitz, J., M.-S. Kim, J. M. Shelton, X. Qi, J. A. Hill, J. A. Richardson, R. Bassel-Duby and E. N. Olson (2008). "Requirement of protein kinase D1 for pathological cardiac remodeling." *Proceedings of the National Academy of Sciences of the United States of America* 105(8): 3059-3063.

Fisher, D. E., C. S. Carr, L. A. Parent and P. A. Sharp (1991). "TFEB has DNA-binding and oligomerization properties of a unique helix-loop-helix/leucine-zipper family." *Dev Biol* 142(1): 2342-2352.

Foletta, V. C., L. J. White, A. E. Larsen, B. Leger and A. P. Russell (2011). "The role and regulation of MAFbx/atrogen-1 and MuRF1 in skeletal muscle atrophy." *Pflügers Arch* 461(3): 325-335.

Gatto, F., B. Rossi, A. Tarallo, E. Polishchuk, R. Polishchuk, A. Carrella, E. Nusco, F. G. Alvino, F. Iacobellis, E. De Leonibus, A. Auricchio, G. Diez-Roux, A. Ballabio and G. Parenti (2017). "AAV-mediated transcription factor EB (TFEB) gene delivery ameliorates muscle pathology and function in the murine model of Pompe Disease." *Sci Rep* 7(1): 15089.

Goldberg, A. L. (1969). "Protein turnover in skeletal muscle. II. Effects of denervation and cortisone on protein catabolism in skeletal muscle." *J Biol Chem* 244(12): 3223-3229.

Gomes, M. D., S. H. Lecker, R. T. Jagoe, A. Navon and A. L. Goldberg (2001). "Atrogen-1, a muscle-specific F-box protein highly expressed during muscle atrophy." *Proc Natl Acad Sci U S A* 98(25): 14440-14445.

Griger, J., Schneider, R., Lahmann, I., Schöwel, V., Keller, C., Spuler, S., ... Birchmeier, C. (2017). Loss of Ptpn11 (Shp2) drives satellite cells into quiescence. *eLife*, 6, e21552. doi:10.7554/eLife.21552

Gustafson-Wagner, E. A., H. W. Sinn, Y.-L. Chen, D.-Z. Wang, R. S. Reiter, J. L.-C. Lin, B. Yang, R. A. Williamson, J. Chen, C.-I. Lin and J. J.-C. Lin (2007). "Loss of mXin α , an intercalated disk protein, results in cardiac hypertrophy and cardiomyopathy with conduction defects." *Circ Res* 101(5): H2680-H2692.

Ha, C. H., & Jin, Z. G. (2009). Protein kinase D1, a new molecular player in VEGF signaling and angiogenesis. *Molecules and cells*, 28(1), 1–5. doi:10.1007/s10059-009-0109-9

Haberland, M., R. L. Montgomery and E. N. Olson (2009). "The many roles of histone deacetylases in development and physiology: implications for disease and therapy." *Nature reviews. Genetics* 10(1): 32-42.

Hayashi, K., K. Dan, F. Goto, N. Tshuchihashi, Y. Nomura, M. Fujioka, S. Kanzaki and K. J. C. S. Ogawa (2015). "The autophagy pathway maintained signaling crosstalk with the Keap1-Nrf2 system through p62 in auditory cells under oxidative stress."

Hemesath, T. J., E. Steingrimsson, G. McGill, M. J. Hansen, J. Vaught, C. A. Hodgkinson, H. Arnheiter, N. G. Copeland, N. A. Jenkins and D. E. Fisher (1994). "microphthalmia, a critical factor in melanocyte development, defines a discrete transcription factor family." *Genes Dev* 8(22): 2770-2780.

Hewitt, G., B. Carroll, R. Sarallah, C. Correia-Melo, M. Ogrodnik, G. Nelson, E. G. Otten, D. Manni, R. Antrobus, B. A. Morgan, T. von Zglinicki, D. Jurk, A. Seluanov, V. Gorbunova, T. Johansen, J. F. Passos

and V. I. Korolchuk (2016). "SQSTM1/p62 mediates crosstalk between autophagy and the UPS in DNA repair." *Autophagy* 12(10): 1917-1930.

Huang, H.-T., O. M. Brand, M. Mathew, C. Ignatiou, E. P. Ewen, S. A. Mccalmon and F. J. Naya (2006). "Myomaxin Is a Novel Transcriptional Target of MEF2A That Encodes a Xin-related α -Actinin-interacting Protein." *Journal of Biological Chemistry* 281(51): 39370-39379.

Hughes, C. S., S. Foehr, D. A. Garfield, E. E. Furlong, L. M. Steinmetz and J. Krijgsveld (2014). "Ultrasensitive proteome analysis using paramagnetic bead technology." *Mol Syst Biol* 10: 757.

Kabeya, Y., N. Mizushima, T. Ueno, A. Yamamoto, T. Kirisako, T. Noda, E. Kominami, Y. Ohsumi and T. Yoshimori (2000). "LC3, a mammalian homologue of yeast Apg8p, is localized in autophagosome membranes after processing." *Embo j* 19(21): 5720-5728.

Kauffman, E. C., C. J. Ricketts, S. Rais-Bahrami, Y. Yang, M. J. Merino, D. P. Bottaro, R. Srinivasan and W. M. Linehan (2014). "Molecular genetics and cellular features of TFE3 and TFE3 fusion kidney cancers." *Nat Rev Urol* 11(8): 465-475.

Kaushal, G. P. (2012). "Autophagy protects proximal tubular cells from injury and apoptosis." *Kidney International* 82(12): 1250-1253.

Kim, M.-S., J. Fielitz, J. McAnally, J. M. Shelton, D. D. Lemon, T. A. McKinsey, J. A. Richardson, R. Bassel-Duby and E. N. Olson (2008). "Protein Kinase D1 Stimulates MEF2 Activity in Skeletal Muscle and Enhances Muscle Performance." *Molecular and Cellular Biology* 28(11): 3600-3609.

Kloetzel, P.-M. (2001). "Antigen processing by the proteasome." *Nature Reviews Molecular Cell Biology* 2(3): 179-188.

Komatsu, M., S. Waguri, T. Ueno, J. Iwata, S. Murata, I. Tanida, J. Ezaki, N. Mizushima, Y. Ohsumi, Y. Uchiyama, E. Kominami, K. Tanaka and T. J. J. C. B. Chiba (2005). "Impairment of starvation-induced and constitutive autophagy in Atg7-deficient mice." 169.

Korolchuk, V. I., A. Mansilla, F. M. Menzies and D. C. Rubinsztein (2009). "Autophagy Inhibition Compromises Degradation of Ubiquitin-Proteasome Pathway Substrates." *Molecular Cell* 33(4): 517-527.

Li, Y. and E. Seto (2016). "HDACs and HDAC Inhibitors in Cancer Development and Therapy." *Cold Spring Harbor perspectives in medicine* 6(10): a026831.

Liu, W. J., L. Ye, W. F. Huang, L. J. Guo, Z. G. Xu, H. L. Wu, C. Yang, H. F. J. C. Liu and M. B. Letters (2016). "p62 links the autophagy pathway and the ubiquitin–proteasome system upon ubiquitinated protein degradation." 21(1): 29.

Mansueto, G., A. Armani, C. Viscomi, L. D'Orsi, R. De Cegli, E. V. Polishchuk, C. Lamperti, I. Di Meo, V. Romanello, S. Marchet, P. K. Saha, H. Zong, B. Blaauw, F. Solagna, C. Tezze, P. Grumati, P. Bonaldo, J. E. Pessin, M. Zeviani, M. Sandri and A. Ballabio (2017). "Transcription Factor EB Controls Metabolic Flexibility during Exercise." *Cell Metab* 25(1): 182-196.

Martina, J. A. (2014). "The Nutrient-Responsive Transcription Factor TFE3 Promotes Autophagy, Lysosomal Biogenesis, and Clearance of Cellular Debris." *Cell Biology*.

Martina, J. A., Y. Chen, M. Gucek and R. Puertollano (2012). "MTORC1 functions as a transcriptional regulator of autophagy by preventing nuclear transport of TFE3." *Autophagy* 8(6): 903-914.

Martina, J. A., H. I. Diab, O. A. Brady and R. Puertollano (2016). "TFEB and TFE3 are novel components of the integrated stress response." *EMBO J* 35(5): 479-495.

Martina, J. A., H. I. Diab, H. Li and R. Puertollano (2014). "Novel roles for the MiTF/TFE family of transcription factors in organelle biogenesis, nutrient sensing, and energy homeostasis." *Cell Mol Life Sci* 71(13): 2483-2497.

Martina, J. A. and R. Puertollano (2013). "Rag GTPases mediate amino acid-dependent recruitment of TFEB and MITF to lysosomes." *Autophagy* 200(4): 475-491.

Masiero, E., L. Agatea, C. Mammucari, B. Blaauw, E. Loro, M. Komatsu, D. Metzger, C. Reggiani, S. Schiaffino and M. Sandri (2009). "Autophagy is required to maintain muscle mass." *Cell Metab* 10(6): 507-515.

Mauthe, M., I. Orhon, C. Rocchi, X. Zhou, M. Luhr, K. J. Hijlkema, R. P. Coppes, N. Engedal, M. Mari and F. Reggiori (2018). "Chloroquine inhibits autophagic flux by decreasing autophagosome-lysosome fusion." *Autophagy* 14(8): 1435-1455.

Milan, G., V. Romanello, F. Pescatore, A. Armani, J.-H. Paik, L. Frasson, A. Seydel, J. Zhao, R. Abraham, A. L. Goldberg, B. Blaauw, R. A. DePinho and M. Sandri (2015). "Regulation of autophagy and the ubiquitin-proteasome system by the FoxO transcriptional network during muscle atrophy." *Nature Communications* 6: 6670.

Millay, D. P., D. G. Gamage, M. E. Quinn, Y.-L. Min, Y. Mitani, R. Bassel-Duby and E. N. Olson (2016). "Structure-function analysis of myomaker domains required for myoblast fusion." *Development* 143(8): 2116-2121.

Millay, D. P., J. R. O'Rourke, L. B. Sutherland, S. Bezprozvannaya, J. M. Shelton, R. Bassel-Duby and E. N. Olson (2013). "Myomaker is a membrane activator of myoblast fusion and muscle formation." *Nature* 499(7458): 301-305.

Mizushima, N. (2007). "Autophagy: process and function." *Cell* 127(22): 2861-2873.

Mizushima, N. and T. Yoshimori (2014). "How to Interpret LC3 Immunoblotting." *Autophagy* 3(6): 542-545.

Mizushima, N., T. Yoshimori and B. Levine (2010). "Methods in mammalian autophagy research." *Cell* 140(3): 313-326.

Moresi, V., A. H. Williams, E. Meadows, J. M. Flynn, M. J. Potthoff, J. McAnally, J. M. Shelton, J. Backs, W. H. Klein, J. A. Richardson, R. Bassel-Duby and E. N. Olson (2010). "Myogenin and class II HDACs control neurogenic muscle atrophy by inducing E3 ubiquitin ligases." *Cell* 143(1): 35-45.

Murmann, O., Niggli, F. & Schäfer, B. (2005). Cloning and Characterization of the Human PAX7 Promoter. *Biological Chemistry*, 381(4), pp. 331-335.

Nabar, N. R. and J. H. Kehrl (2017). "The Transcription Factor EB Links Cellular Stress to the Immune Response." *The Yale journal of biology and medicine* 90(2): 301-315.

Napolitano, G. and A. Ballabio (2016). "TFEB at a glance." *J Cell Sci* 129(13): 2475-2481.

Nezich, C. L., C. Wang, A. I. Fogel and R. J. Youle (2015). "MiT/TFE transcription factors are activated during mitophagy downstream of Parkin and Atg5." *Development* 142(3): 435-450.

Nowak, S. J., P. C. Nahirney, A. K. Hadjantonakis and M. K. Baylies (2009). "Nap1-mediated actin remodeling is essential for mammalian myoblast fusion." *J Cell Sci* 122(Pt 18): 3282-3293.

Palmieri, M., S. Impey, H. Kang, A. di Ronza, C. Pelz, M. Sardiello and A. Ballabio (2011). "Characterization of the CLEAR network reveals an integrated control of cellular clearance pathways." *Hum Mol Genet* 20(19): 3852-3866.

Pena-Llopis, S. and J. Brugarolas (2011). "TFEB, a novel mTORC1 effector implicated in lysosome biogenesis, endocytosis and autophagy." *Cell Cycle* 10(23): 3987-3988.

Perry, R. L. and M. A. Rudnick (2000). "Molecular mechanisms regulating myogenic determination and differentiation." *Front Biosci* 5: D750-767.

Ploper, D., V. F. Taelman, L. Robert, B. S. Perez, B. Titz, H.-W. Chen, T. G. Graeber, E. von Euw, A. Ribas and E. M. De Robertis (2015). "MITF drives endolysosomal biogenesis and potentiates Wnt signaling in melanoma cells." *Proceedings of the National Academy of Sciences* 112(5): E420-E429.

Poggenberg, V., M. H. Ogmundsdottir, K. Bergsteinsdottir, A. Schepsky, B. Phung, V. Deineko, M. Milewski, E. Steingrimsson and M. Wilmanns (2012). "Restricted leucine zipper dimerization and specificity of DNA recognition of the melanocyte master regulator MITF." *Genes Dev* 26(23): 2647-2658.

Qiao, L. and J. Zhang (2009). "Inhibition of lysosomal functions reduces proteasomal activity." *Neuroscience Letters* 456(1): 15-19.

Roczniak-Ferguson, A., C. S. Petit, F. Froehlich, S. Qian, J. Ky, B. Angarola, T. C. Walther and S. M. Ferguson (2012). "The Transcription Factor TFEB Links mTORC1 Signaling to Transcriptional Control of Lysosome Homeostasis." *PLoS One* 7(2): ra42-ra42.

Rozengurt E. (2011). "Protein kinase D signaling: multiple biological functions in health and disease. *Physiology*" (Bethesda, Md.), 26(1), 23–33. doi:10.1152/physiol.00037.2010

Rozengurt, E. Rey O., Waldron RT. (2005). "Protein kinase D signaling" *J Biol Chem*. 280(14):13205-8.

Sakamaki, J. I., S. Wilkinson, M. Hahn, N. Tasdemir, J. O'Prey, W. Clark, A. Hedley, C. Nixon, J. S. Long, M. New, T. Van Acker, S. A. Tooze, S. W. Lowe, I. Dikic and K. M. Ryan (2017). "Bromodomain Protein BRD4 Is a Transcriptional Repressor of Autophagy and Lysosomal Function." *Mol Cell* 66(4): 517-532 e519.

Salma, N. (2017). "Tfe3 and Tfeb Transcriptionally Regulate Peroxisome Proliferator-Activated Receptor γ 2 Expression in Adipocytes and Mediate Adiponectin and Glucose Levels in Mice *Molecular and Cellular Biology* 37(15).

Sardiello, M., M. Palmieri, A. di Ronza, D. L. Medina, M. Valenza, V. A. Gennarino, C. Di Malta, F. Donaudo, V. Embrione, R. S. Polishchuk, S. Banfi, G. Parenti, E. Cattaneo and A. Ballabio (2009). "A gene network regulating lysosomal biogenesis and function." *Science* 325(5939): 473-477.

Sardiello, M. B., A (2009). "Lysosomal enhancement. CLEAR answer to cellular degradative needs." *Cell Cycle*.

Schiaffino, S. and C. Reggiani (2011). "Fiber Types in Mammalian Skeletal Muscles." *Physiol Rev* 91(4): 1447-1531.

Schindelin, J., I. Arganda-Carreras, E. Frise, V. Kaynig, M. Longair, T. Pietzsch, S. Preibisch, C. Rueden, S. Saalfeld, B. Schmid, J.-Y. Tinevez, D. J. White, V. Hartenstein, K. Eliceiri, P. Tomancak and A. Cardona (2012). "Fiji: an open-source platform for biological-image analysis." *Nature Methods* 9: 676.

Schwander, M., M. Leu, M. Stumm, O. M. Dorchies, U. T. Ruegg, J. Schittny and U. Muller (2003). "Beta1 integrins regulate myoblast fusion and sarcomere assembly." *Dev Cell* 4(5): 673-685.

Settembre, C. and A. Ballabio (2011). "TFEB regulates autophagy: an integrated coordination of cellular degradation and recycling processes." *Autophagy* 7(11): 1379-1381.

Settembre, C., R. De Cegli, G. Mansueto, P. K. Saha, F. Vetrini, O. Visvikis, T. Huynh, A. Carissimo, D. Palmer, T. J. Klisch, A. C. Wollenberg, D. Di Bernardo, L. Chan, J. E. Irazoqui and A. Ballabio (2013). "TFEB controls cellular lipid metabolism through a starvation-induced autoregulatory loop." *Nat Cell Biol* 15(6): 647-658.

Settembre, C., R. Zoncu, D. L. Medina, F. Vetrini, S. Erdin, S. Erdin, T. Huynh, M. Ferron, G. Karsenty, M. C. Vellard, V. Facchinetti, D. M. Sabatini and A. Ballabio (2012). "A lysosome-to-nucleus signalling mechanism senses and regulates the lysosome via mTOR and TFEB." *EMBO J* 31(5): 1095-1108.

Sherwood, L. (2007). "Human physiology: from cells to systems " Frontera and Ochala.

Sielaff, M., J. Kuharev, T. Bohn, J. Hahlbrock, T. Bopp, S. Tenzer and U. Distler (2017). "Evaluation of FASP, SP3, and iST Protocols for Proteomic Sample Preparation in the Low Microgram Range." *J Proteome Res* 16(11): 4060-4072.

Sinn, H. W., J. Balsamo, J. Lilien and J. J. Lin (2002). "Localization of the novel Xin protein to the adherens junction complex in cardiac and skeletal muscle during development." *Dev Dyn* 225(1): 1-13.

Steingrimsson, E., N. G. Copeland and N. A. Jenkins (2004). "Melanocytes and the microphthalmia transcription factor network." *Annu Rev Genet* 38: 365-411.

Steingrimsson, E., L. Tessarollo, S. W. Reid, N. A. Jenkins and N. G. Copeland (1998). "The bHLH-Zip transcription factor Tfeb is essential for placental vascularization." *Development* 125(23): 4607-4616.

Stitt, T. N., D. Drujan, B. A. Clarke, F. Panaro, Y. Timofeyeva, W. O. Kline, M. Gonzalez, G. D. Yancopoulos and D. J. Glass (2004). "The IGF-1/PI3K/Akt pathway prevents expression of muscle atrophy-induced ubiquitin ligases by inhibiting FOXO transcription factors." *Mol Cell* 14(3): 395-403.

Sundram, V., Chauhan, S. C., & Jaggi, M. (2011). Emerging roles of protein kinase D1 in cancer. *Molecular cancer research : MCR*, 9(8), 985–996.

Vega, R. B., B. C. Harrison, E. Meadows, C. R. Roberts, P. J. Papst, E. N. Olson and T. A. McKinsey (2004). "Protein kinases C and D mediate agonist-dependent cardiac hypertrophy through nuclear export of histone deacetylase 5." *Mol Cell Biol* 24(19): 8374-8385.

Waddell, D. S., L. M. Baehr, J. van den Brandt, S. A. Johnsen, H. M. Reichardt, J. D. Furlow and S. C. Bodine (2008). "The glucocorticoid receptor and FOXO1 synergistically activate the skeletal muscle atrophy-associated MuRF1 gene." *Am J Physiol Endocrinol Metab* 295(4): E785-797.

Walsh, K. and H. Perlman (1997). "Cell cycle exit upon myogenic differentiation." *Curr Opin Genet Dev* 7(5): 597-602.

Weiss, A., S. Schiaffino and L. A. Leinwand (1999). "Comparative sequence analysis of the complete human sarcomeric myosin heavy chain family: implications for functional diversity." *J Mol Biol* 290(1): 61-75.

Willis, M. S., M. Rojas, L. Li, C. H. Selzman, R. H. Tang, W. E. Stansfield, J. E. Rodriguez, D. J. Glass and C. Patterson (2009). "Muscle ring finger 1 mediates cardiac atrophy in vivo." *Am J Physiol Heart Circ Physiol* 296(4): H997-H1006.

Yaffe, D. and O. Saxel (1977). "Serial passaging and differentiation of myogenic cells isolated from dystrophic mouse muscle." *Nature* 270(5639): 725-727.

Zammit, P. S., T. A. Partridge and Z. Yablonka-Reuveni (2006). "The Skeletal Muscle Satellite Cell: The Stem Cell That Came in From the Cold." *J Cell Biol* 174(1): 1177-1191.

Zhao, J., J. J. Brault, A. Schild, P. Cao, M. Sandri, S. Schiaffino, S. H. Lecker and A. L. Goldberg (2007). "FoxO3 coordinately activates protein degradation by the autophagic/lysosomal and proteasomal pathways in atrophying muscle cells." *Cell Metab* 6(6): 472-483

